Femoral Neck Anteversion: Measurement, Predictors, and Effects on Musculoskeletal Function

Matteo Scorcelletti

PhD 2022

Femoral Neck Anteversion: Measurement, Predictors, and Effects on Musculoskeletal Function

By Matteo Scorcelletti

A thesis submitted in partial fulfilment of the requirements of

Manchester Metropolitan University

for the degree of

Doctor of Philosophy.

Department of Life Sciences

Faculty of Science and Engineering

Manchester Metropolitan University

In collaboration with the

German Aerospace Centre (DLR)

2022

Table of Contents

Acknowledgements

I would like to express my gratitude to my supervisor, Dr. Alex Ireland, for his academic and emotional guidance throughout my PhD. He devoted a great deal of time and energy to both me and the project, always remaining composed and helping me find solutions. I would also like to thank my co-supervisor, Prof. Jörn Rittweger, for providing the necessary infrastructure and expertise of the German Aerospace Agency (DLR) and the Children's Clinic in Cologne, which greatly expanded the possibilities of my PhD. Prof. Neil Reeves, my co-supervisor, deserves special thanks for thoroughly reviewing all of my manuscripts and providing valuable feedback.

I am deeply grateful to the DLR team, including Dr. Jochen Zange, Jonas Böcker, Wolfram Sies, Dr. Patrick Lau, Dr. Uwe Mittag, Dr. Serhan Kara, and Prof. Lothar Seefried, who recruited participants and collected data. I would also like to acknowledge Prof. Oliver Semler and Prof. Eckhard Schönau, who provided excellent feedback on the manuscript for the X-linked Hypophosphatemia study.

Finally, I would like to thank the people that have supported me through my experience at MMU during lunch and as a tutor: Stuart Fielding, Paul Hendrickse, Chris Broughton, Tony Scimone, Xaaly O'Reilly- Berkeley, and Maria Blanco.

Funding

The PhD has been Funded by Manchester Metropolitan University. Parts of the studies have been supported by funding from the Deutsche Luft und Raumfahrt and Kyowa Kirin.

Impact of COVID-19

Starting from March 2020, in response to the COVID-19 pandemic, Manchester Metropolitan University closed the laboratory spaces in accordance with government guidelines. As a result, studies requiring human participants were suspended until February 2021 when the laboratories were partially reopened with limited capacity and strict safety protocols were implemented to ensure the safety of both participants and researchers. The contingency plan involved modifying

the research protocols to accommodate the new safety measures and shifting the focus of the research to data analysis and manuscript writing. This presented substantial challenges to recruitment and conduct of studies even beyond the 11-month laboratory closure, particularly as Manchester was the area within the UK most severely affected by lockdown restrictions.

At the German Aerospace Agency, participant recruitment for research studies was permitted to resume earlier than in the UK. However, recruitment was hampered by travel restrictions and suspected COVID-19 infections among potential participants in the days preceding testing. These challenges persisted until mid-2021 when most of the travel restrictions were lifted and the incidence of suspected infections decreased.

Papers and conference proceedings

Publications

Scorcelletti, M., Zange, J., Böcker, J., Sies, W., Lau, P., Mittag, U., Ireland, A. & Rittweger, J. (2023). Associations between long-term exercise participation and lower limb joint and whole-bone geometry in young and older adults. Frontiers in Physiology, 14, 745.

Scorcelletti, M., Kara, S., Zange, J., Jordan, J., Semler, O., Schönau, E., ... & Seefried, L. (2022). Lower limb bone geometry in adult individuals with X-linked hypophosphatemia: an observational study. Osteoporosis International, 33(7), 1601-1611.

Scorcelletti, M., Reeves, N. D., Rittweger, J., & Ireland, A. (2020). Femoral anteversion: significance and measurement. Journal of anatomy, 237(5), 811-826.

Oral presentations

Scorcelletti M., Zange J., Böcker, J., Sies W., Lau P., Mittag U., Reeves N., Ireland A.,Rittweger. Associations between long-term exercise participation and lower limb bone geometry in young and older adults. *Bone Research Society Conference 2022.*

Scorcelletti, M., Kara, S., Zange, J., Jordan, J., Semler, O., Schönau, E., Rittweger, J., Ireland, A. and Seefried, L. Femoral anteversion (FNA) in individuals with X-linked hypophosphatemia (XLH). *Bone Research Society Conference 2021.*

Poster presentation

Scorcelletti, M., Kara, S., Zange, J., Jordan, J., Semler, O., Schönau, E., Rittweger, J., Ireland, A. and Seefried, L. Lower limb bone geometry in adult individuals with X-linked hypophosphatemia: an observational study. *Bone Research Society Conference 2022.*

Awards and recognitions

New Investigator Award, Bone Research Society Conference 2022

Abstract

Total femoral torsion and other lower limb geometry parameters show substantial inter-individual variation and contribute to clinical outcomes such as hip dysplasia, hip and knee osteoarthritis, atypical fractures, and disadvantageous kinematics. This thesis aimed to identify appropriate methods to assess femoral torsion. Thereafter, to investigate its determinants and relationship to other aspects of lower limb geometry and muscle function.

The literature review identified the clinical importance of femoral torsion, a lack of standardisation in femoral torsion measurement, and the strength and weaknesses of

current methods whilst highlighting the need for quick and accurate techniques employable in children.

The first study proved the concept of a new three-dimensional biomedical imaging device using a standard ultrasound device, with a linear array probe, coupled with a coordinate-measuring system. This achieved only poor-to-moderate test-retest reliability for femoral torsion (ICC=0.329; CI -0.542-0.843) and femoral length (ICC=0.615; CI -0.071-0.919) respectively but identified a number of potential avenues for improvement of the technique.

The second study characterised lower limb geometry in individuals with X-linked hypophosphatemia (XLH) and controls and found large differences in several parameters of lower limb geometry between the two groups. The identification of ~ 18° smaller intertrochanteric rather than shaft torsion in these individuals can inform surgical guidelines.

The third study explored the associations of long-term power exercise with lower limb geometry in young and older adults. Only small associations were observed with training and age as effects on femoral bowing in the order of magnitude of ~2°. The ability to alter skeletal geometry through exercise throughout adulthood seems limited, reinforcing the importance of childhood physical activity for lifelong skeletal health.

This thesis presented novel insights and methodologies regarding the characterisation of lower limb geometry on three planes and the relationship between the different shape parameters, informing future surgical procedures. It also added new evidence of skeletal shape adaptations to chronic exercise in adulthood and impaired phosphate metabolism.

Chapter 1 Introduction

1.1 Bone function

Bone can refer to the whole organ, the tissue of which it is composed, or the material from which the tissue is constructed. At the organ level, bones form the skeleton which is the framework of the human organism and other vertebrate animals. This framework can have different functions such as the protection of vital organs, providing lever arms upon which muscles can act on to produce movement (Scheys et al., 2008, Yavuzer, 2020) or more niche functions such as the propagation of sound. Bone is a metabolic organ which stores minerals and fats (Burr & Allen 2019). The inner part of the bone is also the primary site for white and red blood cell production (Burr & Allen 2019).

Bone is composed of a hierarchical collagen and mineral component structure (Reznikov, Shahar, & Weiner,2014), giving it a balance of stiffness and toughness. It is composed of living cells, and it is irrorated by blood vessels and nerves (Burr & Allen 2019) making it a more dynamic tissue than intuition would suggest.

1.2 Bone types

Bone types are genetically determined to have a specific function. They are classified by their function and shape (Currey, 2008; Black & Tadros, 2020). Flat bones such as the skull bones are designed for protection and containment, whilst other flat bones like the scapula provide an extended surface for muscular attachment. Short bones, like the carpals, support movement. Long bones like the femur and tibia provide long lever arms for muscles to act against, allowing broad and rapid movements (Zirkle and Lovejoy, 2019). Sesamoid bones such as the patella increase lever arms (Dan et al. 2018) and are to be found at the

intersections of some joints, these have smooth surfaces decreasing the friction with the tendon with which they are working.

1.3 Bone structure

The outer shell of the bone is the cortical or compact bone, and the inner part is the trabecular or the cancellous bone. These two differ in density, *i.e.,* the amount of mass per unit of volume. Compact cortical bone typically occupies ~80% of the bone volume, with the honeycomb-like trabecular bone structure having ~20% of its volume composed of bone (Ott 2018).

The cortical bone provides protection for the inner bone and strength to the system. It is composed of cylindrical structures called osteons or Haversian systems. These cylindrical structures align parallel to the forces they must counteract making the bone resistant to longitudinal compression and bending. The osteons are constituted by 10 to 25 layers of lamellae that surround a central blood vessel, depending on whether it is primary osteons, emerging adjacent to the growth plate, or secondary osteons resulting from intracortical remodelling (Gasser and Kneissel, 2017).

Trabecular bone is the inner porous part of the bone in the areas close to the joints. Its functional unit is not the osteon as in the remodelled cortical bone but the trabecula. The trabecula is also constituted by lamellae arranged in sheets or rods. Between the trabeculae we can find bone marrow and blood vessels which keep this region metabolically active. The trabeculae are often aligned to the lines of maximum stress, and this is seen beautifully in the proximal femur (Figure 1). Trabecular bone is generally found in regions of the bone where predominately compressive forces are experienced, such as long bone epiphyses and the vertebrae.

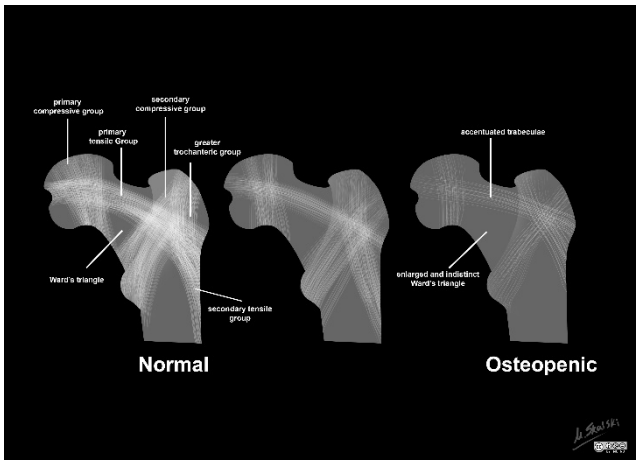

Figure 1 Diagram showing the trabecular structure in individuals with different levels of bone strength. Whilst the normal femur has greater bone mineral content, the orientation of the trabeculae is similar to that in an osteopenic bone in response to similar loading patterns. Case courtesy of Dr Matt Skalski (Skalski, 2022).

Externally the bone has a fine outer and inner layer of periosteum which covers the cortical bone, and a fine layer of endosteum which divides the cortical from the trabecular bone.

1.4 Bone turn-over

The process of bone material formation or osteogenesis is accomplished by the action of cells called osteoblast which produce an osteoid matrix made from collagen fibres that are secondarily mineralized in the two-step process of bone formation. Another cell, called osteoclast, has the role of absorbing bone material. Bone remodelling, therefore, is accomplished by the interaction of osteoblast and osteoclast activity. The cells involved in this process make up the basic multicellular unit also called remodelling unit, of the remodelling process (Rauch, 2006; Sims & Gooi, 2008). The process of remodelling begins with lining cells metabolising bone matrix preparing the site for osteoclasts to attach to by releasing collagenases forming a temporary canopy called bone remodelling compartment (Hauge et al., 2001). The bone remodelling compartment is highly vascular, this suggests

that osteocytes and osteoblasts migrate there via the bloodstream (Sims & Gooi, 2008) in the form of mononuclear osteoclast precursors (Parfit, 2006) and vascular pericytes which could be a source of osteoblast precursors (Eriksen et al., 2007; Sacchetti et al., 2007). The development of osteoclasts is initiated by local factors released by nearby cells from the osteoblast lineage such as pre-osteoblasts, mature osteoblasts, lining cells, osteocytes, and immune cells in the bone marrow (Suda et al., 1999). Most of these signalling mechanisms converge into the activation of the RANK receptor which is the main mediator of osteoclast formation (Dougall et al., 1999). The production of the ligand activating the RANK receptor (RANKL) is stimulated by microcracks in the bone matrix that can either occur under normal skeletal loading or pathological conditions (Parfit, 2022). The osteoblast lineage cells also signal the inhibition of osteoclast formation through osteoprotegerin (Bucay et al., 1998). The resorption phase comes to an end when the osteoclasts undergo programmed cell death, thereby preventing excessive resorption (Xin & Boyce, 2005).

The reversal phase follows where the newly resorbed bone surface undergoes a process of preparation. The removal of unmineralized collagen matrix is orchestrated by cells belonging to the osteoblastic lineage. Subsequently, a non-collagenous mineralized matrix is deposited to facilitate the adherence of osteoblasts (Zhou et al. 1994). Bone formation is then initiated by osteoblasts secreting collagen-rich osteoid matrix and continued with the osteoid mineralization mediated by osteoblasts (Atkins er al., 2012). Upon completion of mineralization, osteoblasts either undergo programmed cell death known as apoptosis, undergo a transformation into bone-lining cells, or become encased within the mineralized bone matrix and terminally differentiate into osteocytes (Sims & Gooi, 2008) which are thought to regulate bone remodelling activity. Bone lining cells are flattened cells on the surface of bones which have a central role in the signalling of bone remodelling by

communicating through the gap junctions with the osteocytes located deep in the bone matrix (Kollet et al., 2006). It is still not clear whether bone lining cells can reactivate into osteoblasts (Bilezikian et al., 2002; Matic et al., 2016) or not (Karsdal et al., 2002; Khosla et al., 2008; Matsuo & Irie, 2008). An imbalance of osteoblast and osteoclast activity will determine whether bone is lost or gained, and this can be seen in the ageing population when osteoclast's activity is higher than the osteoblast one resulting in low bone mineral density at the organ and tissue level, and a disadvantageous bone microarchitecture (Brandi, 2009). Other variables that affect bone formation are genetic disorders like x-linked hypophosphatemia and physical activity (the process of which will be explained in higher detail further down), nutritional deficits, lack of sunlight, hormones, and others.

Another cell called bone lining cell is part of the bone system. Bone lining cells are flattened cells of the osteoblast lineage that cover the surface of bones and have ceased to undergo cell division. In adult mice, these cells are considered to be a precursor to osteoblasts. (Matic et al., 2016).

1.5 A bone's life

The development of bones starts in the first trimester of foetal life and continues through childhood until skeletal maturity. This is driven by two distinct processes: intramembranous ossification and endochondral ossification.

Intramembranous ossification is usually associated with embryonic life as it takes place thanks to the mesenchyme, which is a primitive connective tissue. It is found mostly in embryonic development (Setiawati & Rahardjo, 2019) however, intramembranous ossification can also occur during bone healing after fractures. The process starts with the consolidation of mesenchymal cells which then differentiate into osteoblasts and start

producing collagen matrix in which osteoblasts will become encapsulated and become osteocytes (Allen & Burr, 2018). This process produces small patches of disorganised collagen structure which will expand and connect to similar patches and eventually form more organised lamellar bone.

Endochondral ossification also starts from an aggregate of mesenchymal cells which then differentiate into chondroblasts instead, leading to the formation of cartilage. This cartilage is surrounded by a cellular fibrous membrane called perichondrium which is similar in shape to the mineralized bone (Allen and Burr, 2019). Cells that are part of the perichondrium differentiate into osteoblasts and consequently form layers of bone on top of the cartilage.

During development and growth of the bone, the modelling of the structure will occur through the opposing actions of osteoblast which produce bone, and osteoclast which break bone material down. This process of bone modelling is responsible for shaping the mature adult bone and regulating bone mass as it increases in response to the mechanical stresses experienced during daily activities.

Mature bones undergo a process of bone remodelling. This relies on the coupled activity of osteoclasts and osteoblasts, maintaining continual bone material turnover which results in healing of microdamage and disposal of obsolete material in addition to regulating the level of serum calcium.

1.6 Longitudinal growth and the growth plate

The growth plate is the solution brought by probably millions of years of evolution, to the problem of making bone grow in length when our water bound ancestors felt the need to settle on land and developed a skeleton. The challenge was to develop a tissue that was

firm enough to withstand mechanical stress and soft enough to permit newly developed osteoblasts to provide appositional growth. The growth plate is located between the

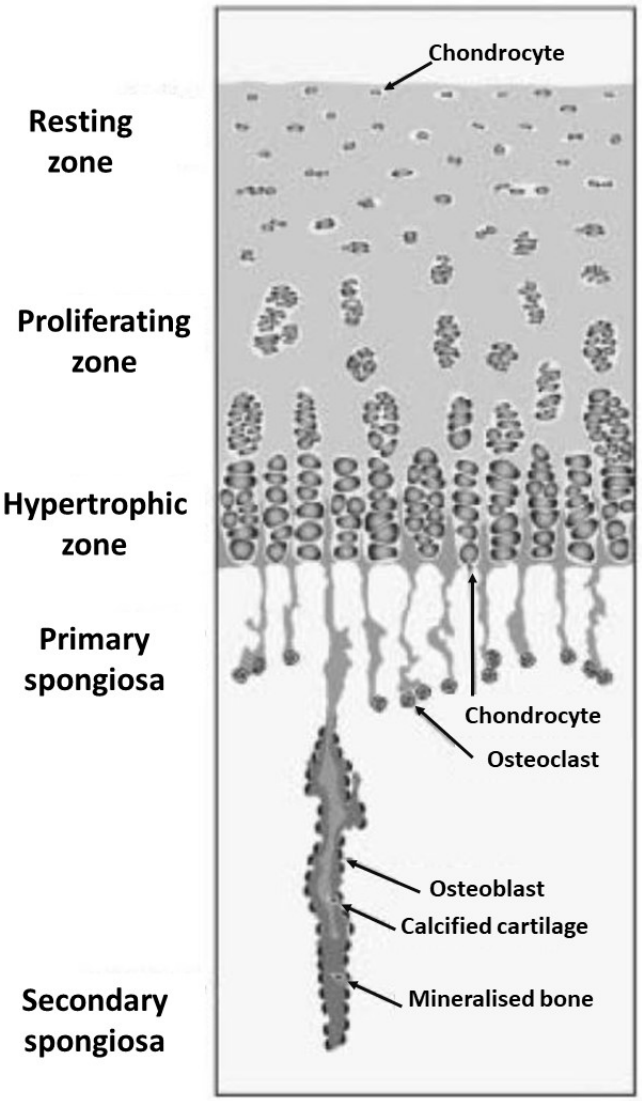

Figure 2 Zones of the growth plate which is situated between epiphyseal and metaphyseal bone. Figure from (Rauch, 2005).

epiphysis and the metaphysis. The growth is unidirectional towards the epiphysis as at the epiphyseal end of the growth plate resting chondrocytes and extracellular and intracellular material are found, which give a direction to the underlying active chondrocyte-producing bone matrix (Figure 2) (Rauch, 2005).

When the proliferating zone “travels” towards the epiphysis chondrocytes start mitosis still providing extracellular matrix and proteins. Subsequently, chondrocytes increase in size and stop proliferating and align themselves longitudinally to the bone while the concertation of calcium increases which is the signal to mineralise the surrounding matrix. At the junction of the hypertrophic zone and the primary spongiosa chondroclasts reabsorb the chondrocytes leaving space for blood vessels to invade the empty columns referred to as septa. The blood vessels, allow for bone precursors to permeate the tissue. Most of the mineralised septa are resorbed in the primary spongiosa and some are used as scaffold of osteoblast to lay bone matrix (Rauch, 2005).

The growth plate plays a central role in longitudinal growth and aligns the bone axes to the predominant mechanical forces (Fabeck et al., 2002; Rauch, 2005). Longitudinal growth ceases following mineralisation of the growth plate at the end of puberty (Jörn Rittweger, 2008).

1.7 Growth in width

While evolutionarily longitudinal bone growth served the increase in size of land-dwelling species, the growth in width was of paramount importance for the stability of bone as they have opposite effects on its strength. There is a positive exponential relationship between bending strength and the width of the elongated object. The ability of an elongated object to resist bending is related to its diameter elevated to the power of three. If we imagine two cylinders made from the same material but one with double the width, the latter would be eight times as resistant to bending and torsion.

Bones gain width from the action of osteoblasts on the periosteal surface, called periosteal apposition (Rauch, 2005). These osteoblasts become soon inactive and turn into osteocytes

when enclosed in the newly deposited bone matrix. During childhood, where bone formation is continuous, the periosteum surrounds the diaphysis being only loosely attached to the external lamellae of the diaphysis and continues into the perichondrium of the growth plate (Rauch, 2005). During adulthood, bone resorption and formation undergo a cyclical phase called remodelling (Frost, 1990).

Through the combined action of osteoblasts and osteoclasts, bone is added where strain is high, and it will be removed where strain is low. The aim of modelling is to move the position of the cortex relative to its central axis. This is called bone drift (Frost, 1990).

1.8 The Mechanostat

That mechanical stimulation influences bone structure was first proposed by Galileo when he asserted that loading is required to preserve bone mass (Uda et al., 2017) and that bones become more robust with increasing body mass. In 1892 Julius Wolff stated that bone remodelling in healthy individuals occurs in response to the forces applied to the bone (Wolff, 1892), now famously known as “Wolff’s Law”. The word “Mechanostat” was effectively first used in 1987 by the American orthopaedic surgeon Harold Frost, who theorised an underlying cellular mechanism of the previously observed bone adaptation induced by load (Frost, 1987). Mechanical loading occurring during daily activities is transduced from the macroscopic structure of skeletal elements to the tissue level, progressively reaching the cellular level (Jacobs et al., 2010). Later authors have suggested osteocytes as the possible mechanoregulatory agent of the bone tissue (Jacobs et al., 2010; Bonewald, 2011; Uda et al., 2017). Evidence includes a 2007 study that demonstrated that transgenic mice with specific osteocyte ablation, leaving osteoblasts intact, did not respond to mechanical unloading, with bone loss (Tatsumi et al., 2007). The stimuli reaching the

osteocytes, through the mineralised extracellular matrix, where osteocytes are located, are a combination of mechanical stresses including shear, compressive pressure, and fluid flow through the lacuno-canalicular system and strain (Thompson et al., 2012). Various structures of the osteocyte have been proposed to work as mechanosensors including its dendrites, the primary cilium, gap junctions, focal adhesions, cytoskeleton, ion channels and pericellular matrix at the lacunar region. Understanding of the osteocyte's transduction system from their mechanosensory to biochemical signals to achieve bone adaptation is still not fully known. All pathways, however, are responsible for the processes of bone formation including the proliferation and differentiation of bone-forming osteoblasts and regulation of their activity and enhancing genesis of bone-reabsorbing osteoclasts (Qin et al., 2020), increasing bone turnover.

1.9 The Femur

This thesis focuses primarily on the femur, which is the largest, strongest bone in the body. The most powerful human movements like jumping and sprinting are accomplished predominately by the interplay of the large muscles attached to the femur. This interaction of lever arms and weight-bearing makes the femur ideal to study adaptation of bone to its mechanical environment.

The femoral shape is detectable already at the end of the embryonic stages (9 weeks) (Suzuki et al., 2019) when the femur is only ~3mm long. At that stage, the femur has undergone the process of chondrification, which is the creation of cartilage, and endochondral ossification has begun. At the beginning of endochondral ossification, it is localised at the circumference at mid-femur (diaphysis), creating a circular structure of lamellae called the bone collar (Setiawati & Rahardjo, 2019). This process will signal to the

perichondrium to transition towards the periosteum, where osteoblasts will become present. The expansion of the mineralised collar results in a reduction of nutrients moving through the cartilage, which promotes apoptosis of the chondrocytes. The freshly mineralised tissue will allow the diffusion of blood vessels to sustain bone metabolism. The peripheral ossification and the presence of blood vessels at the centre allow for the formation of bone marrow (Rauch, 2005). The expansion of mineralized tissue and bone marrow from the diaphysis towards the epiphysis happens at the growth plates located between the junction of metaphysis and epiphysis (Rauch, 2005). It has been theorised that the growth plate aligns perpendicularly to predominant forces (Fabeck et al., 2002)

In addition to longitudinal growth, the femur also increases in width creating a more stable bone. Whilst bone strength in compression is predominately related to bone mineral content, the strength in bending and torsion is also determined by its distribution relative to the central axis (Ferretti, 1998). A practical example of bone drift occurs in individuals with rickets, who commonly have femoral bowing, which decreases following the correction of the condition triggering the disease (Rauch, 2005). The main bulk of bone diameter is gained during youth, therefore, that could be a potential time window where the mechano-adaptative capacity of the modelling phase could be used to develop a more robust skeleton. In defence of this are observations in older tennis players, where there is little evidence of periosteal growth in response to exercise in adulthood, particularly in epiphyseal regions (Ireland et al., 2014a). However, a modest amount of periosteal growth seems to continue throughout life (Riggs et al., 2004).

The femur also faces bone remodelling at the cortical and trabecular level. The type of bone that can withstand mechanical loads, including both cortical and trabecular bone in the metaphyses of the femur, is located near the yellow marrow and has a slow turnover rate

(Parfit, 2002). This type of bone is at risk of developing small cracks due to repetitive stress, known as fatigue microdamage, which must be eliminated. On the other hand, cancellous bone that regulates calcium levels and is located near red marrow has a faster turnover rate to prevent excessive mineralization (Parfit, 2003). A remodelling cycle of a single bone remodelling unit last for about 3-4 months and adds between 40 and 50 μm of bone (Rauch, 2006).

1.10 Femur shape and lower limb alignment

Evolutionarily speaking the shape of the hip and that of the femur is thought to have been shaped by the necessity of giving birth to a primate with a larger head than its hominid counterparts (Lovejoy, 2005b). However, it has to be noted that the hip and femur shape also has mechanical advantages in bipedality decreasing energy expenditure in walking and creating longer lever arms for the muscle to act on (Yavuzer, 2020). The gross shape of bones including the femur is mainly determined genetically, be it between species or among the same species. However, sizeable changes in femoral shape are evident throughout life, more predominantly during foetal life and throughout childhood with lesser changes during adulthood according to the metabolic activity of the bone (Ireland et al, 2014a). The shape of the femur is complex with multiple components of geometry, some of which vary substantially between individuals. The diaphysis of the femur can have lateral and frontal bowing. The diaphysis, especially the midshaft where bending stresses are predominant, is constituted by thick cortical bone. The proximal epiphysis is constituted by the femoral head, femoral neck, and greater trochanter. The femoral head articulates with the acetabulum of the pelvis to constitute the hip joint. The femoral neck creates an angle relative to the shaft in the frontal plane called the femoral neck angle and the mechanical-

anatomical angle is defined by the lines connecting: the femoral head centre to the intercondylar notch and the intercondylar notch to the center of the femur immediately distal to the lesser trochanter. The proximal epiphysis, where compressive and tensile stresses, due to the action of muscle and gravity, are paramount (Singleton & LeVeau, 1975), is constituted mainly by trabecular bone with little cortical bone except from the inferior portion of the femoral neck where thick cortical bone is evident (Figure 3) (Lovejoy, 1988; Aversa et al., 2016). The trabeculae play an important role in stress distribution and modulation of cartilage stress in joints (Lovejoy, 2005a). The distal epiphysis relates with the tibia to constitute the knee joint, through two round prominences called condyles. On the frontal plane also features of lower limb alignment become evident such as the femoro-tibial angle, which describes the relationship of the femur and the tibia by means of varus and valgus alignment, and the mechanical axis which is defined by two lines: one connecting the femoral head centre to the femoral intercondylar notch, and the other from the midpoint of the tibial intercondylar eminence to the midpoint of the distal tibial epiphysis. On the axial plane, one may observe the torsion of the femur, which can be defined as the angle of the femoral neck in relation to that of the knee indicated by the line between the posterior condyles. In the literature it is commonly referred to as femoral neck anteversion, entailing that the torsion is located proximally in respect to the distal femur. However, more recent literature suggests that torsion prevails throughout the whole femur resulting in Inter-trochanteric, shaft and condylar torsion (Seitlinger et al., 2016; Waisbrod et al., 2017; Archibald et al., 2019).

Although it seems intuitive that some components of geometry e.g. femoral torsion/femoral neck angle and the mechanical axis, are related there is little literature exploring this (Cho et al., 2018; Lu et al., 2019; Liu et al., 2021). As a result, the extent to

which they have shared development influences, and the independence of their contributions to clinical outcomes is currently unknown.

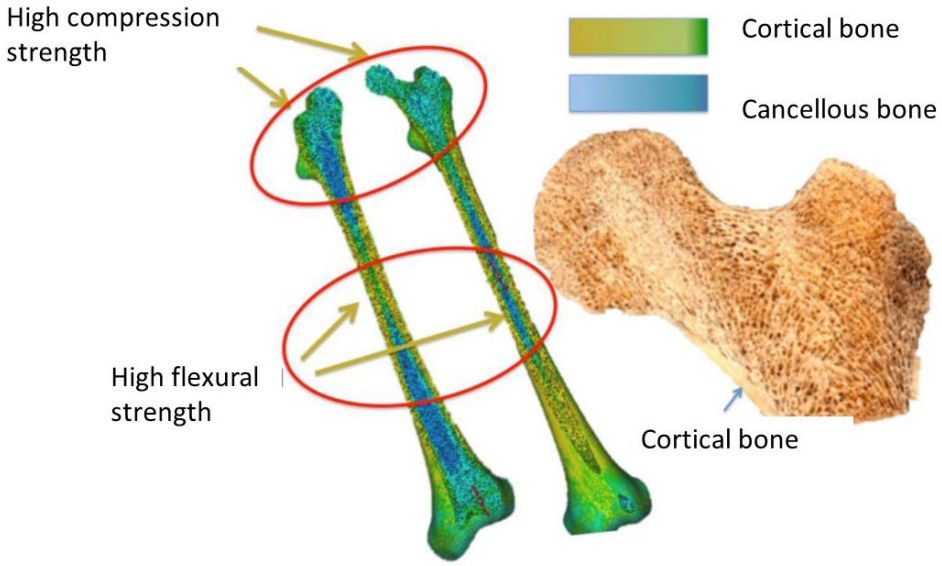

Figure 3 3D representation of trabecular and cortical bone distribution in the entire femur. On the right a longitudinal section of the proximal epiphysis showcasing the internal patterns of the trabecular bone. Adapted from Aversa et al (Aversa et al., 2016).

1.11 Hip joint shape

The human hip shape differentiates human from nonhuman primates and favours upright walking (Zirkle and Lovejoy, 2019). The hip joint, or femoro-acetabular joint, is a synovial ball and socket joint where the femoral head interacts with the concave acetabulum. The femoro-acetabular joint has a joint cavity, or socket covered with articular cartilage and a synovial membrane producing synovial fluid, the round shaped femoral head congruent to the socket and a ligamentous capsule originating on the hip and inserting on the proximal femur surrounding the femoro-acetabular joint (Byrd, 2005). The concave acetabulum is formed of three bone parts: the ilium, forming the superior wall of the acetabulum, and accounting for approximately 40% of the surface area, the ischium, forming the posterior wall, and also ~40% of the acetabulum and the pubis forming the anterior wall, and covering ~20% of the acetabulum (Moore et al., 2013). The characterisation of the acetabulum comprises acetabular inclination, which describes its position relative to the frontal or coronal plane, the acetabular version which describes the acetabulum's position relative to the horizontal or axial plane, and the acetabular coverage which represents the protrusion of the femoral head into the acetabulum.

1.12 Development of femoral shape

As previously stated, genetics is the predominate driver of the femur's gross shape and function. However, local changes can be observed at a structural and geometrical level according to the stresses applied to the femur. During foetal development, most skeletal elements, including the femur are present by week 8.5 (Bardeen and Lewis, 1901) and already have a similar shape to their adult form (Bardeen and Lewis, 1901; Charles R Bardeen, 1905). Primary ossification begins within the centre of the diaphysis, from their

cartilaginous stage after week 9 of gestation (Bardeen and Lewis, 1901; Bagnall et al., 1982) which coincide with independent movement from the foetus (De Vries and Fong, 2006). Further development of joints including the hip occurs throughout gestation (Ráliš and McKibbin, 1973). Skeletal and joint shape, similarly to skeletal strength parameters, undergoes a dramatic change from the 12th to the 40th week of gestation including an increase in femoral anteversion of 40°, an increase of femoral inclination of 7.5°(Walker and Goldsmith, 1981; Li et al., 2019) and a 5 and 3 fold increase in acetabular depth and inclination respectively (Watanabe, 1974). After birth, secondary ossification centres develop within the epiphysis leaving a horizontal cartilaginous layer between the primary and secondary ossification centres were longitudinal growth will occur (Ballock and O'Keefe, 2003; Nilsson et al., 2005) and a second cartilaginous layer surrounding the secondary ossification centre that is responsible for the growth of the most proximal femur (Parvaresh et al., 2018). The secondary ossification centre has been shown to have developed in animals conquering the terrestrial environment and developed as a protective structure for the underlying hypertrophic chondrocytes of the growth plate, from the high mechanical stresses met on land (Xie et al., 2020). Following the intense metabolic activity after birth until pre-pubertal development dramatic changes in lower limb geometry are observed, including a steady decrease in femoral torsion of ~1.5° a year and a decrease from varus lower limb alignment decreasing at birth (+15°±8) to a valgus alignment in healthy children (-5°±8) before the age of 7 (Holt et al., 1954). In the small body of current literature describing femoral shape changes during adulthood, only minor changes have been observed, including a decrease in femoral torsion between younger and older adults of ~3° (Inamdar et al., 2019; Pierrepont et al., 2019), and an increase with age

of lateral femoral bowing with age of ~2° in a large cross-sectional study (Matsumoto et al., 2015).

1.13 Development of acetabular shape

At the end of embryonic development which occurs during week 7-9 of gestation, the hip joint is present as a cartilaginous model and by the 11th week of gestation, the hip joint has developed its characteristic shape, consisting of a spherical femoral head, concave acetabulum, with synovium and an articular capsule. Clinical and experimental studies support the notion that the typical cup shaped acetabular growth is stimulated by the spherical shape of the femoral head during development (Smith et al., 1958; Harrison, 1961). Later, interstitial, endochondral, and appositional bone formation will determine the acetabular shape (Strayer Jr, 1971; Ponseti, 1978). After 8 years of age, similar to the femur, three secondary ossification centres, on the epiphysis of the ilium, of the ischium and the pubis will regulate the acetabular development through intramembranous ossification until they close at age 17-18 (Ponseti, 1978; Parvaresh et al., 2018). In a retrospective study on asymptomatic individuals aged 2 to 19 years, Monazzam et al (Monazzam et al., 2013) reported a significant increase in acetabular version and coverage with age until the age of 12. Acetabular depth is due to interstitial and appositional bone growth occurring in the metaphysis of the adjacent ilium and pubis, and endochondral ossification of the acetabular margin (Ponseti, 1978).

1.14 Pre-natal and post-natal bone adaptation to loading

During prenatal development, exponential growth of the foetus is observed, including the growth of the skeletal system. Intrauterine skeletal loading due to kicking produces

reaction forces on the uterine wall of up to 50 N which translates to a force 4 times the body weight of the foetus, acting directly onto the developing bone (Verbruggen et al., 2018a). Failure of production of foetal movements due to pharmacological or neuromuscular induced foetal akinesia results in thin and hypo-mineralised bones (Rodríguez et al., 1988; Miller and Hangartner, 1999) and dysplastic joints (Aronsson et al., 1994). Also, other events that reduce foetal movement including breech presentation and low level of amniotic fluid influence hip shape (Frysz et al., 2020) including higher femoral torsion in breech position (Hinderaker et al., 1994). Mechanical loading during early development is a driving factor of bone composition (Daly, 2007). Bone strength parameters continue to adapt to loading during childhood with evidence of greater femoral and spinal bone density in children involved in sports compared to inactive children (Grimston et al., 1993). Evidence suggests that high impact exercises, such as plyometric jumping over a period of 9 months may increase bone mineral density during puberty compared to an age and weight matched group not performing a jumping exercise (Witzke and Snow, 2000).

Although available information indicates that bone strength adaptations to loading are greater when loading is applied during development compared to when it is applied during skeletal maturity (Ireland et al., 2014a), bone mass and size adaptations to loading continue during adulthood (Riggs et al., 2004; Nikander et al., 2005; Rittweger et al., 2005; Lauretani et al., 2008; Wilks et al., 2009a). Bone cross-sectional area continues to increase by ~15% after skeletal maturity, informed by large cohort studies analysing individuals from 20 to 97 years of age (Riggs et al., 2004; Lauretani et al., 2008). Bone cross-sectional geometry of the tibia has been identified as larger in athletes rather than controls with greater effect in individuals competing in high-impact events (Nikander et al., 2005; Wilks et al., 2009a) and

bed rest and space flights studies have confirmed loading dependent bone loss in the mature bone (Rittweger et al., 2005; LeBlanc et al., 2007). Some of the cited studies are cross-sectional in nature (Riggs et al., 2004; Nikander et al., 2005; Wilks et al., 2009a), which could be confounded by secular changes in bone accrual due to differences in physical activity, environment, and nutrition. However, longitudinal studies, such as the inCHIANTI study (Lauretani et al., 2008) and others (Ireland et al., 2014a; Rittweger et al., 2005), provide more robust evidence of the notion of skeletal adaptations during adulthood.

Abnormal foetal position such as breach presentation or foetal akinesia could result in developmental deformations (Shea et al., 2015; Yang et al., 2020) including 10° higher femoral torsion (Hinderaker et al., 1994), hip dysplasia (Lambeek et al., 2013; D'Alessandro and Dow, 2019), and congenital bowing of the tibia and fibula (Cheema et al., 2003). Postnatally, mechanical loading assessed through early life motor development parameters, such as age for onset of walking has been evidenced as a lifelong determinant of hip and spine morphology (Daly, 2007; Ireland et al., 2019; Saunders et al., 2020). In individuals with normal skeletal development, a large overcorrection is observed from varus (+15°± 8) at birth, to valgus (-10°± 8) lower limb alignment which stabilises before the age of 7 at -5°±8 valgus alignment (Holt et al., 1954; Salenius and Vankka, 1975). Additional mechanical loading due to participation in sports requiring cutting movement determines a prevalence of increased varus leg alignment after the age of 13 (Yaniv et al., 2006). On the other hand, in children with decreased or abnormal loading due to impaired motor development including cerebral palsy, we can observer valgus knee alignment and intoeing gait (Staheli et al., 1968; Fabry et al., 1973b; Bobroff et al., 1999a; Ward et al., 2006).

Additionally, bone shape parameters, including femoral torsion, which undergoes a steady decrease of ~1.5° until physeal closure during puberty (Svenningsen et al., 1989; Tönnis and

Heinecke, 1991a; Fabry et al., 1994). Notably, femoral torsion does not decrease or remains greater compared to typical values in children with neuromuscular development disorders including cerebral palsy (Fabry et al., 1994; Bobroff et al., 1999a), Down syndrome (Shaw and Beals, 1992) and Charcot-Marie-Tooth disease (Novais et al., 2014). On the contrary femoral torsion has been found lower in an overweight adolescent cohort (Galbraith et al., 1987), suggesting mechanical loading as a determinant for the moulding of skeletal shape. Few studies have studied bone shape adaptation to different mechanical loading in the mature bone. Only modest differences have been observed in skeletal shape parameters, such as increased femoral bowing associated with prolonged squatting activities or decreased femoral bowing associated with heavy lifting tasks during long-term employment (Do et al., 2020).

1.15 Hip and lower limb shape: functional implications

The skeleton is the rigid framework of joints and levers arms upon which the muscle can act on to produce movement. It is therefore evident that changes in the shape of the framework, including the femur, the tibia and the acetabulum will have biomechanical implications. When changing the femoral anteversion angle, the greater trochanter will move posteriorly respective to the femoral head with increasing anteversion. The total femoral torsion therefore results in a change in the lever arms of the hip flexors, extensors, and abductors (Scheys et al., 2008; Kim et al., 2012; Li et al., 2014) i.e., a higher femoral torsion (between 21° and 51°) increases internal rotation moment arm length by 96.5% and decreases the external rotation moment arm length by 86%, compared to a general musculoskeletal model (Scheys, et al. 2008) subsequently affecting gait by favouring the movement with longer lever arms, likely increasing intoeing gait(Scheys et al., 2008;

Uemura et al., 2018). Consequently, whether the contribution to femoral torsion is from the distal femur or from the proximal femur will change the line of action of the muscles and characterise clinical groups (Kim et al., 2012; Seitlinger et al., 2016). Exaggerated femoral torsion also increases hip contact forces (Heller et al., 2001; Li et al., 2014) and low femoral torsion results in greater shear forces on the femoral neck (Pritchett and Perdue, 1988; Fishkin et al., 2006). In a recent investigation by Altai and colleagues (Altai et al., 2021) using musculoskeletal modelling and finite element models it was established that lower femoral neck inclination resulted in higher peak femoral neck strain. Although this finding is counterintuitive to previous literature reporting greater femoral neck fracture risk in osteoporotic women with greater femoral neck inclination angle (Gnudi et al., 2002) it is reasonable to suggest that the femoral necks with higher inclination adapted to a mechanical environment with lower strain resulting in weaker bones. Also, tibial torsion is associated with biomechanical implications such as foot progression angle changes during gait and knee contact pressure changes (Snow, 2021). Acetabular coverage has evidenced its role in femoro-acetabular mechanics, with higher acetabular coverage limiting range of motion (Audenaert et al., 2012; Hayashi et al., 2021).

1.16 Hip and lower limb shape: clinical implications

Alteration of lower limb bone geometry, including femoral and tibial torsion, femoral and tibial bowing and varus alignment is a risk factor for hip and knee osteoarthritis, (Fujishiro et al., 2014; Matsumoto et al., 2015; Shimosawa et al., 2018; Inamdar et al., 2019; Do et al., 2020), femoral and tibial fractures (Sasaki et al., 2012; Caouette et al., 2014; Chen et al., 2014; Shin et al., 2017), hip dysplasia and impingement Tönnis and Heinecke, 1991a; Fujii et al., 2010), and impaired tracking of the patella (Liebensteiner et al., 2016; Peter

Kaiser et al., 2017; Imhoff et al., 2019). Increased femoral torsion in the order of magnitude of ~6° may play a role in the aetiology of hip osteoarthritis (Fujishiro et al., 2014; Li et al., 2014; Inamdar et al., 2019), impaired tracking of the patella (Liebensteiner et al., 2016; Seitlinger et al., 2016; Peter Kaiser et al., 2017) and hip dysplasia (Alvik, 1962; Sugano et al., 1998b; Lerch et al., 2018). In contrast, decreased femoral torsion might contribute to slipped capital femoral epiphyses (Gelberman et al., 1986). Increased femoral or tibial bowing, in the order of magnitude of ~3-5°, has been found to be prevalent in individuals with knee osteoarthritis (Matsumoto et al., 2015; Shimosawa et al., 2018) and lower limb atypical fractures (Sasaki et al., 2012; Caouette et al., 2014; Chen et al., 2014; Shin et al., 2017). The inclination, version and depth of the hip acetabulum and its relationship with the femoral head and neck contribute to osteoarthritis, hip dysplasia and femoro acetabular hip impingement (Tönnis and Heinecke, 1999; Chadayammuri et al., 2016). In particular decreased acetabular version in the order of magnitude of ~2-6° and femoro-acetabular congruence have been shown to be relevant to hip osteoarthritis, dysplasia and impingement (Tönnis and Heinecke 1999, Fujii, Nakashima et al. 2010). Over half of adults aged over 55 years have radiographic evidence of osteoarthritis (D'Ambrosia, 2005), whilst hip impingement is prevalent in up to 75% of the population from a recent metanalysis. (Dickenson et al., 2016). In addition, multiple aspects of hip geometry have been associated with an increased fracture risk., including hip axis length and femoral neck angle which were both associated with a ~50% greater risk (Fajar et al., 2018). Therefore, it is clear that, perhaps unsurprisingly, femoral geometry is a key determinant of several burdensome skeletal problems, and therefore a substantial burden to healthcare services presented by these conditions. Whilst femoral geometry and joint alignment have been recognized as contributory factors in the development of osteoarthritis, the precise quantification of their

relative impact on this multifactorial degenerative disease is challenging, given the diverse array of factors that are known to play important roles in its onset and progression. These factors include advanced age, which increases the risk of osteoarthritis by 18-19 times (Vrezas et al., 2010; Cameron et al., 2011), obesity, associated with a 50%-90% higher risk of osteoarthritis (Wills et al., 2012; Lee et al., 2013; Reyes et al., 2015), metabolic syndrome, which elevates the risk by 32% (Mohajer et al., 2021), socioeconomic status accounting for up to 23% of osteoarthritis incidence after adjusting for obesity (Reyes et al., 2015), as well as occupation, nutrition, and other factors (Allen et al., 2022). The complex interplay of these factors underscores the multifaceted nature of osteoarthritis as a clinical condition.

1.17 Characterisation of lower limb joint shape in clinical populations

In addition to the substantial variation evident within the general population, differences in femoral geometry have been identified in a number of clinical populations. In particular, those where either bone metabolism is affected or those where mechanical loading differs as a result of body size, neuromuscular function or physical activity.

Among those where bone metabolism is affected, like X-linked hypophosphatemia (XLH), the literature focuses on clinical outcomes such as osteoarthritis, waddling gate entheses and varus alignment (Capelli et al., 2015; Skrinar et al., 2019). In individuals with osteogenesis imperfecta the focus lies on fractures and “lower limb deformities” with no comprehensive characterisation of lower limb geometry components (Rauch and Glorieux, 2004; Forlino et al., 2011; Marr et al., 2017), and a similar approach is used in the literature studying achondroplasia (Wright and Irving, 2012; Park et al., 2015).

Broader, non-bone diseases such as cerebral palsy often analyse single or few separate components of lower limb geometry i.e. femoral and tibial torsion (Fabry et al., 1973b;

Davids et al., 2002; Chung et al., 2010), coxa valga deformity (Carriero et al., 2011) and clinical implications such as intoeing or waddling gate (Fabry et al., 1973b; Shefelbine and Carter, 2004). Commonly across all clinical investigations only a single or few components of joint shape are examined, and little comprehensive characterisation of lower limb geometry, even in the healthy population, has been done. Additionally, to our knowledge few studies have explored to what extent lower limb geometry components are inter-related (Gose et al., 2010).

1.18 Summary

Femoral geometry varies substantially between individuals, and is also associated with clinical conditions. However, there is currently limited comprehensive characterisation of lower limb geometry, and most studies only examine a single or few components of lower limbs bone and joint shape. Additionally, there is little understanding of the inter-relationship between different components of lower limb geometry.

In particular, femoral neck anteversion shows substantial inter-individual variability, with typical values between 7° to 24° observed in healthy individuals (Starker et al., 1998; Sugano et al., 1998a; Kuo et al., 2003; Toogood et al., 2009; Botser et al., 2012; Sutter et al., 2015; Lerch et al., 2018). It also appears highly modifiable in response to early life loading. Given this, its relevance for lower limb mechanics and its potential impact on various clinical outcomes, there is a clear need for further research addressing knowledge gaps relating to it determinants and functional consequences in addition to that of other aspects of limb geometry. Therefore, this study had the following aims:

- To identify the most appropriate assessment techniques for femoral neck anteversion via literature review, as detailed in Chapter 2.

- Having identified limitations of current femoral neck anteversion assessment techniques, to develop a new ultrasound-based technique as detailed in Chapter 3.

- To evaluate the inter-relationships between different components of lower limb bone and joint geometry, and the utility of more comprehensive assessments of geometry in a clinical context. These assessments were performed in individuals with X-linked hypophosphatemia (XLH), a rare bone condition associated with substantial skeletal deformity, as well as controls as described in Chapter 4.

- To address gaps in knowledge around the effect of long-term power discipline participation on whole lower limb geometry, including femoral neck anteversion, and the consequences of bone shape on compound movements such as squat jumps and single leg hopping as described in Chapter 5.

Chapter 2 Femoral anteversion: significance and measurement

2.1 Abstract

Background

Femoral neck anteversion (FNA) is the angle between the femoral neck and femoral shaft, indicating the degree of torsion of the femur. Differences in FNA affect the biomechanics of the hip, through alterations in factors such as moment arm lengths and joint loading. Altered gait associated with differences in FNA may also contribute to the development of a wide range of skeletal disorders including osteoarthritis.

Aim

The aim of this narrative review was to describe the biomechanical and clinical consequences of FNA, factors influencing FNA, and the strengths and weaknesses of different methods used to assess FNA.

Methods

A literature search was conducted on PubMed searching for the key words “Femoral neck anteversion” OR “Femoral torsion.” 155 articles were selected based on their relevance to address the aim for this narrative review.

Results

FNA varies by up to 30° within apparently healthy adults. FNA increases substantially during gestation and thereafter decreases steadily until maturity. There is some evidence of a further decrease at a much lower rate during adulthood into old age, but the mechanisms behind it have never been studied. Development of FNA appears to be strongly influenced by mechanical forces experienced during everyday movements. This is evidenced by large differences in FNA in groups where movement is impaired, such as children born breech or

individuals with neuromuscular conditions such as cerebral palsy. Several methods can be used to assess FNA, which may yield different values by up to 20° in the same participant. Whilst MRI and CT are used clinically, limitations such as their cost, scanning time and exposure to ionising radiation limit their applicability in longitudinal and population studies, particularly in children. More broadly applicable measures such as ultrasound and functional tests exist, but they are limited by poor reliability and validity. These issues highlight the need for a valid and reliable universally accepted method. Treatment for clinically problematic FNA is usually de-rotational osteotomy while passive, non-operative methods do not have any effect. Despite observational evidence for the effects of physical activity on FNA development, the efficacy of targeted physical activity remains unexplored.

Conclusions

FNA affects lower limb kinematics and is a risk factor for skeletal disorders. Derotational osteotomy is currently the only effective treatment available to correct altered FNA. Future studies should explore the potential for early life relevant forces and shaping FNA throughout the lifespan. Free hand ultrasound may replace MRI and CT for FNA imaging. Standardization of measuring techniques can aid comparison of FNA measurements.

2.2 Overview

Femoral neck anteversion (FNA), also called femoral torsion or femoral version, is the angle between the projection of two lines in the axial plane perpendicular to the femoral shaft; one line going through the proximal femoral neck region and the second one through the distal condylar region (Figure 4), indicating the degree of 'twist' of the femur.

FNA affects the biomechanics of the hip, as moment arms and the line of action of muscles

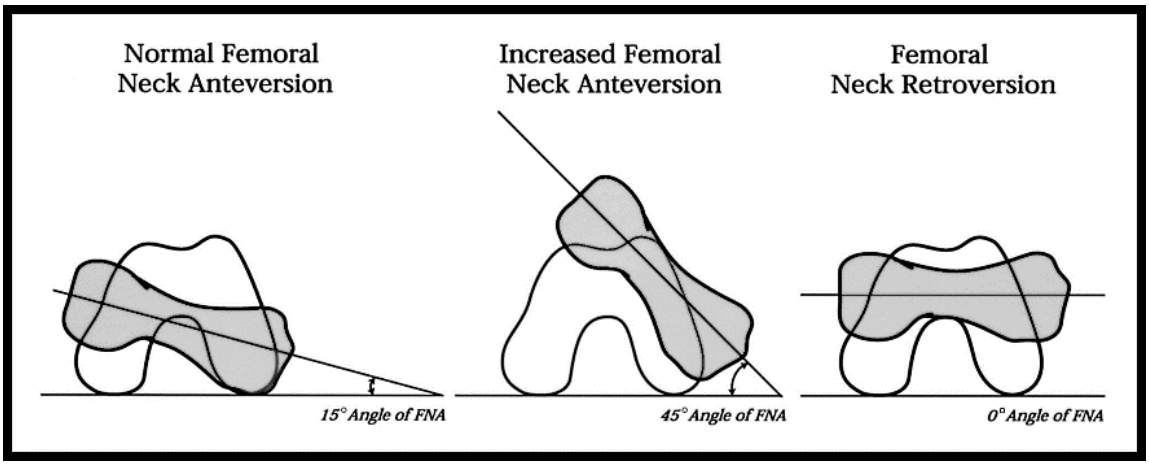

Figure 4 Axial schematic representation of the right femur and of the femoral neck anteversion (FNA). The grey area represents the femoral neck, the white area represents the distal condylar region. From (Cibulka, 2004).

around the joint are altered (Scheys et al., 2008; Kim et al.,2012). As a result, FNA is associated with differences in gait (Laplaza & Root, 1994, Uemura et al. 2018), and is a risk factor for clinical problems including osteoarthritis (McSweeny, 1971; Reikerås and Høiseth,1982; Li et al., 2014; Fujishiro et al., 2014; Inamdar et al., 2019) and slipped capital femoral epiphysis (Gelberman, 1986). FNA goes through substantial development during growth with a change from 0° in early gestation to 30° at birth (Watanabe, 1974; Walker and Goldsmith, 1981; Jouve et al., 2005; Li et al., 2019), decreasing to 15° in adulthood Fabry et al., 1973; Svenningsen et al., 1989; Tönnis and Heinecke, 1991). In addition to age, FNA appears to be strongly affected by mechanical loading during movement, such that

several clinical conditions associated with delayed or impaired locomotion are associated with greater FNA (Fabry et al., 1973; Bobroff et al., 1999).

There are several methods to assess FNA, including imaging using radiography, fluoroscopy, computed tomography (CT), ultrasound (US), and magnetic resonance imaging (MRI) as well as functional assessments. Even within each imaging method, there are variations in how anatomical landmarks are identified (Kaiser et al. 2016). Differences in cost, time, availability, repeatability, and radiation exposure mean that certain methods are not applicable *e.g.,* for clinical studies or those involving children.

The aim of this review is to discuss the implications of altered FNA, both in terms of its effects on movement and clinical consequences. In addition, to describe normal variation and factors affecting FNA in healthy and clinical populations of different ages. Finally, outline the different methods and landmarks used to assess FNA and evaluate their strengths and weaknesses with regard to a defined study setting.

2.3 Biomechanical significance of FNA

A change in FNA affects the position of the trochanter and therefore the line of action of the muscles surrounding that region. Regional torsional changes along the femur also result in a change of lever arms (Kim et al., 2012). A higher FNA results in a slightly shorter hip extension moment arm and an increase in hip flexion moment arm of the abductor muscles. Furthermore, high FNA results in a shorter abductor lever arm (Scheys et al., 2008; Li et al., 2014), and also considerably increases internal rotation moment length by an average of 96.5% for all hip muscles (Figure 5), apart from the iliopsoas, which was not evaluated, and the gluteus maximus anterior which decreases internal rotation moment arm length by 86% (Scheys et al., 2008).

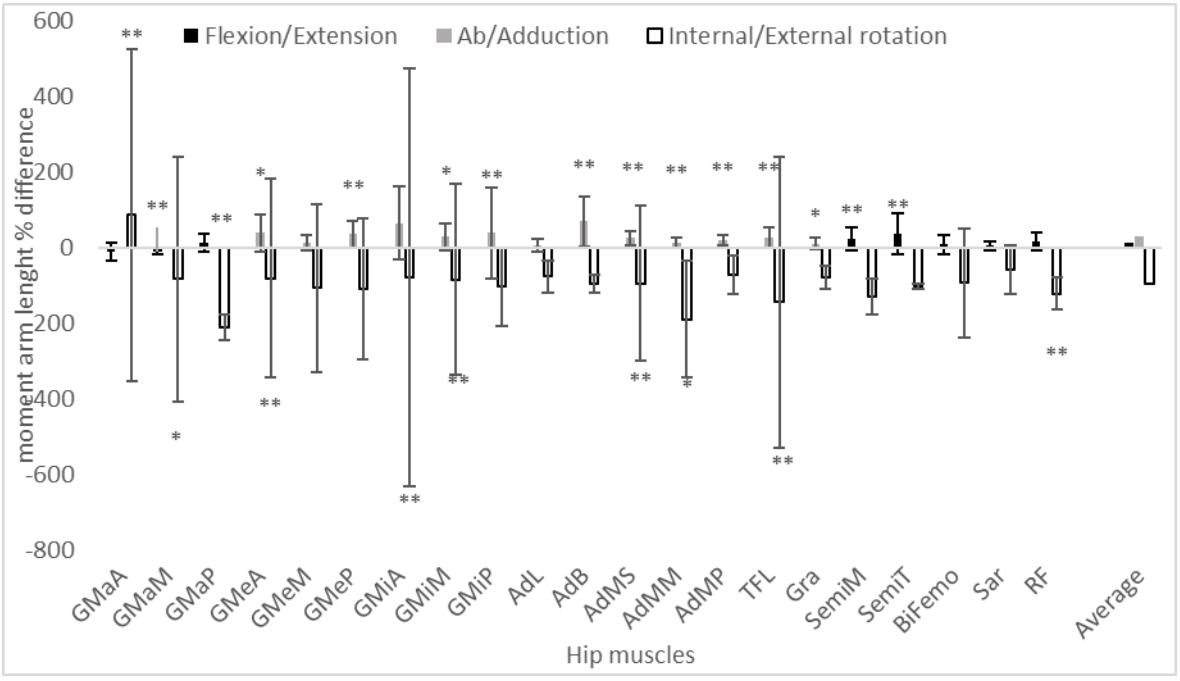

Figure 5 Effects of altered femoral neck anteversion (FNA) on reference moment arm length (MAL), calculated as the difference between subject specific models and a general model. The subject specific model is taken as the reference, therefore negative values indicate a higher value in subject specific models and vice versa. The subject specific model is an average of subjects with a high FNA (ranging from 25 to 51). The moment arm length is averaged over the whole range of motion (10° extension 90° flexion,50° abduction 20° adduction, 40° external and 40° internal rotation). Only the main function is recorded for every muscle and the internal/external rotation. Conventionally positive values are used for flexion abduction and internal rotation. Figure created using data from Scheys et al (Scheys et al., 2008). Abbreviations: GMaA Gluteus maximus anterior, GMaM Gluteus maximus medialis, GMaP Gluteus maximus posterior, GMeA Gluteus medius anterior, GMeM Gluteus medius medialis, GMeP Gluteus medius posterior, GMiA Gluteus minimus anterior, GMiM Gluteus minimus posterior, AdL Adductor longus, AdB Adductor brevis, AdMS Adductor magnus superior, AdMM Adductor magnus middle, AdMP Adductor magnus inferior, TFL tensor fascia latae, Gra gracilis, SemiM Semimembranosus, SemiT Semitendinosus, BiFem Biceps femoris long head, Sar Sartorius, RF Rectus femoris. Significance is shown with *p<0.05 and **p<0.01.

A higher FNA also affects muscle activation, as lower gluteus medius and vastus medialis activity has been recorded during isometric hip abduction (Nyland et al., 2004) probably due to the change in moment arm length. The higher FNA, and therefore the shorter abductor lever arm, also changes the mechanics of the hip joint resulting in up to 24% higher hip contact forces during gait with an anteversion of 30° or 8% higher forces with FNA of 14°, when compared to an anteversion of -2° (Heller et al., 2001; H. Li et al., 2014). On the other hand, reduced FNA results in higher shear forces on the femoral neck-head

junction (Pritchett and Perdue, 1988), quantifiable as a 42% increase with an FNA of 0° and 86% with an FNA of -12.5° compared to an FNA of 12.5° (Fishkin et al., 2006).

2.4 Consequences of altered FNA for Health

Altered movement associated with differences in FNA also appears to have consequences for musculoskeletal health. The shorter hip extension moment arm and longer moment arm for hip flexion shown with increased FNA is consistent with the gait pattern in individuals with cerebral palsy and shorter abductor and adductor lever arm is likely to produce pelvic instability during gait (Laplaza and Root, 1994; Scheys et al., 2008). The increased internal rotation moment arm length, combined with a decreased external rotation moment arm length, is likely to be part of the cause of in-toeing gait in children with cerebral palsy (Gelberman et al., 1987; Fabry et al., 1994; Scheys et al., 2008; Uemura et al., 2018) as a strategy to increase the abductor lever arm during movement (Arnold et al., 1997; Uemura et al., 2018). Self-adjustment of in-toeing gait is often accompanied by the compensatory external rotation of the tibia (Fabry et al., 1973b). Greater FNA is also associated with an increased risk of anterior cruciate ligament injury (Nyland et al., 2004; Shultz et al., 2008; Amraee et al., 2017), which might relate to altered knee kinematics during landing (Howard et al., 2011), lower hip abductor and vastus medialis activity (Nyland et al., 2004), and impaired tracking of the patella (Reikerås, 1992; Lee et al., 1994; Kaiser et al., 2017; Imhoff et al., 2019). Greater hip load and the altered relationship with the acetabulum - resulting from increased FNA (Reikerås et al., 1983b) - may play a role in the genesis of osteoarthritis (McSweeny, 1971; Reikerås and Høiseth, 1982; Fujishiro et al., 2014; Li et al., 2014; Inamdar et al., 2019). This suggestion is reinforced by a prevalence of unilateral osteoarthritis in limbs with higher FNA (Halpern et al., 1979; Piazzolla et al., 2018). The decreased congruity could also result in hip dysplasia, a condition that displays

FNA averages of 6° to 18° above normal (Alvik, 1962; Fabry et al., 1973b; Anda et al., 1991; Sugano et al., 1998b; Li et al., 2014; Lerch et al., 2018), whilst hip congruity (Reikerås et al., 1983b) and loading (Heller et al., 2001; Satpathy et al., 2015) might be a contributor to femoral acetabular impingement (Sutter et al., 2015; Chadayammuri et al., 2016; Gómez-Hoyos et al., 2016; Lerch et al., 2018). On the other hand, the aforementioned increased shear forces occurring with reduced FNA could explain the association of slipped capital femoral epiphysis with populations which have low FNA (R. H. Gelberman et al., 1986). Not only is increased or decreased FNA a risk factor for clinical conditions, but asymmetries in FNA also appear to influence musculoskeletal health, as shown by Piazzolla (Piazzolla et al., 2018). In this study, participants with unilateral osteoarthritis of the hip with higher anteversion reported lower back pain whereas unilateral osteoarthritic participants with symmetrical FNA did not. FNA has been shown to affect the accuracy of clinically-relevant bone mineral density measures (Cheng et al., 1997). However, little is known about whether FNA and altered biomechanics could also affect bone mineral density, other bone strength indicators or the risk of femoral fractures either through these factors or altered fall mechanics.

2.4 Epidemiology

Normative data for FNA in the healthy adult population is highly dependent on the landmarks identified and imaging technique used (P. Kaiser et al., 2016a), with mean values in the range of 7° to 24° (Starker et al., 1998; Sugano et al., 1998a; Kuo et al., 2003; Toogood et al., 2009; Botser et al., 2012; Sutter et al., 2015; Lerch et al., 2018). In addition, there is substantial variation within the population, with individual values ranging by more than 30°, independent of the method used (Yoshioka et al., 1987a; Waidelich et al., 1992;

Toogood et al., 2009; Rosskopf et al., 2014; Sangeux et al., 2014). FNA is at least partly hereditary, with a polygenetic influence on this and other features of proximal femur shape (Hogervorst et al., 2012). However, another key factor is the influence of mechanical loading during everyday movements and exercise. Both the greater trochanter and the epiphyseal growth plate (Figure 6) are accountable for shaping the proximal femur (Fabeck et al., 2002).

Bone growth has been shown to be directed perpendicularly to the direction of the growth

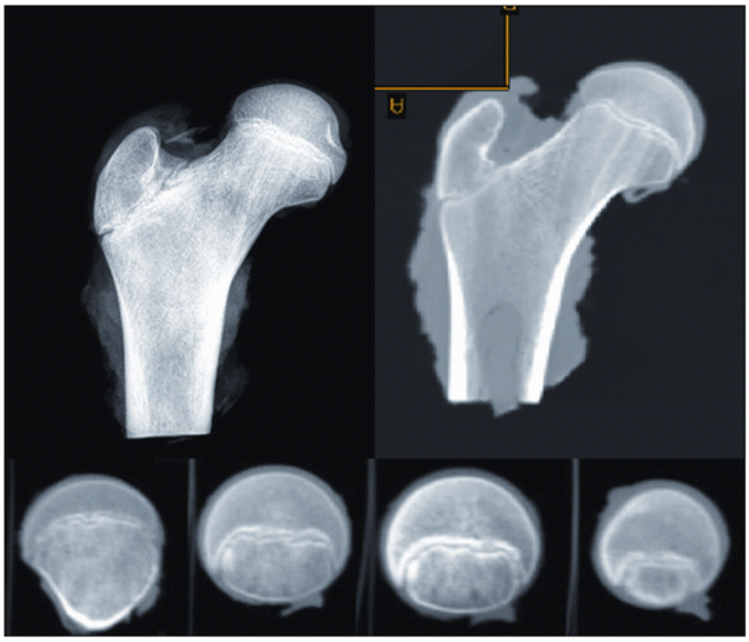

Figure 6 Epiphyseal growth plate: Radiography and computer tomography (CT) of cadaveric proximal femur of 13-year-old individual. Coronal view on top panels, axial view in bottom panel. Slices through the femoral head in the bottom panels go from distal to proximal (Kandzierski et al., 2012).

plate (Dallek and Jungbluth, 1984; Hunziker, 1994), which is orientated in line with the forces acting on it (Pauwels and Maquet, 1979; Carter et al., 1987; Fabeck et al., 2002). The growth rate of growth plate cartilage is influenced by mechanical loading, such that increased compressive and tensile loading increases growth rate up to a point, with additional loading leading to reduced growth rate and potential damage (Rauch, 2005).

This effect of mechanical loading likely contributes to the dramatic changes in FNA observed throughout prenatal development and childhood. An increase of around 30° in FNA during foetal life has been observed (Figure 7) (Watanabe, 1974; Walker and Goldsmith, 1981; Jouve et al., 2005; Li et al., 2019), particularly during the second trimester.

In the womb, the hip has a high angle of flexion, and the femur is levered against the

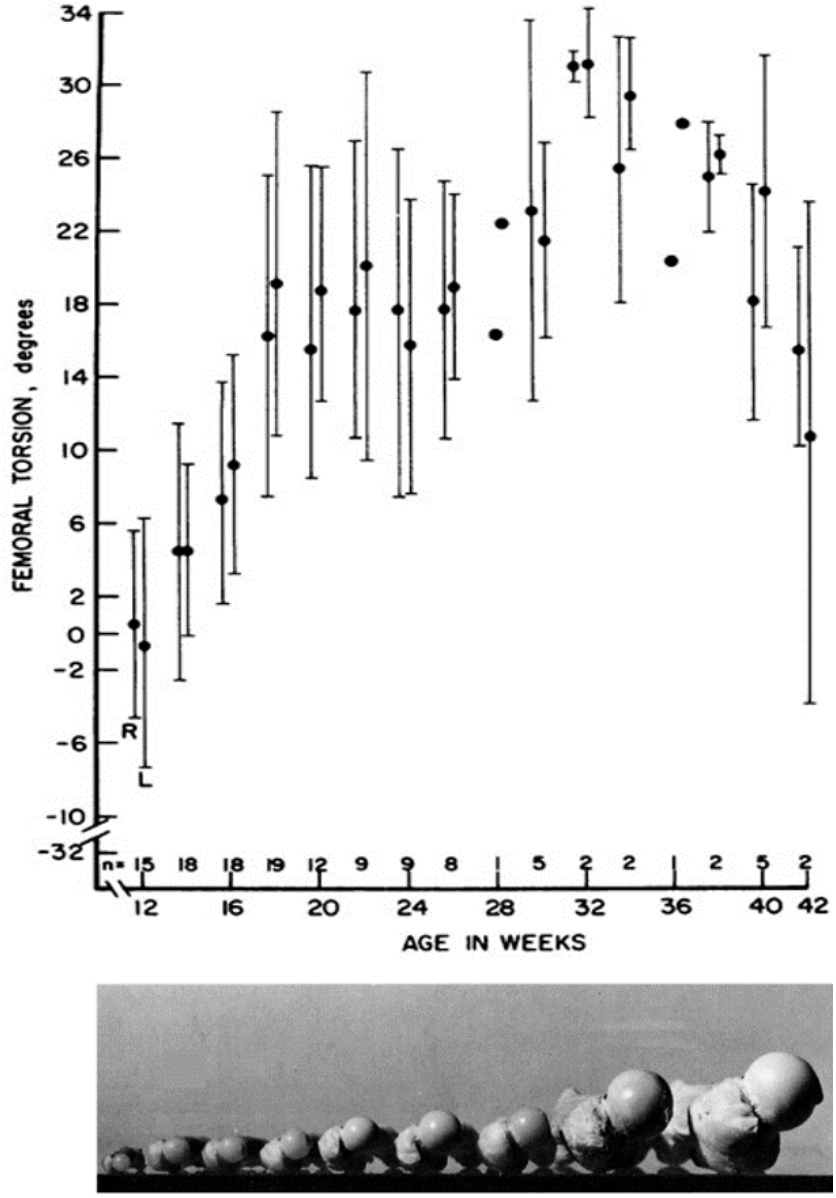

Figure 7 Femoral neck anteversion (FNA) means and standard deviation of foetuses at different stages of gestation. Bottom panel shows photos of typical foetal femur samples at different developmental stages (12 weeks to term). Figures adapted from Walker and Goldsmith (Walker and Goldsmith, 1981).

antero-superior iliac spine, thereby increasing the torsional strain favouring anteversion

(Hogervorst et al., 2012). The internally rotated position of the hip joint during foetal life could also result in increased anteversion, and the opposite is true for external rotation (Watanabe, 1974). This theory is supported by animal studies with forced internal rotation (Wilkinson, 1962) and confirmed by the 10° higher FNA found in children born with breech presentation (Hinderaker et al., 1994); these children often have an internally rotated position in the womb resulting in reduced kicking forces and lower femoral stress and strain during foetal movements (Verbruggen et al., 2018b).

During childhood, a steady ~1.5° a year decrease in anteversion until completion of growth has been recorded (Figure 8) (Fabry et al., 1973b; Svenningsen et al., 1989; Tönnis and Heinecke, 1991a). This decrease during growth might depend on the action of hip muscles during gait, which may shape the FNA (Yadav et al., 2017) and keep the resultant forces during the maximal weight bearing period perpendicular to the growth plate (Fabeck et al., 2002). There is some evidence from large cohort cross-sectional studies to suggest that FNA also decreases, at a lower rate, during adulthood (Waisbrod et al, 2017; Pierrepont et al., 2019). This raises the question of whether 50-70 years ago children were more active, and whether secular rather than within-individual changes are being observed. Furthermore, a recent longitudinal study in individuals with hip osteoarthritis suggests that FNA decreases with time over a period of three years (Inamdar et al., 2019). This might be due to either localized addition of bone on the periosteal surface with increasing age, microfractures, or by the bony erosion due to the osteoarthritic condition. Most studies show a higher FNA in the female population with sex differences ranging from 2° to 8° (Fabry et al., 1973b; Cyvín, 1977; Bråten et al., 1992; Tamari et al., 2006; Decker et al., 2013; Fujishiro et al., 2014;

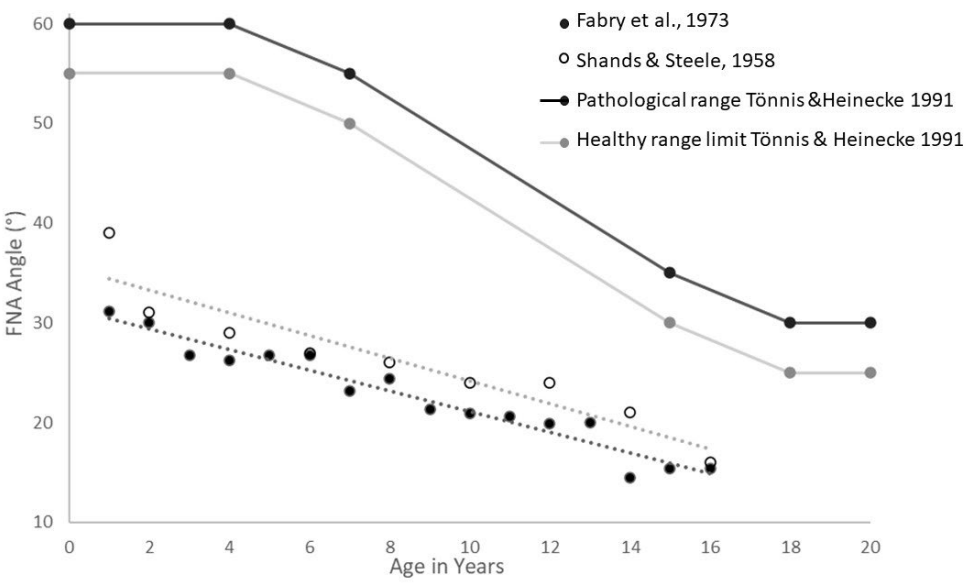

Figure 8 Mean values of femoral neck anteversion (FNA) in children of different ages as measured by different investigators (Shands Jr and Steele, 1958; Fabry et al., 1973a). The light grey continuous line indicates the limit of the healthy range of variation, the continuous black line denotes the limit of the pathological range (Tönnis and Heinecke, 1991b).

Sutter et al., 2015; Chadayammuri et al., 2016; Lerch et al., 2018).

It is known that growth plate fusion occurs at an earlier age in women than men (Grumbach, 1992), therefore a shorter growth period could be a cause of the higher FNA in women. Whilst FNA values reported in individuals from different ethnic groups have differed substantially, this may relate to the use of different measurement methods. More recent CT studies have found no differences in FNA based on ethnicity (Koerner et al., 2013). The importance of mechanical loading for FNA during development is also evident from altered values in children with compromised motor development and movement. Notably, children with CP do not show a decrease in FNA during development (Figure 9) (Fabry et al., 1973b; Bobroff et al., 1999a).

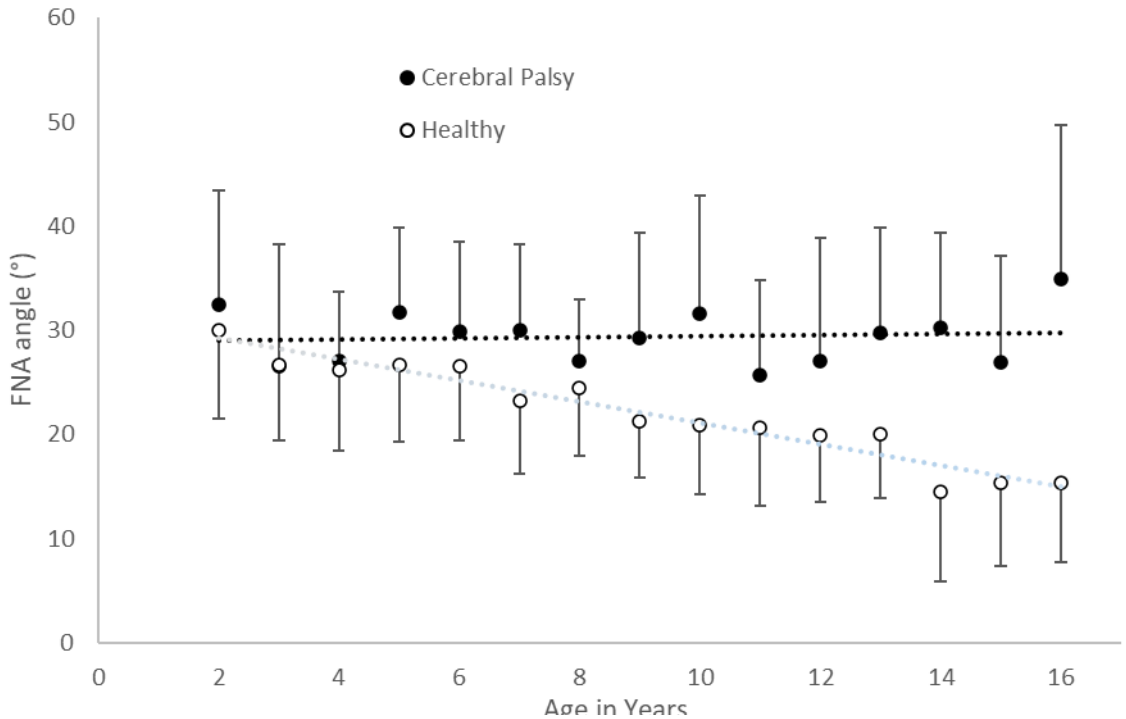

Figure 9 Femoral neck anteversion (FNA) in children with cerebral palsy (CP) and typically developing controls during growth, presented as mean and standard deviation. Adapted from Bobroff et al., 1999 (Bobroff et al., 1999b).

Typically, FNA is around 10° higher in older children with CP than unaffected children, with similar differences evident between the affected and unaffected limbs in children with hemiparetic CP (Staheli et al., 1968). This is thought to be caused by spasticity or decreased activation of certain muscle groups, which is frequent in the clinical spectrum of CP Individuals. In particular, it was suggested that increased activity of adductor and extensor muscles predicts higher FNA, as does reduced activity of hip flexors (Yadav et al., 2017). This was confirmed in animal studies resecting either internal or external rotator muscles (Haike, 1964). Interestingly, ambulant children with CP have higher FNA than non-walking children with CP (Bobroff et al., 1999a). This suggests that the alterations in muscle activity and subsequent joint loading during gait in children with CP contribute to development of FNA. This suggests that healthy motor development is an important factor in development of the proximal part of the femur (Yadav et al., 2017). This is supported by reports suggesting that differences in FNA between children with CP and normally-developing

children emerge at around 12 months, or the typical age of independent walking onset (Beals, 1969; Fabry et al., 1973; Tönnis &Heinecke, 1991; Bobroff et al., 1999a).

FNA has also been reported to differ from typical values in children with other conditions affecting neuromuscular development, such as Down syndrome, with an average of 33° (Shaw and Beals, 1992) and Charcot-Marie-Tooth disease where the mean FNA is 28° (Novais et al., 2014). In addition, higher values are observed in children with a range of disorders affecting skeletal development. For example, Blount's disease causing bowing of the tibia (Aird et al., 2009), Legg-Calvé-Perthes disease resulting in avascular necrosis of the femoral head (Lerch et al., 2018) and achondroplasia (Song et al., 2006), which results in substantially reduced limb length. On the other hand, obesity in adolescence is associated with an FNA of only 0.4° ± 13° (Galbraith et al., 1987). This could be due to the increased muscular forces required to move a greater body mass during development.

2.5 Treatment

In the case of idiopathic altered anteversion in early childhood, this usually corrects itself without intervention (Fabry et al., 1973b; Svenningsen et al., 1989; Staheli, 1993). In cases where increased FNA does not correct itself and results in in-toeing and tripping, the most effective method to change FNA is femoral de-rotational osteotomy. It can be performed either at a distal supracondylar level (Hoffer et al., 1981) or at a proximal sub-trochanteric or intertrochanteric level (Payne and DeLuca, 1994). The contribution of these different regions to total anteversion differs between clinical groups (Kim et al., 2012; Seitlinger et al., 2016). Therefore, it has been suggested that the planning of osteotomies should take into account this segmental variation in order to ensure healthy post-operative hip biomechanics and prevent further clinical problems (Kim et al., 2012; Ferlic et al., 2018). It

has been shown to be a successful technique in the treatment of in-toeing children with cerebral palsy (Saglam et al., 2016; Sung et al., 2018) and patellar instability (Imhoff et al., 2019). However, it must be taken into account that complications might arise and the whole recovery process could be a traumatic experience (Staheli, 1993). Therefore, surgery is suggested only in disabling or symptomatic instances, only after the age of 10 and, depending on the condition, in cases of a measured anteversion from above 20° (Nelitz et al., 2015; Weber et al., 2016; Nelitz, 2018) and internal rotation higher than 80° (Staheli, 1993; Leonardi et al., 2014). Non-operative methods to lower FNA such as shoe wedges, twister cables and night splints have been proposed, but do not appear to be effective (Fabry et al., 1973b; Knittel and Staheli, 1976). The effects of movement and motor development on FNA described earlier suggest that physical therapies and targeted exercises may alter FNA during growth, but, to our knowledge, this remains unexplored.

2.6 Femoral axes

There is evidence that femoral torsion occurs throughout the femoral shaft, below the lesser trochanter, and at the intertrochanteric level (Seitlinger et al., 2016; Waisbrod et al., 2017; Archibald et al., 2019). As well as variation in clinical cases identified above, substantial variation in torsion within each of these regions has been identified in non-clinical populations (Seitlinger et al., 2016; Ferlic et al., 2018). FNA is considered the "total" femoral torsion. The definition of FNA and the chosen femoral axes determine the measurement. The femoral axes are defined as follows: the neck shaft axis, the femoral shaft axis, and the condylar axis. The shape of the proximal part of the femur is complex, as the lateral part of the femoral neck is elliptical and its major axis tilts anteriorly (Backman, 1957), and the femoral head is not usually centred on the femoral shaft (Kingsley

and Olmsted, 1948). The femoral neck axis can be defined as the line connecting the femoral head centre to the femoral shaft axis (Murphy et al., 1987; Waidelich et al., 1992), the line going through the centre of the femoral head to the narrowest part of the neck (Yoshioka et al., 1987a; Kim et al., 2000), the centre of the femoral neck (Reikerås et al., 1983b), the centre of the greater trochanter (Batailler et al., 2018) or the edge of the greater trochanter (Sangeux et al., 2015), the latter being referred to as a functional axis as it takes into account the contact point of the hip and the insertion of the adductor muscles. The femoral neck axis could also be defined as the line parallel to the femoral neck (Weiner et al., 1978; Wedge et al., 1989), without taking into account the trochanter or the femoral head (Figure 10).

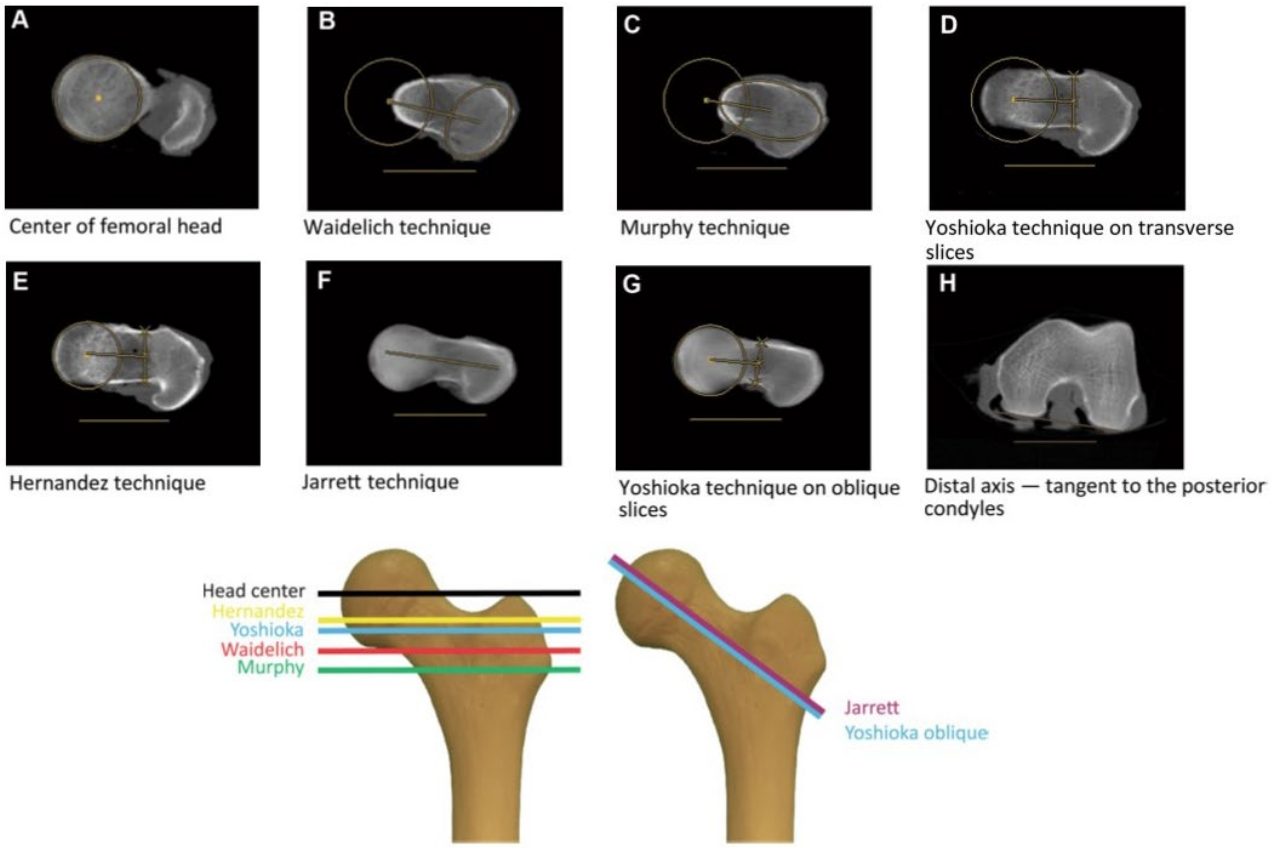

Figure 10 **Top**: Examples of different methods of femoral neck anteversion (FNA) assessment and how they affect the assessed geometry: A, B, C, D, E are transverse slice methods (Hernandez et al., 1981; Murphy et al., 1987; Yoshioka and Cooke, 1987; Yoshioka et al., 1987b;Waidelich, and Schneider, 1992; Jarrett et al., 2010), and F and G use oblique slices (Yoshioka and Cooke, 1987; Jarrett et al., 2010). The location of the slices in the coronal plan is shown in the lower panel. H shows that the posterior condylar line was taken as reference for all methods.Figure from (P. Kaiser et al., 2016b).

These reconstructions are available in single cross sections of the femoral neck or on two different slices, further increasing differences even with similar definitions. For 3D models the femoral neck axis may either be determined using a line of best fit of the centroids of the slices defining the neck by hand (Sugano et al., 1998a) or by using principal component analysis on a point cloud covering the femoral neck determined semi-automatically (Berryman et al., 2014). The anatomical femoral shaft axis is difficult to define accurately, due to the anterior curvature of the shaft. Its distal point can be found either at the anterolateral border of the posterior cruciate ligament (Yoshioka et al., 1987a), at the centre of the medial and lateral articular margins (Walmsley, 1933), the midpoint of the centroids of each condyle (Berryman et al., 2014), the centre of the segment joining the

two midpoints of the line connecting the anterior and posterior points of each condyle (Egund and Palmer, 1984), the centroid of an axial cross section of the femoral condyle (Murphy et al., 1987) or the most proximal aspect of the intercondylar fossa (Sangeux et al., 2015). The proximal point of the femoral axis has been defined using the centroid of the slice taken between the lesser trochanter and the greater trochanter (Murphy et al., 1987; Buddenbrock et al., 1997; Berryman et al., 2014), under the lesser trochanter (Egund and Palmer, 1984; Sangeux et al., 2015), or the head centre if the functional weight bearing axis is used as the rotational axis (Yoshioka et al., 1987a). The femoral shaft axis in most cases is used either as the rotation axis of the femur (Yoshioka et al., 1987a; Kim et al., 2000), as a fixed point to determine the neck axis (Murphy et al., 1987; Buddenbrock et al., 1997) or as a reference for femoral rotation (Egund and Palmer, 1984). In 3D models it is possible to establish the anatomical femoral axis via the interpolation of the centroids of multiple slices taken along the femoral shaft (Eckhoff et al., 2016).

The distal axis (Figure 11) has been defined in various ways: as the posterior edge of the lateral and the medial condyle (posterior condylar line) (Kingsley and Olmsted, 1948; Egund and Palmer, 1984; Murphy et al., 1987; Berryman et al., 2014; Sangeux et al., 2015; Eckhoff et al., 2016), the midline between the anterior condylar line and the posterior condylar line (Ruby et al., 1979; Hernandez et al., 1981), or as a line connecting the peak of the epicondyles on a transverse view (epicondylar line) (Weiner et al., 1978; Yoshioka et al., 1987a).

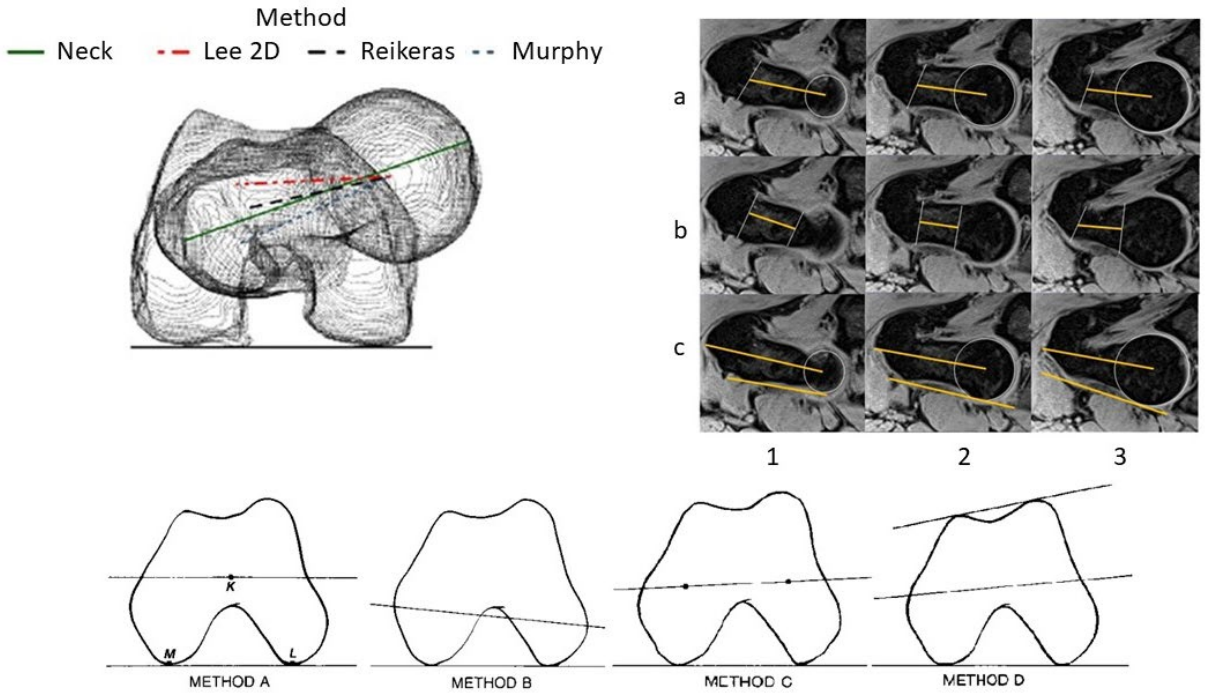

Figure 11 Different methods used to define the distal femoral axis Method A (posterior condylar line) classical table top method, with posterior condyles lying on the table. Method B (epicondylar line) most medial and lateral extremes of the condyles on the axial view (Weiner et al., 1978). Method C identifies the centroids of the medial and lateral condyles. Method D bisects the angle formed by the posterior and anterior condylar lines. Figure from Murphy et al (Murphy et al., 1987).

2.7 Measurement of FNA

Computed Tomography (CT)

Computed tomography can be used to acquire images of single cross sections or volumes of bone. Because the x-ray attenuation is very different between bone and soft tissue, CT provides a sharp contrast between bone and soft tissue, and is therefore good in depicting mature, well-ossified bones. CT scanning times per slice are lower than 2 seconds and for 3D rendering of hip structures, which requires multiple slices, this can go up to 40 seconds (Falchi and Rollandi, 2004). CT is considered cheap in respect to MRI due to shorter scanning time. CT results in ionising radiation exposure of 0.3-0.5mSv for 6 slices in adults (Muhamad et al., 2012); this dose would be double in neonates (Brenner and Hall, 2007).

Single axial slices using CT can be used to define the neck axis (Weiner et al., 1978; Hernandez et al., 1981; Jend, 1986; Beebe et al., 2017). However, the height (Jend, 1986; Sugano et al., 1998a) and angle of slices used for the 3D reconstruction (Schneider et al., 1997; Tomczak et al., 1997; Beebe et al., 2017) affect the final result since the femoral neck has an asymmetrical shape (Backman, 1957). Alternatively, two axial slices can be taken to define the femoral neck axis, one at the femoral head and the other at different heights of the distal femoral neck (Egund and Palmer, 1984; Murphy et al., 1987; Waidelich et al., 1992; Buddenbrock et al., 1997). Where scans are not aligned with the femoral shaft axis, calculation may be needed to transform the torsion to a reference plane, as positioning-related measurement errors can be as large as 8.8° (Hermann and Egund, 1997). After 3D rendering of the proximal femur it is possible to take an oblique slice along the femoral neck angle in the coronal plane (Kim et al., 2000; Jarrett et al., 2010) or compute the femoral neck axis in 3D (Sugano et al., 1998a; Kim et al., 2000; Berryman et al., 2014). The distal femoral axis can be evaluated with one single axial slice with reference to one of the axes described earlier.

Magnetic resonance imaging (MRI)

Magnetic resonance imaging obtains similar features of the transverse femoral cross-section to CT. MRI uses strong magnetic fields and radio waves to exploit paramagnetic properties, mostly of freely movable protons to generate images and is therefore free from ionizing radiation. Different from the bone approach with CT, which is measuring the presence of bone apatite, MRI measures in bone the absence of freely movable protons. Moreover, MRI's magnetic field often limits the application to participants free from metal implants, pacemakers, or other contraindications. In addition, undergoing an MRI measure of the femur means remaining still within a narrow, confined tube for between 5 (Koenig

et al., 2012) and 20 minutes (Tomczak et al., 1995), depending on the sequence type and scanner used, or up to 45 minutes where 3D rendering is required (Botser et al., 2012), which limits its application in young children without sedation. In the following chapters of this thesis, a 3 Tesla Siemens Biograph was used using a DIXON sequence with 1.2 mm x 1.2 mm x 4 mm voxel size and interslice thickness of 4 mm was used, allowing for scanning times of 20 minutes for one lower limb. MRI scanning times can be reduced with novel hardware and software which is not yet commonly present in clinics and research institutes (Florkow et al., 2022). Furthermore, MRI is usually expensive and not available in all research and clinical facilities. It has been suggested that MRI can be superior to CT in depicting the proximal and distal femoral contours in children with immature bones (Tomczak et al., 1997; Rosskopf et al., 2017b).

The orientation of scan slices is virtually equally achievable with CT and MRI (Koenig et al., 2012; Beebe et al., 2017; Rosskopf et al., 2017b) although alignment of CT scans requires post-scan reconstruction. In contrast, MRI scans can be directly aligned to anatomical features such as the femoral neck (Tomczak et al., 1995), thereby allowing the depiction of the whole region. This is particularly useful at high femoral neck inclination angles, where positioning bias is greatest (Jarrett et al., 2010). The distal femoral axis can be evaluated with one single axial slice with reference to one of the axes described earlier.

Ultrasound Imaging (US)

Ultrasound imaging with most clinical scanners only enables two-dimensional cross-sectional views of soft structures but only identifies the outer surface of mature (fully mineralized) bones. On the other hand, the imaging of whole cross sections is possible in neonates and young infants where the bone is not yet mineralised and remains permeable by sound waves. US is free from ionising radiation, cheap compared to other imaging

techniques, and fast in terms of image acquisition, with the whole protocol lasting up to 10 minutes (Kulig et al., 2010b). Free-hand ultrasound approaches use motion capture or other techniques to track the probe in 3D and are therefore more expensive and time-consuming, taking between 8 and 15 minutes (Passmore et al., 2016a; Greatrex et al., 2017) if only particular landmarks are of interest, as with FNA, or longer if a 3D model of the whole femur is required (Świątek-Najwer et al., 2014).

Some methods place the probe horizontally and measure the inclination on the image on the screen or later on the printed image (Moulton and Upadhyay, 1982; Upadhyay et al., 1987; Elke et al., 1991) but results are not consistent at high angles of anteversion (Phillips et al., 1985; Terjesen and Anda, 1987; Elke et al., 1991) where the distal part of the femoral neck becomes deeper and harder to image. To adjust for this issue, others use inclinometers mounted on the probe (Terjesen and Anda, 1987;Terjesen et al., 1993; Aamodt et al., 1995; Ehrenstein et al., 1999) and take the measurement when the chosen features are showing horizontally on the screen, or use additional hardware to place the femur in internal rotation (Elke et al., 1991). Free hand US couples the ultrasound with video or motion capture localizers (Keppler et al., 1999; Keppler et al., 2007; Świątek-Najwer et al., 2014; Passmore et al., 2016a; Greatrex et al., 2017).

Several features have been used to determine the proximal femur axis: 1) the head-trochanter tangent (Terjesen and Anda, 1987; Upadhyay et al., 1987; Aamodt et al., 1995; Keppler et al., 1999), the femoral neck (Clarac et al., 1985; Ehrenstein et al., 1999), and the intertrochanteric plane (Elke et al., 1991; Kulig et al., 2010b; Passmore et al., 2016a) (Figure 12).

However, taking only the anterior border into account means that inter-individual differences in the angle between the anterior border and centre of the femoral neck is ignored.

The features used to draw the inter-condyle axis are the posterior condyles (Keppler et al., 1999), the epicondyles (Moulton and Upadhyay, 1982), the epicondyles and the anterior condyles (Upadhyay et al., 1987), or the anterior condyles only (Ehrenstein et al., 1999). The posterior condylar line can also be inferred by using the tibia as a perpendicular

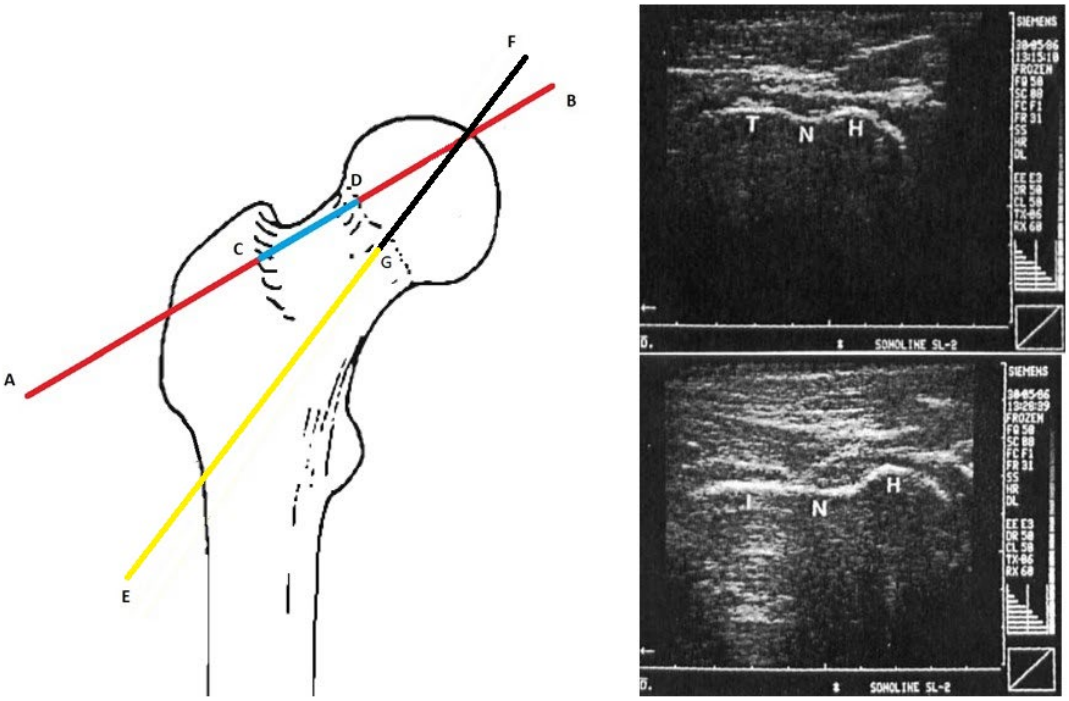

Figure 42 Left panel adapted from (Elke et al., 1991). Frontal view of different ultrasound approaches: the head-trochanter line approach features the peak of the red "head" section BD and the peak of the red "trochanter" section AC (Terje Terjesen and Anda, 1987; Upadhyay et al., 1987; Aamodt et al., 1995; Keppler et al., 1999). The femoral neck approach assesses the region parallel to the blue CD section (Clarac et al., 1985; Ehrenstein et al., 1999). The intertrochanteric plane approach assesses the bone parallel to the yellow GE line (Elke et al., 1991; Kulig et al., 2010a; Passmore et al., 2016b). Right panel: ultrasound images used to define FNA. H= femoral head, N= femoral neck, T= greater trochanter and I intertrochanteric plane. The head-trochanter line and parallel to the neck line can be drawn from the top right panel. The parallel to the intertrochanteric plane can be drawn from the bottom right panel. Figure from (T Terjesen et al., 1993).

reference (Terjesen and Anda, 1987; Elke et al., 1991; Terjesen et al., 1993; Günther et al., 1996) aware of the fact that varus or valgus knee deformation could affect the end result.

Radiography

The images yielded from radiography are projections of the bone structures in the space between the generator and the detector. The detection of the femoral neck axis can be done by either single-plane radiographs giving a 2D image (Dunn and Notley, 1952), biplanar radiography allowing two different projections (Dunlap et al., 1953; Ryder and Crane, 1953; Rippstein, 1955; Magilligan, 1956; Lee et al., 1992) or a 3D computer reconstruction (Chaibi et al., 2012). The actual image acquisition takes seconds, whilst positioning depends on the participant but is usually 1-2 minutes (Rosskopf et al., 2014). Analysis of single-plane images involves drawing a line through the femoral neck axis and is therefore quick. In biplanar and 3D models, the post-processing can take from 2 minutes for approaches where only gross features are identified, to 20 minutes for techniques requiring the identification of a large number of landmarks and evaluation of the whole lower limb (Rosskopf et al., 2014). In the biplanar method, lines are drawn through the chosen landmarks and then converted using trigonometric conversion tables (Dunn and Notley, 1952; Dunlap et al., 1953; Ryder and Crane, 1953; Rippstein, 1955; Magilligan, 1956; Lee et al., 1992). In 3D reconstructions, the images are evaluated by the software. The recently introduced EOS imaging technique (a low dose radiography system) semi-automatically draws the silhouette of the bone and 3D models the lower limb (Chaibi et al., 2012).

Furthermore, radiography is cheap and available in most clinical facilities. The downside of the method is that it uses ionising radiation, not lower than 0.25 mSV for low dose radiography (Kalifa et al., 1998).

Biplanar methods involve an initial anteroposterior radiograph either supine (Ryder and Crane, 1953; Rippstein, 1955; Magilligan, 1956) prone (Dunlap et al., 1953) or standing (Lee et al., 1992; Chaibi et al., 2012). The second image is taken either with the hip flexed at 90° with various degrees of abduction for each method (Dunlap et al., 1953; Ryder and Crane, 1953; Rippstein, 1955; Ogata and Goldsand, 1979), with the detector parallel to the femoral neck inclination (Magilligan, 1956), or standing (Lee et al., 1992; Chaibi et al., 2012). In most methods the proximal axis is taken as parallel to the femoral neck (Dunlap et al., 1953; Rippstein, 1955; Magilligan, 1956; Ogata and Goldsand, 1979) and in others the femoral head- trochanter line (Lee et al., 1992; Chaibi et al., 2012) or head-neck centre are assessed (Ryder and Crane, 1953). The distal axis can be defined using the posterior condylar line (Chaibi et al., 2012), alternatively the tibia is considered perpendicular to the condylar line (Dunlap et al., 1953; Ryder and Crane, 1953; Rippstein, 1955; Magilligan, 1956; Ogata and Goldsand, 1979; Lee et al., 1992).

Functional assessment

It is reported to be possible to measure the FNA without any imaging methods by assessing the angular range of motion (ROM) of the hip joint in the axial plane. FNA can be assessed using the ratio of internal rotation over external rotation, with greater internal rotation associated with greater FNA (Cibulka, 2004; Chadayammuri et al., 2016). In this case the assumption is that the end of the internal and external rotation gives information about where the femoral head stops gliding in the acetabulum and the femoral neck prevents further rotation by touching the acetabulum's contour. Another way of measuring FNA is by measuring the angle of rotation at the point where the greater trochanter feels most prominent, via palpation of the lateral hip (Ruwe et al., 1992; Davids et al., 2002). In this case, the assumption is that when the trochanter is most lateral during the rotation of the

femur, the femoral neck is parallel to the floor and the angle of the tibia will indicate the FNA. This method is called the trochanteric prominence angle test (TPAT) or Craig's test. The downside, however, is the accuracy and precision of these functional methods. These are cheap and convenient, requiring only a goniometer or camera to take measurements. These methods are an indirect indicator of femoral version and are also dependent on both capsular and muscular restraints, as well as acetabular version (Gelberman et al., 1987; van Arkel et al., 2015; Chadayammuri et al., 2016).

The measurement of the rotation has been performed both with an extended or flexed hip (Ruwe et al., 1992; Davids et al., 2002; Botser et al., 2012; Kelly et al., 2012; Chadayammuri et al., 2016), and the degree of flexion can affect the measured FNA by 15° (Chadayammuri et al., 2016). A hip flexion of 45° was used to yield intermediate results between 0° and 90° of flexion (Tönnis and Heinecke, 1991a). It has been suggested that performing functional tests in extended and in flexed positions will give additional information on capsular restraint and acetabular involvement (Gelberman et al., 1987; Cibulka, 2004; van Arkel et al., 2015; Chadayammuri et al., 2016). In all of these methods, the tibia is taken as the perpendicular reference of the posterior condyles (Gelberman et al., 1987; Ruwe et al., 1992; Chung et al., 2010; Botser et al., 2012; Sangeux et al., 2014; Chadayammuri et al., 2016; Uding et al., 2019).

Differences between methods

FNA measurements are dependent on the imaging technique and the landmarks used with differences in mean-values between methods of up to 10° (Kaiser et al., 2016a), which can increase to 20° when people with exaggerated anteversion are tested (Schmaranzer et al., 2019). Mean intra-observer error for CT scans was between 0.8° and 2.9° for the methods of Waidelich, Jarret, Yoshioka, Murphy, and Hernandez, with a range up to 11.4° in

Hernandez's method (Kaiser et al., 2016a). Inter-observer repeatability is excellent for both oblique (interclass correlation ICC 0.95) (Buck et al., 2012; Kaiser et al., 2016a; Beebe et al., 2017) and axial CT techniques (ICC 0.87, 0.93-0.96) (Kaiser et al., 2016a; Beebe et al., 2017; Schmaranzer et al., 2019).

Inter- and intra-operator reliability of MRI in the measurement of FNA has been shown to be comparable to CT (ICC 0.90- 0.97) (Schneider et al., 1997; Tomczak et al., 1997; Muhamad et al., 2012; Beebe et al., 2017). A number of studies have compared CT and MRI measures comparing different methods (Günther et al., 1996; Schneider et al., 1997; Tomczak et al., 1997); in some cases, different landmarks (Kaiser et al., 2016a) or even different samples (Muhamad et al., 2012). However, studies comparing the same methods, meaning the same slice height, orientation and landmark choice, with either MRI or CT show a systematic lower result of 8.9° in MRI with differences up to 37° (Figure 13 left) (Botser et al., 2012) or up to 13.6° variation between measures in another study (Figure 13 right) (Beebe et al., 2017). It has been suggested that the reason for this systematic error might be the long scanning time of the MRI, which leads to the participant relaxing and changing positions between the scanning of the proximal and distal femur. Alternatively, differences in the appearance of bone tissue between MRI and CT may lead to differences in the positioning of identified landmarks.

Comparisons of US with different imaging techniques such as radiography, MRI and CT have shown mean differences of FNA of 0.5° ranging up to more than 10° (Terjesen and Anda, 1987; Upadhyay et al., 1987; Elke et al., 1991; Aamodt et al., 1995; Tomczak et al., 1995; Ehrenstein et al., 1999; Keppler et al., 1999; Kulig et al., 2010b; Passmore et al., 2016a) .

US has shown to have lower inter- and intra-observer reliability than MRI or CT for the 2D methods (Tomczak et al., 1995) but appears more reliable in dried bones (Upadhyay et al., 1987). This may be due to the ability to detect landmarks directly on the dried bone visually, rather than relating them to images on screen through the soft tissue.

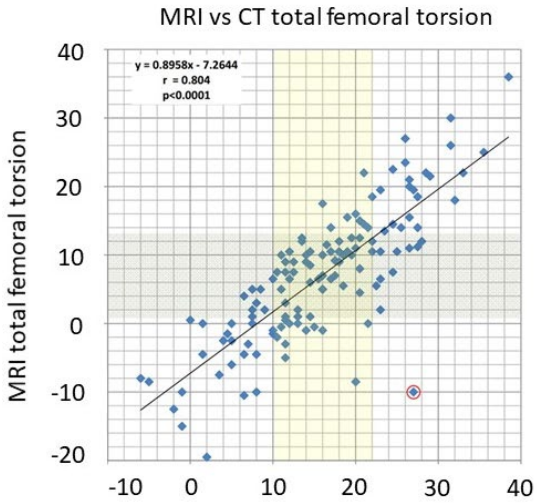

N.	Side	CTA	CTO	MRA	MRO
1	R	6.1	3.5	7.5	8.3
2	R	8.5	9.3	5	13.7
3	R	22.3	15.4	21.8	29
4	R	5.2	-2.2	6.7	3.4
5	L	12.9	15	19	19.8
6	L	22.2	20.6	23.1	32.5
7	L	-3.7	-2.5	-3.4	-2.6
8	L	10.3	10.2	10.1	11.5
9	L	4.2	1.5	5.3	7
10	R	5	5.3	2.6	4.2
11	R	10.9	12.4	12.9	20
12	R	15.7	18.4	17.8	26.3

Figure 13 Left: Comparison of oblique magnetic resonance imaging (MRI) and computer tomography (CT) measurements of the FNA. Figure from (Botser et al., 2012). The yellow shaded area represents the middle two quartiles of the CT measurement, and the green shaded area represents the middle two quartiles of the MRI measurement. The red circled data point is the one with highest discrepancy between CT and MRI FNA values. The black line is the line of best fit and the blue line is the identity line. Right: comparison of CTA (Computer Tomography Axial), CTO (Computer Tomography Oblique), MRA (MRI Axial) and MRO (MRI Oblique). Note the systematic difference between MRI and CT values in the left panel. In addition, the large differences occurring in same specimens using the same reference axes to measure FNA but different imaging techniques (MRI and CT). Adapted from (Beebe et al., 2017).

US has been considered only a good screening method for FNA because of either lower inter- and intra-reliability or only moderate correlation (r= 0.57-0.87) with other imaging techniques (Terjesen and Anda, 1987; Elke et al., 1991; Aamodt et al., 1995; Tomczak et al., 1995) even though these discrepancies also result from errors in the compared methods. US results are closer to MRI than to CT (Tomczak et al., 1995), which may be because the landmarks can be obtained in line with the inclination of the femoral neck. However, the free-hand US methods appear more repeatable compared to regular US (Keppler et al.,

1999; Keppler et al., 2007; Passmore et al., 2016a) with average errors as low as 1.8° (Passmore et al., 2016a) compared to MRI and ICC of 0.95 (Greatrex et al., 2017).

total average difference can be found for biplanar radiography compared to dried femoral measurements of 2.6° to 3.6° with good correlation (r= 0.82-0.91) (Dunlap et al., 1953; Rippstein, 1955; Ogata and Goldsand, 1979; Lee et al., 1992). However, in living participants, the error could be as high as 20° due to positioning errors (Wissing and Spira, 1986). The EOS system yields total average differences compared to CT of 0° to 5° (Buck et al., 2012; Rosskopf et al., 2014). Inter-reader agreement is high for the low dose EOS system (ICC 0.95) with an average difference of 0.1° and 3.4° (Buck et al., 2012; Rosskopf et al., 2014). Error sources might include inaccurate positioning due to physical impairments (such as spasticity, pain, skeletal deformities, or obesity), and inaccurate location of the axes on the roentgenogram (Gibson, 1967) because of lack of clear guidelines. Additionally, soft tissue can obscure the bone outline, making detection of the bony structure more difficult in obese populations. Davids (Davids et al., 2002) showcases that, even though the total mean difference of functional methods is below 5°, in 45% of the sample the error is more than 10° compared to CT. However, internal rotation test or TPAT are good at predicting a low, normal, or high anteversion (Kelly et al., 2012; Muhamad et al., 2012; Chadayammuri et al., 2016; Uding et al., 2019). Correlations with CT methods are highly variable, with regression coefficients ranging from less than 0.25 to 0.79 (Chung et al., 2010; Botser et al., 2012; Sangeux et al., 2014; Uding et al., 2019) for the internal rotation test, and from 0.12 (Sangeux et al., 2014) to 0.86 (Chung et al., 2010; Uding et al., 2019) for TPAT. The reliability of the method is good; the inter-observer ICC value for internal ROM is 0.89 and for the TPAT it is 0.81 (Chung et al., 2010).

2.8 Conclusions

Abnormal FNA changes the biomechanics of the hip, altering muscular lever arms, hip contact forces and femoral neck shear forces, which may contribute to development of a wide range of skeletal disorders, such as osteoarthritis and alter the kinematics of the lower limbs. FNA grows in line with the growth plate, which seems to adjust according to mechanical forces acting on the proximal femur during movement, increasing the FNA during gestation to more than 30° and thereafter decreasing steadily until completion of growth. This decrease is less pronounced or absent in individuals with conditions causing neuromuscular and movement impairment such as cerebral palsy. Interestingly, FNA in older adults is consistently lower than in younger adults, raising the question of mechanisms behind the modelling of the femur at a mature age following growth plate closure, or whether factors such survivor bias or secular changes in physical activity during childhood contribute. Treatment for altered FNA is usually derotational osteotomy, suggested only in the case of disabling conditions while passive, non-operative methods such as braces or wearable cables do not have any effect. Despite observational evidence for the effects of muscular activity on FNA development during growth, the efficacy of targeted physical activity remains unexplored. Large variations between methods evaluating the FNA limit the ability to synthesise the large number of studies on the topic, as normative values must be set, relative to the method. It is not possible to draw conclusions on the choice of which femoral axis to utilise, and further studies are needed to determine the relevant forces shaping it. However, the authors endorse identification of landmarks which consider the femoral head and trochanter part of the femoral neck axis. Further studies are needed to explore the distal axis and whether the usual posterior condylar axis is the most relevant one. As for the imaging technique, it is situation driven,

with MRI and CT giving the best images and measurement precision; MRI is superior to CT in terms of radiation hazard and CT is quicker and cheaper. The biplanar radiography EOS system seems to be a quick, low radiation option, but not as reliable as the aforementioned approaches. However, both within clinical and basic science research, limitations of these methods prevent their broader application in healthy children and population studies. New US techniques already permit a 3D depiction of the femur with systems of probe localization. Further improvements in US imaging and data analysis could provide a cheap, quick, non-invasive, and more broadly applicable alternative to MRI and CT.

2.9 Following research

The literature review identified a pressing need for the development of a non-invasive and clinically viable alternative to MRI and CT for assessment of FNA, as well as a more user-friendly and adaptable option compared to current Free-hand ultrasound devices. Such a tool would facilitate investigations of lower limb and joint morphology in infants and children, enabling the longitudinal tracking of relevant parameters, such as femoral torsion, and yielding novel insights into the determinants of bone mechanoadaptation when analysed alongside variables such as muscle volumes, physical activity, and kinematic parameters. To address this need, a new ultrasound-based technique was developed and assessed, which is detailed in Chapter 3.

Chapter 3 A new three-dimensional biomedical imaging device

3.1 Abstract

Background

Accurate imaging of musculoskeletal structures is essential for diagnostic and research purposes. Current techniques such as magnetic resonance imaging, computed tomography or radiography are either time consuming, expensive or expose participants to radiation hazards. Ultrasound (US) imaging is not accurate for three dimensional structures. These characteristics are un-suitable particularly in the case of imaging children and infants or for the use in large scale studies needing accurate musculoskeletal measurements. This study aimed to propose a cost effective and quick three-dimensional biomedical imaging device based on ultrasound, and to assess its reliability.

Methods

11 adults (28±3.7 years old) were recruited and their thigh scanned in a supine position, with a standard US scanner with linear array probe coupled with a commercially available three-dimensional coordinate system (FAROARM®). The landmarks to measure femur length and total femoral torsion were identified on the video stream of the US. Test-retest reliability was assessed on two repeated scans of each thigh with intraclass correlation coefficients (ICC) and Pearson correlation and Bland Altman plots.

Results

Test-retest ICC was moderate (ICC=0.615; CI -0.071-0.919) for femoral length, and poor (ICC=0.329; CI -0.542-0.843) for femoral torsion.

Discussion

The US-FAROARM® is a quick and inexpensive device. However, currently the reliability for assessment of gross anatomical features is only poor to moderate. Improvements need to be made during data a collection to accurately analyse data on the video stream. However, a future application of this concept could use three-dimensional reconstruction from individual frames of the US stream.

3.2 Introduction

Musculoskeletal disorders affect 1.71 billion people globally (Cieza et al., 2020) and are the leading cause of disability (Bouziri et al., 2022) and work-related absence (Kang et al., 2014) worldwide. Accurate imaging of musculoskeletal structures is essential for diagnosis and assessment of treatment efficacy, in addition to an understanding of the underlying pathophysiology. The cost of musculoskeletal imaging amounts to $3.6 billion a year in the United States alone (Parker et al., 2008). Current imaging modalities to diagnose musculoskeletal disorders are radiography (RX), computer tomography (CT), magnetic resonance (MR) and ultrasound imaging (US). These methods are either expensive (CT and MR), have long scanning times requiring sedation of young children (MR), expose the participant to radiation (RX and CT), or are not accurate for three-dimensional skeletal structures (RX and US) (Scorcelletti et al., 2020). US imaging is cheap, quick and does not involve ionising radiation, but the two-dimensional images produced cannot capture important variation in three-dimensional musculoskeletal structures such as hip geometry or spine curvature.

The EOS RX imaging system has a much lower radiation dose compared to CT and to deliver a three-dimensional model of bony structures through software (Buck et al., 2012; Rosskopf et al., 2017a). Freehand US combines US images with a motion capture system to locate the coordinates of the US images in three-dimensional space allowing reconstruction of either a three-dimensional measurement (Passmore and Sangeux, 2016; Frederick Greatrex et al., 2017) or model (Świątek-Najwer et al., 2014). However, current freehand US systems are bulky, require expensive equipment, and both setup and post processing procedures are time-consuming and require substantial expertise (Świątek-Najwer et al., 2014; Passmore et al., 2016a; Greatrex et al., 2017). Further improvement of this technique could provide an inexpensive, and more broadly applicable alternative to CT, MR and RX for three-dimensional musculoskeletal imaging.

A relatively cheap and portable commercial coordinate measuring system, FAROARM® , was identified to substitute the expensive and laborious motion capture systems used in previous studies (Świątek-Najwer et al., 2014; Greatrex et al., 2017; Passmore et al., 2018) and was coupled with a conventional US imaging device. The aim of this pilot study was to test the repeatability of the FAROARM® integrated with a conventional US device to measure skeletal landmarks.

3.3 Methods

Ethics

The ethical application was reviewed by the Science and Engineering Research Ethics and Governance Committee and was approved on the 14/11/2019 (EthOS Reference Number: 12344). All procedures performed in studies involving human participants were in accordance with the ethical standards of the institutional and/or national research committee and with the 1964 Helsinki declaration and its later amendments or comparable ethical standards. Participants provided written consent and they were informed that their participation was voluntary and that they could withdraw from the study at any time.

Participants

11 right thighs of 11 participants (28.0 ±3.7 y) were scanned amongst staff and students at the Manchester Metropolitan University. The exclusion criteria to participate in the study were having skin conditions on the regions of interest that would not allow the data collection, having any hip or knee replacement and having any current musculoskeletal injury. The study was approved by the Faculty of Science and Engineering Ethics Committee.

Data collection

The individual was asked to lay supine on a physiotherapy bed. The right lower leg was then abducted to approximately 40°, allowing the posterior distal part of the femur to be free. The foot and tibia were strapped into a leg holder, to minimise movement during the data collection (Figure 14).

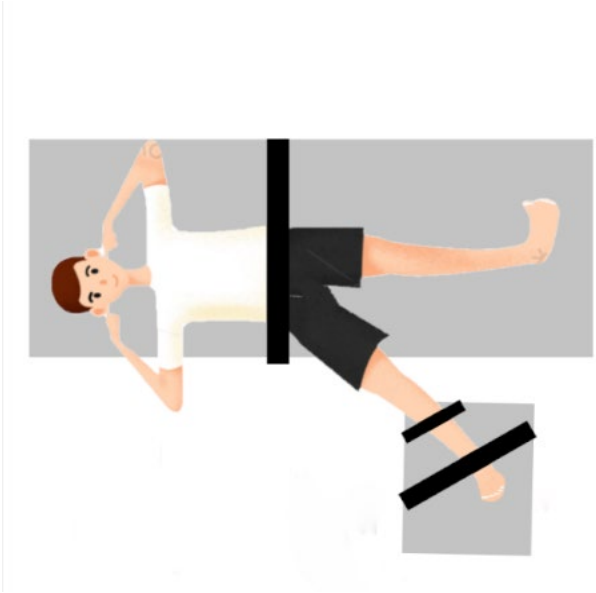

Figure 14 Axial representation of a participant lying on a physiotherapy bed (in Gray) with the right leg strapped (rectangles in black) on a foot and leg holder (also in Gray). Note the foot is at 90° in a neutral position, and the posterior condyles of the leg are not on the table, making them accessible for the scanning US probe.

A continuous stream of US images at 25Hz was collected at the proximal femur, covering the frontal and the sagittal plane of the femoral head, greater trochanter, and proximal femoral shaft. The distal part of the femur was also scanned, covering the posterior and lateral part of the condylar region and the distal part of the femoral shaft. For each region, around 40-80s of images were collected until the whole region had been captured. One set of data collection was considered to be the combination of one proximal and one distal scan, during which the participant was encouraged to hold still. The participant was allowed to move between the two sets of data collection.

Ultrasound FAROARM® (US-FAROARM®)

The US-FAROARM® device consists of a standard US scanner (MyLab Twice, Esaote, Genova, Italy) with linear array probe (Esaote LA923) at 14Hz, 7 cm field view depth, coupled with a commercially-available FAROARM® (Quantum^{S}, FARO®, FARO Technologies Inc., USA) coordinate measurement system. The FAROARM® consists of a multi-jointed arm which encodes the three-dimensional position and angle of a probe mounted on the most distal arm segment (Figure 15). The US probe was fixed to the top of the FAROARM® through a three-dimensional printed probe holder.

US imaging (B-mode, 25 *Hz*) and FAROARM® coordinates including Euler angles were acquired asynchronously via a bespoke multithreaded C++ software application. The US was acquired using the libraries for the Sensoray 2255 software development kit (SDK: http://www.sensoray.com/products/2255.htm), and FAROARM® data were acquired using the libraries for the Faro SDK (no public version; available on request from manufacturer) . Data were acquired using a streaming queue buffer, saved directly to disk in a background worker thread. Faro hardware timestamps were recorded as well as system clock timestamps, which were associated with US and FAROARM® data points. The system clock was used to approximately synchronise both data streams after data acquisition.

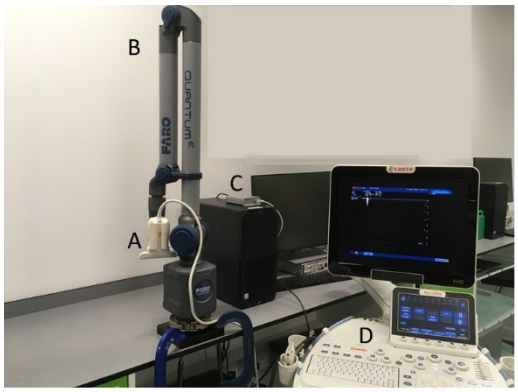

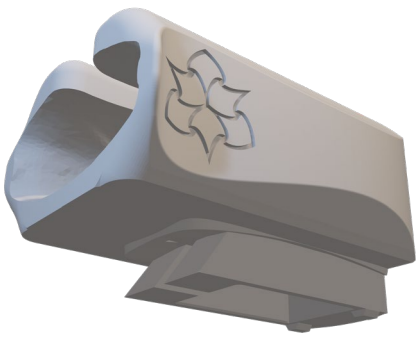

Figure 15 A) Custom designed probe holder, with probe. B) Quantum^{S}. C) Frame grabber, connected to computer and ultrasound scanner. D) Ultrasound scanner. Right panel: 360 view of the custom made probe holder.

Image analysis

A custom Matlab plugin (MathWorks R2021a, 64-bit win64) was developed to allow the user to identity the three-dimensional coordinates of chosen landmarks on the frames of the US output. Landmarks were identified based on video footage, specifically when the desired landmark was visible. The three-dimensional coordinate was retrieved the FAROARM® coordinate system, thereby obviating the need for a priori standardization of data collection planes. The landmarks were selected from the video and when the desired landmark was visible. The dimensional coordinate was then determined by the coordinate system, making an a priori standardization of data collection location superfluous. Leg length was defined as the distance between the apex of the greater trochanter, and the intercondylar notch. Femoral torsion was defined as the line parallel to the anterior edge of the femoral neck and the posterior condylar line. On the femoral neck two points were selected, one proximal and one distal to the femoral head where the femoral neck was flat. The posterior condylar line was identified by the most prominent point on each condyle (Figure 16).

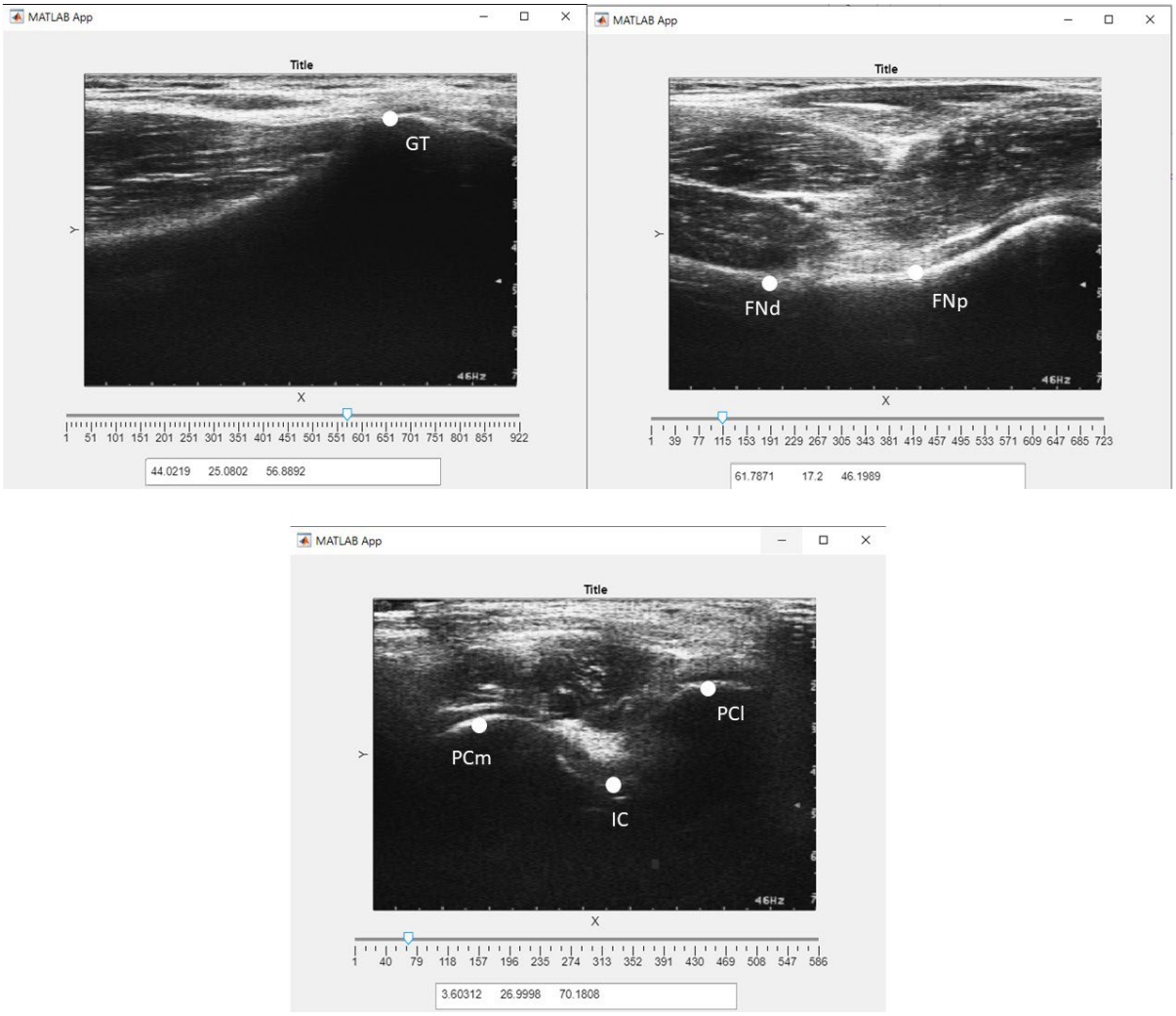

Figure 16 Custom MatLab plugin showing identified landmarks as follows: GT) apex of the greater trochanter. FNp) and FNd) two points proximal and distal to the femoral neck on the anterior border of the femoral neck. PCm) and PCl) medial and lateral posterior condyles. IC) intercondylar notch.

The three-dimensional coordinate from the custom MatLab plugin were then entered into the trigonometric formulas (Equation 1) to yield the femoral length and femoral torsion measurement.

$$\overline{Femoral\ Length} = \sqrt{(ICx - GTx)^2 + (ICy - GTy)^2 + (ICz - GTz)^2} \quad (1)$$

$$Femoral\ Torsion = \quad (2)$$

$$\cos^{-1}\left(\frac{(PCmx - PClx) * (FNpx - FNdx) + (PCmy - PCly) * (FNpy - FNdy) + (PCmz - PClz) * (FNpz - FNdz)}{\sqrt{(PCmx - PClx)^2 + (PCmy - PCly)^2 + (PCmz - PClz)^2} * \sqrt{(FNpx - FNdx)^2 + (FNpy - FNdy)^2 + (FNpz - FNdz)^2}}\right) - 90$$

Equation 1 (1) is the equation to calculate femoral length from the coordinates x, y, z of the selected landmarks. IC) is the intercondylar landmark, GT) is the apex of the greater trochanter (Figure 2). (2) is the equation to calculate femoral torsion from the coordinates x, y,z of the selected landmarks. PCm) and PCl) are the medial and lateral posterior condyles. FN) p and FNd) are the points proximal and distal to the femoral head on the border of the femoral neck.

Statistical analysis

Test-retest Intraclass correlation coefficient (ICC) estimates and their 95% confident intervals (CI) were calculated using the Rstudio statistical environment (Version 3.5.0, www.r-project.org) based on single rater, absolute-agreement, 2-way mixed-effects model (Koo and Li, 2016).

3.4 Results

Only 8 of the 11 participants had landmarks that were recognisable during the image analysis. (Figure 17)

Test-retest intraclass correlation coefficient for femoral length was moderate (ICC=0.615; CI -0.071-0.919) with a mean absolute error between the two measurements of 1.4±1.5 cm (range 0.0cm-4.7cm).

Test-retest intraclass correlation coefficient for femoral torsion was poor (ICC=0.329; CI -0.542-0.843) with a mean absolute error of 11.9±9.2° (range 0.8°-27.7°).

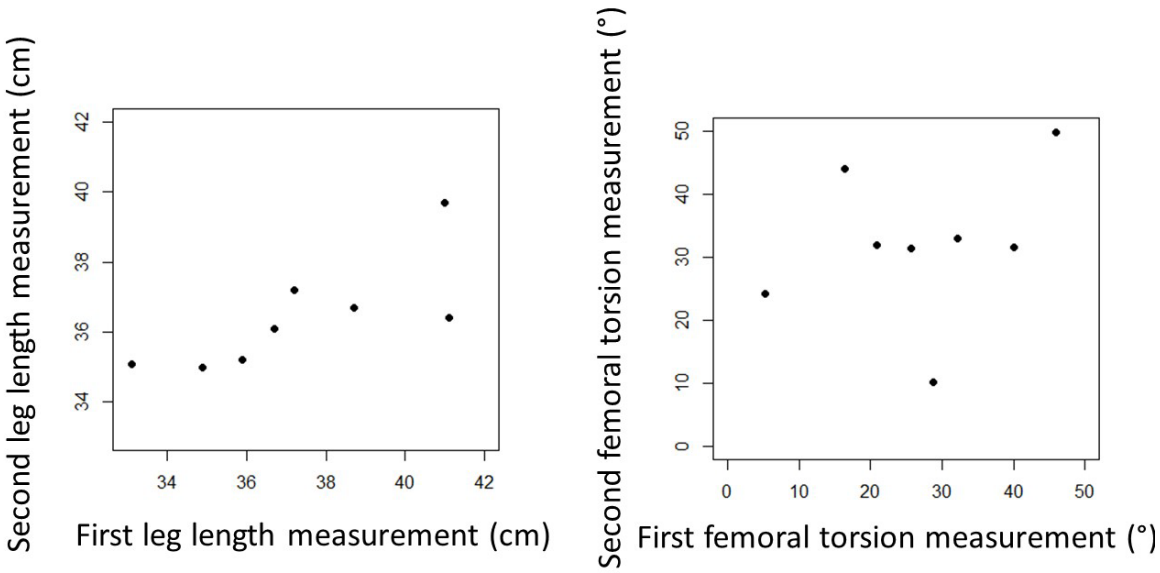

Figure 17 Scatter plots for femoral Length measurement on the left panel and femoral torsion on the right panel.

3.5 Discussion

The purpose of this study was to test the repeatability of the US-FAROARM® three-dimensional measurement, which is potentially a very cost efficient, non-invasive, portable, and quick musculoskeletal imaging system. Musculoskeletal disorders are a leading cause of disability (Bouziri et al., 2022), accurate imaging systems are essential for diagnosis and assessment of treatment efficacy. Current methods such as CT, MR, RX, and US are either expensive, time consuming, invasive, or inaccurate for three-dimensional musculoskeletal assessment (Scorcelletti et al., 2020).

The results of the test-retest ICC showed that the US-FAROARM® device was only moderately reliable in measuring femoral length with errors ranging from 0.0 to 4.7 cm. Current imaging devices such as CT, MR, RX, and EOS RX measure femur length with an excellent reliability (ICC>0.91) with errors ranging from 0 to 1.1 cm (means<0.4 cm) (Leitzes et al., 2005; Doyle and Winsor, 2011; Escott et al., 2013). Few studies have used US to measure femur length with an analogical coordinate system, with differences up to 0.7 cm

compared to the RX measure and errors below 0.5 cm for retest reliability (Terjesen et al., 1991; Junk et al., 1992). When using a free hand US device retest ICC is 0.99 (p=0.49) (Greatrex et al., 2017).

The reported results of the test-retest ICC for femoral torsion of the US-FAROARM® device showed only fair reliability, with errors ranging from 0.8° to 27.4° (mean 11.9±9.1°). Current imaging devices such as CT, MR EOS RX measure femoral torsion with excellent reliability (ICC>0.87) with mean errors lower than 3.4° ranging up to 11.4° (Kaiser et al., 2016a; Beebe et al., 2017; Schmaranzer et al., 2019; Scorcelletti et al., 2020). US methods have test retest errors lower than 5° for femoral torsion measurements (Upadhyay et al., 1987; Scorcelletti et al., 2020), three-dimensional approaches seem promising with excellent repeatability (ICC=0.95, p=0.74) (Greatrex et al., 2017).

Current methodologies, although presenting clear limitations in their applications particularly clinically, have greater reliability than the US-FAROARM® in measuring femur length and femoral torsion. Compared to already present three-dimensional US methods using a more expensive and time consuming to set up, motion capture system as a coordinate measurement device (Greatrex et al., 2017), the US-FAROARM® had lower ICC of 0.24 for the femoral length and 0.64 for the femoral torsion.

The Quantum^{s} FAROARM® coordinate measurement system has an accuracy of 0.05mm and can be ruled out as the source of low reliability of this method. The main source of error was the difficulty in determining the appropriate landmarks in post analysis. The data had been collected with the intention of subsequently reconstructing a three-dimensional model of the proximal and distal region of the femur and analysing landmarks in the context of the model. By analysing the two-dimensional US video, it was not always possible to determine the position of the probe or its inclination which can affect the femoral torsion

up to 10° (Scorcelletti et al., 2020). This limitation can be solved in future studies by recording the landmarks of interest more clearly and labelling them with a trigger signal similar to past studies (Terjesen and Anda, 1987; Upadhyay et al., 1987; Elke et al., 1991; Keppler et al., 1999; Kulig et al., 2010b). Alternatively, by reconstructing and interpolating images to create a three-dimensional volume from which landmarks can be more clearly identified. Furthermore, the inexperience of the person taking the ultrasound scans need to be acknowledged

In conclusion the US-FAROARM® is a quick, inexpensive device requiring little processing post-data capture. The concept of using the Quantum^{s} FAROARM® as a coordinate measuring system is promising in principle, considering its accuracy and portability. However, the initial data collection showed only poor to moderate reliability for assessment of gross anatomical measures. Improvements must be made during data collection to allow more accurate measurement of distance and rotational parameters on musculoskeletal systems from the US image stream. However, future applications of the US-FAROARM® are more likely to be in three-dimensional modelling of musculoskeletal systems, allowing for quick and minimally invasive scans ideal for screening infants' and children's musculoskeletal development. As such, the limitations evident in the current study would not be relevant in future iterations of the technique.

Chapter 4 Lower limb bone geometry in adult individuals with X-linked hypophosphatemia: an observational study

4.1 Abstract

Background

Individuals with X-linked hypophosphatemia (XLH) are at risk of lower limb deformities and early onset of osteoarthritis. These two factors may be linked, as altered biomechanics is a risk factor for osteoarthritis. This exploratory evaluation aimed provide an objective, quantitative characterisation of multiple clinically-relevant components of lower limb bone geometry in individuals with XLH and controls.

Methods

For this observational study, 13 participants with XLH (11 have had corrective surgery), aged 18-65yr (6 female), were compared with sex age and weight matched healthy individuals at a single German research centre. Femoral and hip joint geometry, including femoral and tibial torsion, femoral and tibial shaft bowing, bone cross-sectional area (CSA), acetabular version and coverage measured from magnetic resonance imaging (MRI) scans.

Results

Total femoral torsion was 29° lower in individuals with XLH than in controls ($p<0.001$), mainly resulting from lower intertrochanteric torsion (ITT) ($p<0.001$). Femoral lateral and frontal bowing, tibial frontal bowing, mechanical axis, femoral mechanical-anatomical angle, acetabular version, and acetabular coverage were all greater and tibial torsion lower in individuals with XLH as compared to controls (all $p<0.05$). Greater femoral total and marrow cavity CSA, and greater tibial marrow cavity CSA and lower cortical CSA were observed in XLH (all $p<0.05$).

Discussion

Large differences were observed in clinically-relevant measures of tibia and particularly femur bone geometry in individuals with XLH compared to controls. These differences were evident despite changes attributable to corrective surgeries performed to correct deformations. These differences in geometry plausibly contribute to clinical manifestations of XLH such as early onset osteoarthritis, pseudo fractures and altered gait and therefore should be considered when planning surgeries.

4.2 Introduction

X-linked hypophosphatemia (XLH) is a rare genetic disorder with an assumed incidence rate of 1 in 20,000 (Beck-Nielsen et al., 2009) caused by pathogenic variants in the Phosphate Regulating Endopeptidase Homolog, X-linked (PHEX) gene located at Xp22.1(Francis et al., 1995). The pattern of inheritance is X-chromosomal dominant with supposed complete penetrance. However, family history is negative in about one third of cases suggesting a relevant proportion of *de novo* mutations or an asymptomatic / undiagnosed parental status (Carpenter, 1997; Gaucher et al., 2009). By still not completely elucidated mechanisms, pathogenic, loss of function variants in PHEX lead to elevated levels of the phosphatonin Fibroblast Growth Factor 23 (FGF-23). Resulting renal phosphate wasting and compromised production of 1,25 dihydroxyvitamin D along with further disease mechanisms cause a wide spectrum of clinical manifestations (Beck-Nielsen et al., 2019). Specifically, skeletal issues including short stature and limb deformities, joint problems and early onset osteoarthritis are a universal finding in almost all participants (Francis et al., 1995; Carpenter et al., 2011; A. S. Lambert et al., 2019; Skrinar et al., 2019; Steele et al., 2020). Common deformities of the weight bearing lower limbs in XLH comprise abnormal diaphyseal bowing and torsion including unphysiological femoral torsion (alternatively known as femoral neck anteversion or FNA) (Carpenter et al., 2011; Seefried et al., 2020). These deformities have clinical relevance, as differences in joint geometry likely contribute to increased risk of pseudo-fractures (Pritchett and Perdue, 1988; Genest and Seefried, 2018; Scorcelletti et al., 2020) and impaired joint congruity both directly through altered biomechanics as well as indirectly through effects on muscle tractive forces and gait in individuals with XLH (Mindler et al., 2020; Steele et al., 2020). In addition to direct effects of PHEX deficiency and elevated FGF-23 on mineral metabolism and skeletal development,

other disease associated manifestations such as delayed motor development (Linglart et al., 2014; Skrinar et al., 2019) and greater incidence of childhood obesity in children with XLH (Zhukouskaya et al., 2020) likely contribute to differences in joint development and degeneration (Galbraith et al., 1987; Bobroff et al., 1999a). Moreover, hip joint geometry has been identified to have predictive value with regards to developing osteoarthritis independent of clinical risk factors (Castaño-Betancourt et al., 2013) and recent analyses highlight that specifically femoral torsion is on the one hand influenced by mechanical loading while on the other, it can contribute to osteoarthritis development (Scorcelletti et al., 2020)

Whilst the incidence of skeletal deformities in XLH has been reported according to clinical assessment thresholds or by self-report (Capelli et al., 2015; Skrinar et al., 2019), objective characterisation of bone geometry in adults with XLH has not been completed. Therefore, I assessed multiple components of lower limb geometry in individuals with XLH and compared them to those in an age and sex-matched control group. I hypothesised that I would observe altered joint geometry in individuals with XLH.

4.3 Methods

Ethical approval

Ethical approval for the study was obtained from the competent ethics committees of the medical faculties at the universities of Cologne (No. 19-1020) and Wuerzburg (128/19). The study is registered with the German Register for Clinical Studies (DRKS00016074). All participants provided written informed consent prior to any study-related procedures.

Cohort

Evaluations are based on data obtained from an exploratory clinical study comparing 13 participants with X-linked hypophosphatemia (XLH) and 13 unaffected, age, sex and weight

matched controls. Per selection criteria, participants were 18-65 years old and did not have any acute disorders or conditions that would interfere with planned assessments.

For all XLH participants, genetic confirmation of the diagnosis was available. Data regarding their previous medical and surgical treatment was based on medical history. Accessible information included age at initiation of medical treatment and number of surgeries to the leg under consideration and is provided in Table 1. Considering participants' age and the fact that most treatments were initiated in childhood, written documentation, and medical records regarding dosage over time and formulations of substitutional treatment or technical details regarding surgeries could not be reproduced by the participants. However, surgeries mostly focus on correcting lower limb alignment and comprise techniques such as osteotomies, guided growth, hexapod fixators, or intramedullary nails (Mindler et al., 2021). Control group participants were recruited among participants' friends and spouses who did not have any bone disease, bone targeted medication nor a history of corrective surgery to the evaluated leg.

While the core study is intended to comparatively evaluate muscle fatigue and physical performance in XLH vs healthy controls, data presented here is dedicated to a sub analysis of MRI-data based evaluation of leg and hip geometry. Height and body mass were recorded.

Identity	***Gender***	***Genotype***	***Age at assessment***	***Age at initiation of substitutional treatment***	***Number of corrective Interventions***	***Number of corrective Interventions***
		PHEX			***Femur***	***Tibia***
1	F	Exon 11 c.1235delG p.Ser412Metfs*12	55	15	1	0
2	F	Exon 8 c.871C>T p.Arg291*	56	31	0	2
3	F	IVS15 c.1645+1G>A p.? (Splicing)	41	22	0	0
4	F	Exon 3 - 22 c. (187+1_188-1)_(*1_?)del, p. Ala62_Trp749del	36	1	2	1
5	F	Exon 9, c.1005dupC, p.Ser336Leufs*13	55	5	0	1
6	F	Exon 2, deletion	51	32	1	1
7	M	Exon 2 deletion	61	60	0	1

Identity	*Gender*	*Genotype*	*Age at assessment*	*Age at initiation of substitutional treatment*	*Number of corrective Interventions*	*Number of corrective Interventions*
		PHEX			***Femur***	***Tibia***
8	M	IVS 21, c.2148-2A>G, p.? (Splicing)	40	1	1	2
9	M	Exon 4 c.415T>A, p. Tyr139Asn	37	3	1	1
10	M	IVS 13, c.1483-2A>G, p.?	58	54	0	1
11	M	Exon 9 c.1022T>A, p. Val341Asp	48	1	0	1

Table 1 Individual information of the XLH cohort. Genotypic PHEX mutation is reported. Since the surgery information is mostly based on medical history as recalled by the participant's memory, appropriate details about the type of previous surgical interventions were not available.

Magnetic Resonance Imaging (MRI) scan parameters

In this study 5 sets of 64 transverse images each were recorded from the right leg and body side reaching at least from the foot to the lower part of the lumbar spine using a 3 Tesla Siemens Biograph. Images were recorded using a turbo 2 echo DIXON sequence with following parameters: flip angle 10°, TR 7.02 ms, TE1 2.46 ms, TE2 3.69 ms, 300 mm x 300 mm field of view at 1.2 mm x 1.2 mm x 4 mm voxel size. In this study, only images covering the region of the femur and tibia were evaluated.

Image analysis

MRI images were analysed using ImageJ (Version1.52h). The total femoral torsion was defined using the femoral-neck line and the posterior condylar line. The femoral-neck line was defined as the line between the femoral head centre, and the shaft centre directly distal to the lesser trochanter. The posterior condylar line was defined as the line joining the posterior apices of the condyles in the image where the condyles were most prominent.

The inter-trochanteric torsion (ITT) was defined as the angle between the femoral neck line and the lesser trochanter line. The lesser trochanter line was defined as the line between the apex of the lesser trochanter at peak lesser trochanter size, and the shaft centre. The shaft torsion (ST) is the angle between the lesser trochanter line and the posterior distal shaft line, which is aligned with the flat posterior distal shaft surface immediately proximal to the posterior condyles. The condylar torsion (CT) is the angle between the posterior distal shaft line and the posterior condylar line (Figure 18). Tibial torsion was measured by the angle of the posterior tibial condylar line as reference and the line connecting the medial and lateral malleoli. The angle will be negative when the distal tibia rotates externally respective to the proximal tibia.

To measure femoral lateral and frontal bowing, the shaft centre was identified at four landmarks; immediately distal to the lesser trochanter, at 1/3 proximal-distal femoral shaft length; at 2/3 proximal-distal femoral shaft length (Shaft is between slice “c” and “d” in Figure 18), and at the femoral intercondylar notch. Likewise, tibial lateral and frontal bowing were defined using shaft centre at the intercondylar notch, the proximal third of the tibia, the distal third of the tibia at the distal tibial plateau.

The two lines used to define the mechanical axis are those connecting the femoral head centre to the femoral intercondylar notch, and from the midpoint of the tibial intercondylar eminence to the midpoint of the distal tibial epiphysis. The two lines defining the femoro-tibial angle were those connecting the femoral shaft centre at the distal third of the femur and the intercondylar notch, and the intercondylar notch and the proximal third of the tibia. Lastly, the femoral mechanical-anatomical angle is defined by the lines connecting: the femoral head centre to the intercondylar notch and the intercondylar notch to the centre of the femur immediately distal to the lesser trochanter.

The acetabular version was assessed in the cross-section where the femoral head was greatest. It was defined as the angle between the anterior and posterior acetabular margins of the acetabulum and the sagittal plane (Figure 18). On the same slice the acetabular coverage was assessed as the angle between the posterior margin of the acetabulum and the femoral head centre and the anterior margin of the acetabulum and the femoral head centre.

To calculate the relevant angle λ in the frontal plane the coordinates of the desired landmarks were calculated using the formula:

$$\lambda = arctan\left(\frac{\frac{ay-by}{ax-bx} - \frac{cy-dy}{cx-dx}}{1+\frac{ay-by}{ax-bx} * \frac{cy-dy}{cx-dx}}\right)$$

where "a" and "b" represent the respectively the proximal and distal reference points of the proximal axis and "c" and "d" the proximal and distal reference points of the distal axis. “B” and “c” overlap in the case of the mechanical axis and femoro-tibial angle (Figure 18). “Y” and “x” on the other hand are respectively the antero-posterior coordinates, and the medio-lateral coordinates.

Statistical analysis

Femoral and tibial geometry, femoro-tibial alignment and acetabular parameters were compared in individuals with XLH and in control participants. Data from both groups were tested for normal distribution with the Shapiro-Wilk test. Parametric data were expressed as mean ± SD, non-parametric data as median and inter quartile range (IQR).

For parametric data, homogeneity of variance was checked with the Levene’s test, and the student t-test was implemented to assess group differences. For non-parametric data, the Mann–Whitney U test was applied to test for group differences. Repeatability of the measures performed has been calculated using SPSS statistical package version 23 (SPSS Inc, Chicago, IL) by intraclass correlation coefficient (ICC). It was calculated based on a mean rating of 3 image analysis, absolute effects, using a 2-way mixed effects model to assess repeatability of the image analysis by the same examiner at three different times in random order (Koo and Li, 2016). ICC was found to be excellent for total femoral torsion (ICC:0.989), ITT (ICC:0.968), femoral lateral bowing (ICC: 0.978), femoral frontal bowing (ICC: 0.904), tibial torsion (ICC:0.93), tibial lateral bowing (ICC: 0.938), mechanical axis (ICC:0.958), femoral mechanical-anatomical angle (ICC:0.974). Values for CT (ICC0.843), tibial frontal bowing (ICC:0.768), acetabular version (ICC:0.859) and acetabular coverage (ICC:0.855) showed good reliability.

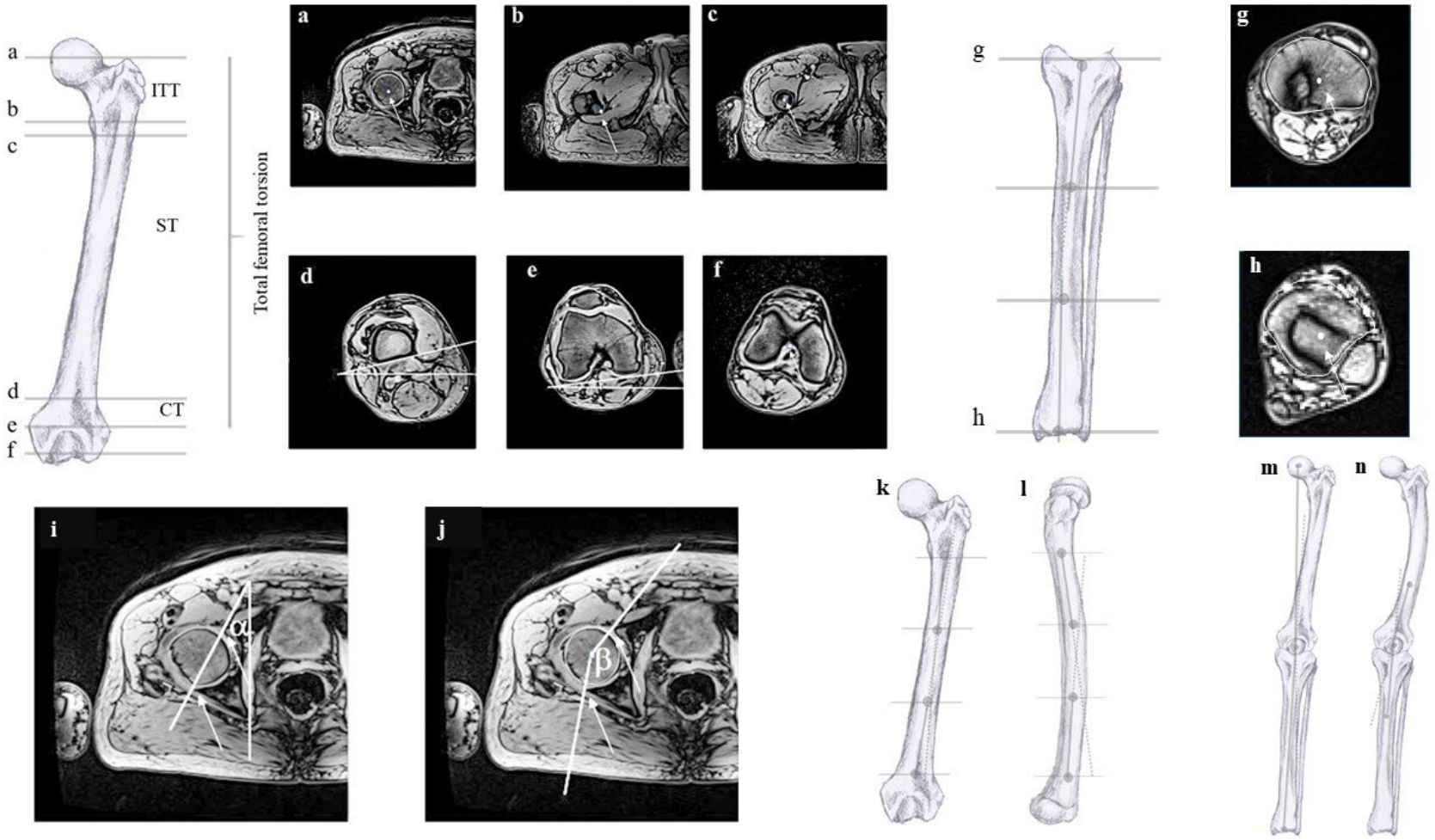

Figure 18 Angle definitions: a) femoral head centre, b) tip lesser trochanter, c) shaft centre, d) posterior distal shaft line, e) posterior condylar line, f) intercondylar notch. Total femoral torsion is the angle between the line joining a and c and the reference in e. ITT is the angle connecting the landmarks in a-c and b-c, ST is the angle connecting c-b and the upper line in d, CT is the angle between d and c. g) and h) tibial lateral and frontal bowing landmarks. i) Acetabular version α and j) acetabular coverage β. The slice where the circumference of the femoral head was largest was chosen for analysis. The arrows show the rim of the acetabulum. k) femoral lateral bowing landmarks. l) femoral frontal bowing landmarks. m) mechanical axis landmarks. n) femoro-tibial angle landmarks. Figure adapted with permission from Scorcelletti and colleagues, illustrations by Xaali O'Reilly-Berkeley.

4.4 Results

Out of 13 participants enrolled per group, whole leg MRI imaging could be evaluated from 11 individuals with XLH (mean age 48.7±9.2y, 6 female, 77.3kg,) and 13 age, sex and weight-matched controls (mean age 48.8±7.6y,6 female, 79.9kg, p>0.677). The mean height of the XLH individuals was 1.56m and the control group height was 1.69m (Table 2). For two male participants in the XLH group, MRI data could not be analysed due to extensive artefacts from metal implants.

Variable	**XLH (n=11)** **5 male / 6 female**		**Control (n=13)** **7 male / 6 female**		**t-test**
	mean	*SD*	*mean*	*SD*	*p-value*
Age (years)	48.7	9.2	48.8	7.6	0.995
Height (m)	1.56	0.10	1.68	0.09	0.006
Weight (kg)	77.3	16.5	79.9	13.2	0.677
BMI (kg/m^2)	32.0	8.5	28.4	4.6	0.223

Table 2 Mean, standard deviation (SD) and group comparison p-values for descriptive variables of the studied groups. BMI: body mass index.

Both basic characteristics and each of the measured angles were normally distributed apart from tibial frontal bowing. Individuals with XLH and control participants had similar age, body mass and BMI although control participants were taller than individuals with XLH (p=0.006).

The total femoral torsion in the XLH group was 8.4±20.2° and thus significantly lower than in the control group with 37±14.2° (p<0.001, Figure 19). When evaluating regional torsion on different levels along the femoral axis, group differences in femoral torsion appeared to primarily result from significantly lower inter-trochanteric torsion (ITT) in the XLH group with 36.4±12.3° as compared to the control group with 54.9±9.5° (p<0.001), as well as a

lower condylar torsion (CT) in in XLH vs Control with 1.5±5.3° *vs* 7.2±2.9°, respectively (p<0.005, Figure 19). In contrast, the shaft rotation or shaft torsion (ST) was similar in both XLH participants (-29.5± 17.9°) and controls (-26.3±12.05°), (p=0.620). The tibia was less externally rotated in individuals with XLH -8.7±13.5° than in the control group -37.2±11.8° (p<0.001).

Substantial between group differences were also evident regarding limb bowing. Femoral

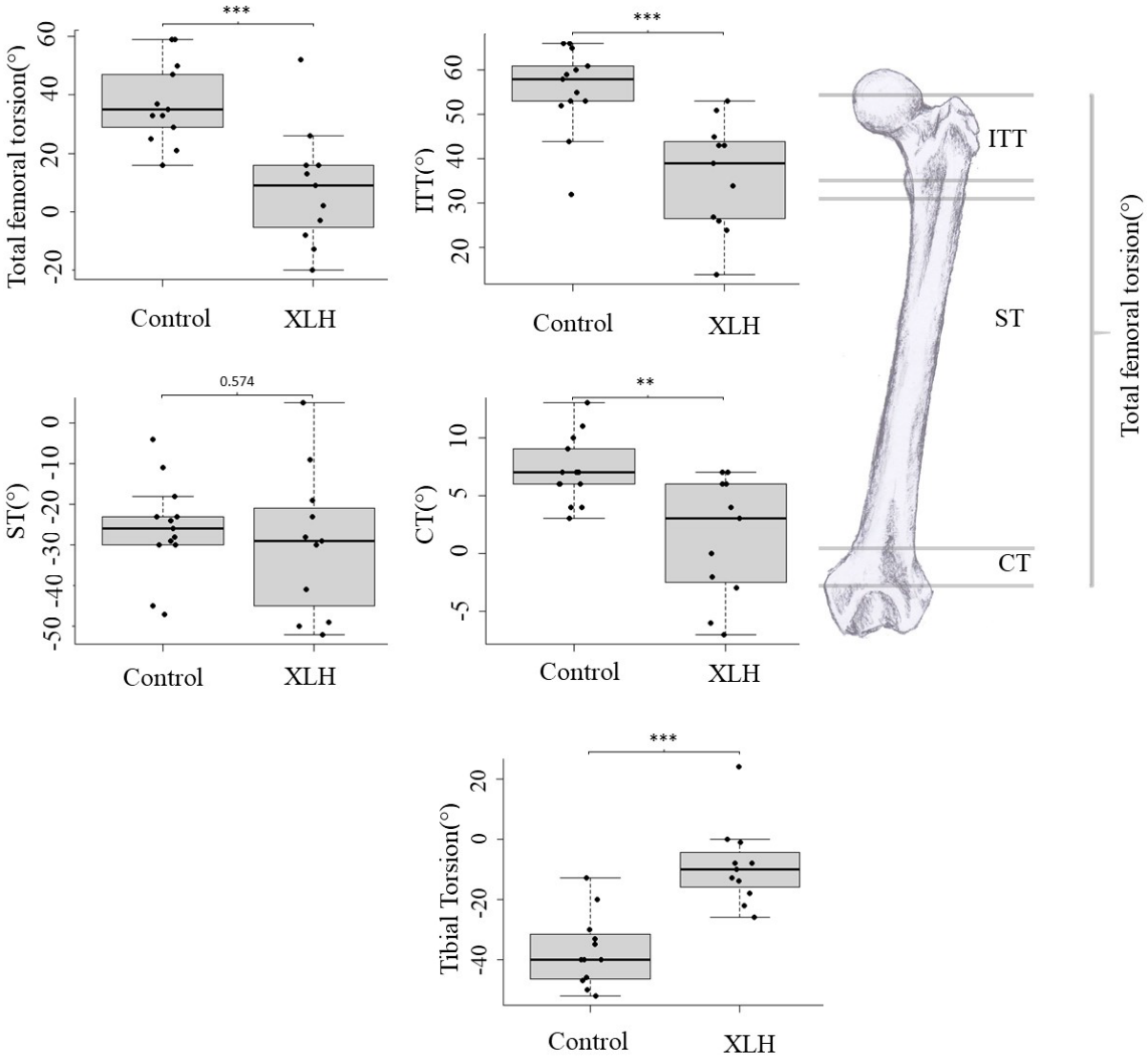

Figure 19 Total and regional torsion of the femur compared between control participants and individuals with XLH. Boxplots indicate median, interquartile range, minimum and maximum values. Femoral torsion, ITT - intertrochanteric torsion, ST - shaft torsion, CT - condylar torsion. Positive degrees represent external torsion from the frontal plane. Asterisks indicate results of group comparisons - * - p<0.05, ** - p<0.01, *** - p<0.001. Illustrations by X. O'Reilly-Berkeley.

bowing was significantly enhanced in individuals with XLH vs controls for both lateral

bowing with 13.1±7.0° vs. -1.0±2.5° (p<0.001), as well as frontal bowing with 31.4±7.3° vs 17.8±1.4° (p<0.001), respectively.

There was no apparent difference in tibial lateral bowing, whereas for tibial frontal bowing (which was not normally distributed) the median value of 11.6° (IQR 7.8°, 19.5°) for individuals with XLH was higher than that in controls 5.0° (IQR: 2.9°-7.7°, p<0.005, Figure 20).

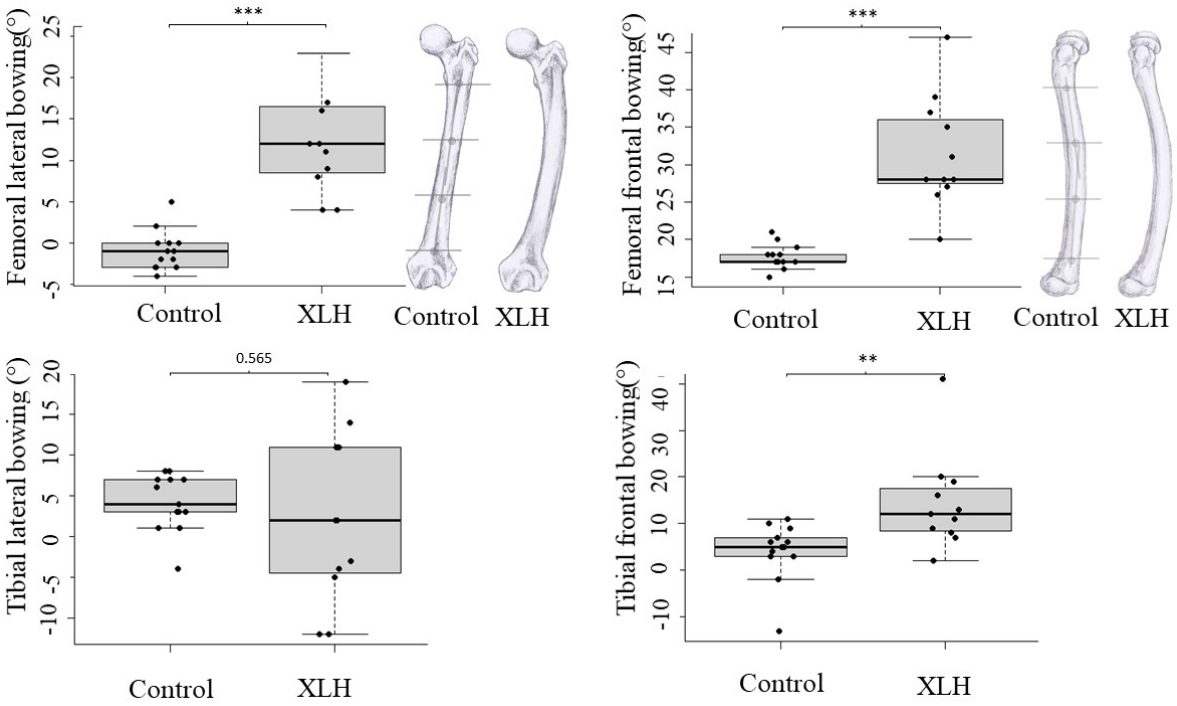

Figure 50 Femoral and tibial bowing in the two groups, positive values indicate anterior and lateral bowing. Boxplots indicate median, interquartile range, minimum and maximum values. * p<0.05, **p<0.01, ***p<0.001. Illustrations by X. O'Reilly-Berkeley depict the scale of differences described by the results.

In terms of lower limb alignment, there was an enhanced valgus of the mechanical axis in the XLH group (5.6±5.3°) as compared to the control group (1.5±2.5°, p<0.05) In contrast, the average femorotibial angles were not significantly different between the groups. Accordingly, there was a significant difference in the femoral mechanical-anatomical angle, representing the difference between the mechanical and the anatomical axis. In that

regard, average femoral mechanical-anatomical angle was 9.1±2.2° in the XLH group and only 5.1±0.8° in controls (p<0.001, Figure 21).

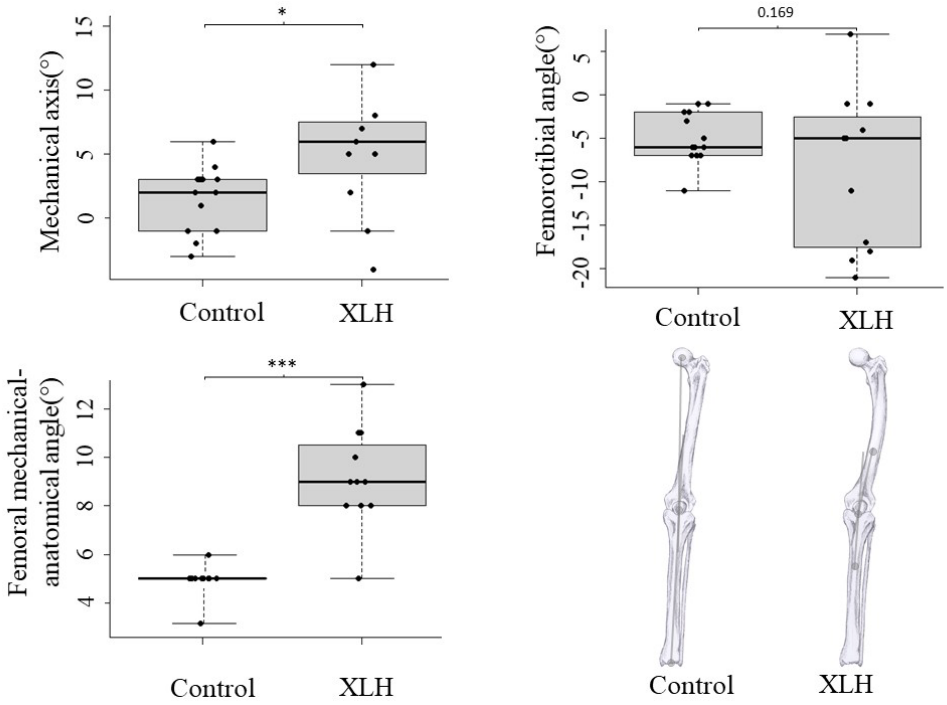

Figure 21 Mechanical axis, femorotibial angle and femoral mechanical-anatomical angle in the two groups. Boxplots indicate median, interquartile range, minimum and maximum values. Positive degrees are outward lateral. * p<0.05, **p<0.01, ***p<0.001. Bottom right panel shows visual representation of lower limb alignment. Also, the mechanical axis is drawn on the control limb and the femorotibial angle on the XLH limb. Illustrations by X. O'Reilly-Berkeley.

Acetabular version was significantly increased in individuals with XLH (23.6±8.4°) as compared to those in the control group (17.5±3.9°, p<0.05). Additionally, acetabular coverage was 32.6° higher in individuals with XLH (192.5±22.6°) than the control group (159.9±9.1°, p<0.001, Figure 22).

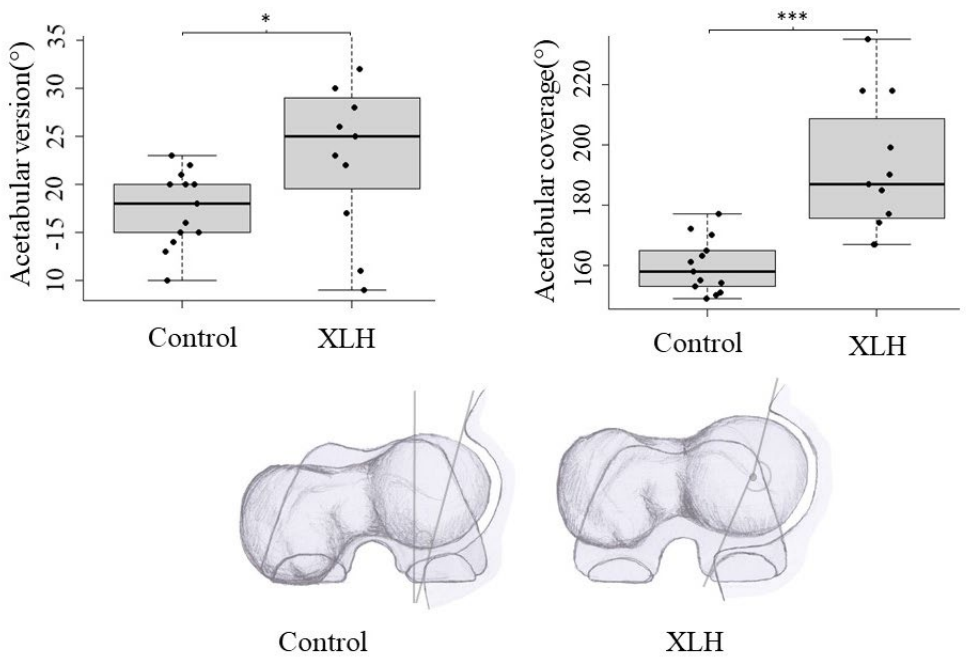

Figure 22 Acetabular version and acetabular coverage for the two groups. For acetabular version positive values indicate anterior rotation from a lateral position, for the acetabular coverage values indicate the portion of the femoral head within the acetabulum. Boxplots indicate median, interquartile range, minimum and maximum values. * p<0.05, **p<0.01, ***p<0.001. Bottom panel shows a visual representation of the acetabular geometry, the femoro-acetabular relationship, and the total femoral torsion. Control panel displays acetabular version measurement, the XLH panel shows acetabular coverage measurement. Illustrations by X. O'Reilly-Berkeley.

The total CSA of the femoral head and at the lesser trochanter showed no differences between the two groups. The total CSA of femoral shaft sites was ~21-24% greater in individuals with XLH compared to the control group ($p<0.015$). The bone marrow cavity of the femoral shaft sites was also greater in XLH individuals (all $p<0.05$), such that cortical bone area was similar between groups. The total CSAs of the three tibial shaft sites and the talus were similar between the groups. The bone marrow cavities of the proximal and mid tibial shaft sites were greater ($p<0.05$) and cortical CSAs at all shaft sites lower ($p<0.05$ except proximal sites $p=0.069$) in the XLH individuals compared to the control participants. (Table 3 and Figure 23).

Bone	***Site***		***Total CSA (mm^2)***						***Bone marrow CSA (mm^2)***						***Cortical bone CSA (mm^2)***					
			XLH		Control		Difference		XLH		Control		Difference		XLH		Control		Difference	
			mean	*SD*	*mean*	*SD*	*%*	*p*	*mean*	*SD*	*mean*	*SD*	*%*	*p*	*mean*	*SD*	*mean*	*SD*	*%*	*p*
Femur	Head centre		1840	274	1923	303	-4	*0.559*												
	Under lesser trochanter		1093	223	966	159	13	*0.182*												
	Shaft	Proximal 3rd	823	132	674	104	22	***0.015***	389	116	172	39	126	***<0.001***	431	117	502	75	-14	*0.147*
		Middle	829	137	671	100	24	***0.011***	355	128	203	64	75	***0.004***	452	138	468	67	-3	*0.752*
		Distal 3rd	853	202	703	108	21	*0.062*	382	54	312	72	22	***0.042***	487	180	391	59	25	*0.136*
	Distal flat shaft		1790	277	1551	174	15	***0.039***												
Tibia	Shaft	Proximal 3rd	701	144	670	93	5	*0.592*	439	92	344	73	28	***0.026***	262	87	326	50	-20	*0.069*
		Middle	526	86	516	75	2	*0.79*	278	81	164	28	70	***<0.001***	247	61	351	66	-30	***0.003***
		Distal 3rd	460	78	469	136	-2	*0.881*	214	60	158	124	35	*0.254*	246	57	310	44	-21	***0.014***
	Talus		1755	220	1618	230	8	*0.221*												

Table 3 Cross sectional area (CSA) of femur and tibia at multiple locations. Where Marrow cavity was not present, only total CSA has been evaluated.

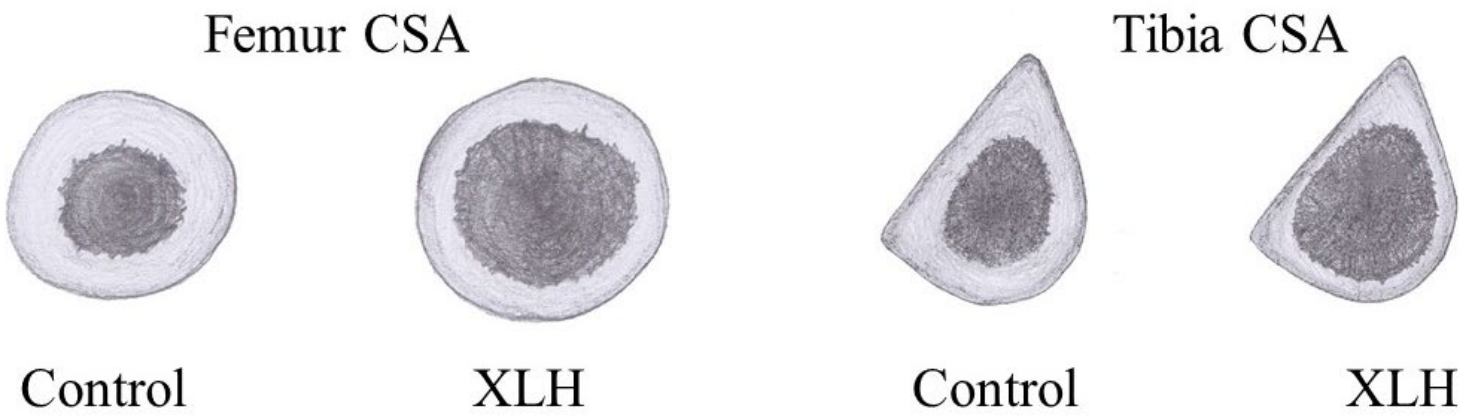

Figure 23 visual representation of femur CSA on the left, and tibial CSA on the right. Illustrations by X. O'Reilly-Berkeley.

4.5 Discussion

Summary of Key findings

This study was the first to objectively characterise and compare multiple components of lower limb bone geometry between individuals with XLH and controls. I observed considerable differences in multiple clinically relevant aspects of geometry, extending previous qualitative clinical and self-reports (Skrinar et al., 2019; Mindler et al., 2020) with which the current study findings were broadly in line. Specifically, individuals with XLH exhibited significantly lower femoral torsion as compared to controls. Further detailed analysis revealed this difference to result mainly from a lower proximal, intertrochanteric torsion. Whilst lower distal condylar torsion also appeared to contribute, no group differences in shaft torsion were evident. In that regard, one may speculate that this could be due to enhanced torsional strain towards the joint, i.e., at the intertrochanteric and the condylar area. However, other clinical populations have shown different contributions of subtrochanteric and supertrochanteric torsion to total femoral torsion (Kim et al., 2012). This is clinically important, as when pharmacological treatment during growth to prevent femoral deformities has failed and femoral osteotomy is considered (Sharkey et al., 2015), it is important to correct torsion in the correct region (Kim et al., 2012; Scorcelletti et al., 2020). To date, surgical protocols focus on frontal plane deformations (Carpenter et al., 2011; Gizard et al., 2017; Horn et al., 2017), therefore assessment of femoral torsion should also inform development of future guidelines. Furthermore, characterising the overall lower limb geometry of this clinical group could inform about possible sources of joint incongruity, fractures, osteoarthritis and gait disturbances other than frontal plane deformations. Moreover, I observed significantly increased acetabular coverage of the hip joints in the XLH cohort. This is particularly important since both, reduced femoral torsion and increased acetabular coverage are known to predispose to hip osteoarthritis

development (Zeng et al., 2016). A recent large study on knee osteoarthritic individuals found correlations between coronal alignment, CT and tibial torsion (Valgus- high CT, valgus - high tibial torsion) (León-Muñoz et al., 2021) opposite to the average XLH individual in the current study (valgus - low CT, valgus - low tibial torsion), suggesting that mechanisms of knee osteoarthritis in the XLH individuals might be different from the general osteoarthritic population. and these findings may be important contributions to better understand early osteoarthritis development in XLH (Insogna et al., 2018; Steele et al., 2020). Moreover, it is important to keep in mind that increased acetabular coverage and diminished ITT as the main contributor to low femoral torsion are not directly affected by corrective surgeries in XLH, usually addressing the diaphyseal / distal femur and the proximal tibia. Along the diaphyseal segment, I observed increased frontal and lateral bowing in the XLH cohort at the femur, while differences concerning bowing of the tibia were less pronounced and only significant with regards to frontal bowing. Finally, there was lower external rotation of the tibia (tibial torsion) in line with previous reports (Carpenter et al., 2011).

There was larger inter-individual variation for most aspects of skeletal geometry in people with XLH, and the causes and consequences for this need to be identified. The above results agree with current qualitative literature about deformities in participants with XLH (Carpenter et al., 2011; Horn et al., 2017; Haffner et al., 2019), however, detailed quantification of limb geometry in this clinical group was not yet available in the literature.

Bone cross-sectional area

The observation of a significantly greater total cross-sectional area of the femur is remarkable, considering the overall reduced body size of XLH participants as compared to controls. This is in line with a previous peripheral quantitative computed tomography (pQCT) study in tibia in children and adults (age 23±13y) with XLH (Veilleux et al., 2013). Looking at it more closely, the difference results from an enlarged marrow cavity on all

height levels along the femoral axis while cortical cross-sectional area is not significantly different on these levels. In contrast, the generally larger tibia marrow cavity in the absence of a pronounced advantage in total CSA in XLH resulted in lower cortical CSA throughout tibia length. One may speculate if the pronounced femoral hypertrophy results from childhood rickets with compromised bone quality and deficient mineralization leading to enhanced mechanical strain and increased bone turnover with intensified endosteal bone resorption and periosteal apposition.

Factors contributing to observed findings.

Overall, there are likely a number of factors which contribute to the observed findings. Fundamentally, the osteoid content of participants with osteomalacia results in higher ductility of the bone structure (Hadjab et al., 2021). This abnormality likely leads to changes in deformation patterns caused by mechanical loading during daily activities and exercise, in addition to the resultant adaptive response in bone geometry. In addition, increased bone ductility may also underlie the higher acetabular coverage due to the pressure of the femoral head on the acetabulum. Altered bone composition and mechanical loading may also contribute to the greater variance observed in the group with XLH. In relation to mechanical loading, XLH is associated with muscle weakness (Veilleux et al., 2018) and altered gait (Mindler et al., 2020; Steele et al., 2020) which likely result in altered bone loading. In a similar vein, childhood motor development, which has been shown to affect development of bone geometry (Ireland et al., 2014b; Ireland et al., 2019) is delayed in children with XLH (Zhang et al., 2019).

Clinical implications

These results have both functional and clinical implications for individuals with XLH. Waddling gait and early osteoarthritis at weight bearing joints are commonly diagnosed in

individuals with XLH (Carpenter et al., 2011; Mindler et al., 2020; Steele et al., 2020). In particular, the high prevalence of osteoarthritis in up to 55% even in individuals under the age of 30 is of particular concern (Hardy et al., 1989; Skrinar et al., 2019). Also, altered femoral geometry likely contributes to the high prevalence of lower limb and specifically femoral pseudo fractures in XLH (Portale et al., 2019). Femoral torsion and proximal femur varus deformities have been shown to change the lever arms of hip muscles and therefore decrease hip muscle strength (Scheys et al., 2008; Kim et al., 2012; Li et al., 2014). This alteration has been hypothesized to be the cause of waddling gait (Horn et al., 2017). Recent gait analysis in participants with XLH has found that waddling gait was correlated to varus limb alignment (Mindler et al., 2020) and degenerated hip, knee, and ankle joints and enthesopathy of the hip abductors (Steele et al., 2020). Lower femoral torsion and high acetabular coverage, both confirmed risk factors of hip osteoarthritis (Zeng et al., 2016), impede hip internal rotation in XLH (Bedi et al., 2011; Steele et al., 2020) which results in enhanced risk of femoro-acetabular hip impingement and consecutive joint pain (Carpenter et al., 2011; Seefried et al., 2020). The lower femoral torsion also increases the shear forces on the femoral neck (Pritchett and Perdue, 1988), this could contribute to development of coxa vara which is common in this population. Tibial torsion also contributes to altered gait as identified in pediatric populations with XLH (Mindler et al., 2020).

Corrective surgery: present and future

Corrective surgery is a common practice in individuals with XLH, with >57% of adults with XLH and frontal plane deformities (Carpenter et al., 2011; Gizard et al., 2017; Horn et al., 2017) having already undergone at least one procedure. In the analysis presented here, the average femorotibial angle was similar in both groups. While this finding appears to conflict with the common perception of XLH being associated with varus deformity of the leg axis,

it most likely reflects that all but two participants in the XLH cohort evaluated here have undergone femoral osteotomies which are usually aimed at correction of frontal plane deformities (Gizard et al., 2017). In addition, average mechanical valgus angle was actually increased in the XLH group as compared to controls, along with an increased femoral mechanical-anatomical angle, reflective of an enhanced femoral offset and further supporting this perception. While this aspect of previous corrective osteotomies has to be considered a limitation of the study, otherwise findings represent real world data and evidence of the condition of XLH individuals.

However, when planning osteotomies taking into account transverse plane parameters such as regional femoral torsion could be beneficial (Seitlinger et al., 2016; Waisbrod et al., 2017), for example to restore advantageous muscular lever arm length. The restoration of limb alignment in multiple planes could decrease the chances of early arthrosis due to malalignment (Khan et al., 2008).

Strengths and limitations

To our knowledge this is the first study to quantitatively characterize multiple objectives and clinically-relevant measures of lower limb bone geometry, in individuals with XLH. Previous studies had reported the incidence of identified deformities such as tibial bowing without a description of the magnitude of deviation or the degree of within-group variance (Capelli et al., 2015; Skrinar et al., 2019).

There are several limitations to this study which have to be kept in mind. Importantly, all statistical analyses and interpretations have to be seen against the background of the limited number of cases for this complex assessment in a rare disorder, and lack of significance in some parameters may be related to the low number of participants enrolled. Furthermore, all but two participants with XLH had corrective surgery on the lower limbs

during their lifetime, therefore observed differences are not solely attributable to differences in natural growth. Indeed, outcome of corrective interventions and the risk for recurrent deformity or overcorrections are subject to multiple modifiers, including but not limited to surgical technique and performance, age at surgery and quality of accompanying medical treatment. However, considering that it is unethical to let XLH participants grow into adulthood without treating their deformities and understanding limitations regarding availability of data on treatments that occurred 10-50years ago, real world data provided here still represent best available evidence. Having said that, data presented here should not be perceived to reflect natural bone development in XLH but rather to provide a real-world inventory of bone deformities in adult XLH participants.

Moreover, the fact that specific differences particularly concerning aspects of rotation and bowing persist even following surgery both highlights the scale of the effects and that different interventional approaches *e.g.,* pharmacological treatments or physiotherapy/exercise may be required to comprehensively address this issue. Even though the participants were recruited from a broad clinical cohort, the sample size is small. Although individuals with XLH were originally matched, due to dropout unmatched comparisons were made. This will have reduced study power, and in addition could introduce confounding by group differences in relevant variables although key measures such as age and weight were very similar between the two groups. Therefore, whilst the observed group differences were large and statistical evidence for them was strong, these findings require replication in a larger cohort. Furthermore, only the left leg was scanned for every participant, as scanning both legs would have quadrupled scanning times. I was therefore unable to assess inter-limb asymmetries, which may contribute to gait and other problems within individuals with XLH. Detailed information on previous pharmacological and other treatments from childhood was not available for all participants, and future

studies should examine whether surgical or other treatments impact on bone geometry. Femoral torsion was assessed on two cross section slices and not on one oblique slice which is now standard practice. Whilst the latter results in slightly smaller torsion values within-population variance is similar (Sutter et al., 2015) therefore I believe that this would not substantially impact the main findings. Finally, all frontal plane measurements were assessed using cross sectional MRIs, and not by the usual clinical method of anteroposterior radiographs.

4.6 Conclusions

In conclusion, adults with XLH have substantial differences and greater inter-individual variation in hip and femur bone geometry, principally lower femoral torsion originating in the intertrochanteric region, lower tibial torsion, and higher lateral and frontal femoral bowing. Large difference in acetabular coverage and version were also observed, whilst differences detected between the groups in the mechanical axis and tibiofemoral angle are minimal. These differences are likely to be due to the higher malleability of the bones, variations in gait, delayed motor development and impaired muscle function. These differences were evident despite most individuals within the current study having undergone corrective frontal plane surgery. Accordingly, these observations should be considered when planning corrective surgery in XLH in the future. The presented results have the potential for increased femoral fracture risk, disadvantageous joint mechanics during daily physical activity and could be part of the cause of the osteoarthritis, pain, and waddling gait commonly experienced in this clinical group.

Chapter 5 Associations between long-term exercise participation and lower limb bone geometry in young and older adults

5.1 Abstract

Background

Features of lower limb bone geometry are associated with movement kinematics and clinical outcomes including fractures and osteoarthritis. Therefore, it is important to identify their determinants. Lower limb geometry changes dramatically during development, partly due to adaptation to the forces experienced during physical activity. However, the effects of adulthood physical activity on lower limb geometry, and subsequent associations with muscle function are relatively unexplored. The aim was to investigate associations of long-term exercise in adulthood with lower limb bone geometry parameters.

Methods

43 adult males were recruited; 10 young (20-35y) trained *i.e.,* regional to world-class athletes, 12 young sedentary, 10 older (60-75y) trained and 11 older sedentary. Skeletal hip and lower limb geometry including acetabular coverage and version, total and regional femoral torsion, femoral and tibial lateral and frontal bowing, and frontal plane lower limb alignment were assessed using magnetic resonance imaging. Muscle function was assessed recording peak power and force of jumping and hopping using mechanography. Associations between age, training status and geometry were assessed using multiple linear regression, whilst associations between geometry and muscle function were assessed by linear mixed effects models with adjustment for age and training.

Results

Trained individuals had 2° (95%CI:0.6°-3.8°; p=0.009) higher femoral frontal bowing and older individuals had 2.2° (95%CI:0.8-3.7°; p=0.005) greater lateral bowing. An age-by-training interaction indicated 4° (95%CI:1.4°-7.1°; p=0.005) greater acetabular version in younger trained individuals only. Lower limb geometry was not associated with muscle function (p>0.05).

Conclusions

The ability to alter skeletal geometry via exercise in adulthood appears limited, especially in epiphyseal regions. Furthermore, lower limb geometry does not appear to be associated with muscle function.

5.2 Introduction

Specific alterations to lower limb bone geometry are important factors that could lead to clinical problems such as fractures (Shin et al., 2017) and osteoarthritis (Do et al., 2020; Scorcelletti et al., 2020). Whereas increased femoral torsion, which is the angle between the femoral neck and the distal femur on the transverse plane, increases the risk of hip impingement, knee, and hip osteoarthritis, decreased anteversion increases the risk of femoral neck fractures (Scorcelletti et al., 2020). Increased lateral femoral and tibial bowing are also associated with increased incidence of knee osteoarthritis (Matsumoto et al., 2015; Shimosawa et al., 2018), and femoral and tibial fractures (Chen et al., 2014). Acetabular geometry and femoro-acetabular congruence have been shown to be relevant to hip osteoarthritis, dysplasia, and impingement (Dortmund Tönnis and Heinecke, 1999; Fujii et al., 2010). Therefore, given their clinical significance, it is important to identify key factors influencing components of lower limb geometry, and how the latter affects physical function.

Skeletal geometry is not only clinically relevant but also has an effect on movement biomechanics with femoral torsion affecting muscle lever arm length and the line of action of hip muscles (Scorcelletti et al., 2020), and hip shape having an impact on gait (Lewis et al., 2017) and hip range of motion (Ross et al., 2014). Increased femoral torsion affects kinematics during walking and landing (Scorcelletti et al., 2020), but little is known about how skeletal geometry affects components of physical function such as peak jump power relevant to clinical outcomes as well as sporting performance.

Lower limb geometry changes dramatically during childhood with femoral torsion decreasing by ~1.5° every year from the onset of walking until completion of growth is established (Scorcelletti et al., 2020). Varus bowing is also greatest at birth (+15°± 8), then

overcorrects to valgus alignment during the first years of life (-10°± 8) and stabilizes (-5°±8) later in development in healthy children (Salenius and Vankka, 1975). Mechanical loading in early life is a key determinant of bone shape development (Fabeck et al., 2002; Daly, 2007; Janz et al., 2014; Ireland et al., 2019; Saunders et al., 2020) and bone composition (Janz et al., 2001; Daly, 2007; Janz et al., 2014). Individuals who have conditions that do not permit normal gait during development, such as children with cerebral palsy, will often face lower limb misalignments such as increased femoral torsion, tibial torsion, valgus knee alignment and intoeing (Staheli et al., 1968; Fabry et al., 1973b; Bobroff et al., 1999a; Ward et al., 2006).

Modest changes in lower limb geometry continue to occur throughout adulthood. Bone cross-sectional area increases by ~15% from 20y to 90y (Riggs et al., 2004; Lauretani et al., 2008), whereas femoral torsion also appears to decrease by ~3° across a similar age range (Waisbrod et al., 2017; Inamdar et al., 2019; Pierrepont et al., 2019). Studies of athletes, who continue to train and compete, have been conducted to examine the effects of physical activity on adult bone cross-sectional geometry. Previous studies have identified greater tibia and femoral cross-sectional area in athletes rather than controls, with larger advantages in athletes competing in high-impact events (Nikander et al., 2005; Wilks et al., 2009a). These advantages appear to diminish with age, possibly because of lower muscular forces produced by older athletes (Wilks et al., 2009b). In addition, evidence from master tennis players suggests that the pattern of bone adaptation to exercise differs after skeletal maturity with the ability to adapt bone outer geometry (particularly in epiphyseal regions) substantially diminished compared to adaptations to exercise during development (Ireland et al., 2014a).

Whilst the effects of adulthood physical activity on lower limb bone cross-sectional geometry have been well explored, comparatively little is known about other clinically relevant aspects of lower limb geometry on the sagittal and frontal plane such as bowing, femoral torsion and acetabular geometry. For example, femoral bowing might be increased by prolonged squatting tasks or decreased by prolonged heavy lifting tasks due to farming activity in the order of magnitude of 1-3° (Do et al., 2020). Therefore, the primary aim was to examine the impact of continued participation in exercise during adulthood on lower limb geometry by comparing young and old sedentary individuals with young and old power athletes. In secondary analyses, I explored associations between femoral and tibial bone shape, and limb alignment on peak lower limb power and peak force during countermovement jumps and vertical hopping.

5.3 Methods

Study setting

The study was performed between September 2020 and May 2021 at the envihab facility (www.envihab.org) at the German Aerospace Centre in Cologne. The study conformed with the declaration of Helsinki. Prior to commencement, it had received ethical approval (Ärztekammer Nordrein, lfd.Nr. 2018269) and had been registered at the German clinical trials register (www.drks.de, registration number DRKS00015764. Recruitment focused on healthy adult males, considering age and training status of the participants. The inclusion criteria for this study were to be either 20-35 years of age (young group) or 60-75 years of age (old group) and male. The participants were selected from individuals either running ≥4 hours per week and participating in track and field competitions including sprinting, jumping, and throwing events (athletic, Table 5) or reporting ≤ 25 metabolic units of physical activity per week (sedentary). The body mass index for all participants was ≤ 25

kg/m². Combined groups of 24 individuals per age and training category (young/old, trained/untrained) would give over 75% study power to detect a large (0.8SD) difference between groups.

Initially, recruitment was planned for spring 2020, which had to be postponed due to the SARS-CoV-2pandemic. Recruitment was challenging due to travelling restrictions and suspected SARS-CoV-2 infections, and candidates were screened from the whole of Germany. Recruitment had to stop when the envihab facility became unavailable in June 2021. All participants gave their written informed consent prior to the testing session. Participants and/or the public were not involved in the design, or conduct, or reporting, or dissemination plans of this research.

Magnetic Resonance Imaging (MRI) scanning protocol

In this study, 5 sets of 52 cross-sectional images each were acquired from the left leg, hip and lower trunk reaching at least from the foot to the mid lumbar spine. Using a 3 Tesla Siemens Biograph MR, the images were recorded by means of a 6-echo DIXON turbo sequence with the following parameters: flip angle 5 °, TR 10 ms, TE1 1.35 ms, TE2 2.64 ms, TE3= 3.69 ms, TE4= 5.22 ms, TE5= 6.51ms, TE6= 7.80 ms, field of view 300 mm x 300 mm, voxel size of 1.17 mm x 1.17 mm x 5 mm. Only images covering the femur and tibia region were evaluated in this study.

The position of the participants was standardized with a foot-holder and soft wedges keeping the feet perpendicular to the table and the malleoli, epicondyles, and trochanter parallel to the table.

Image Analysis

MRI images were analysed using ImageJ (version 1.52h) as in Scorcelletti et al. (Scorcelletti et al., 2022). Total femoral torsion (FNA) was defined using the femoral neck line and

posterior condylar line. The femoral neck line was defined as the line between the centre of the femoral head and the centre of the shaft directly distal to the lesser trochanter. The posterior condylar line was defined as the line joining the posterior apices of the condyles in the image where the condyles were most prominent. Intertrochanteric torsion (ITT) was defined as the angle between the femoral neck line and the lesser trochanter line. The lesser trochanter line was defined as the line between the apex of the lesser trochanter at the peak of the lesser trochanter size and the centre of the femur just under the lesser trochanter. Torsion of the shaft (ST) was defined as the angle between the lesser trochanter line and the distal posterior shaft line, which is aligned with the flat surface of the distal posterior shaft immediately proximal to the posterior condyles. Condylar torsion (CT) is the angle between the posterior distal shaft line and the posterior condylar line (Figure 24). Intra-observer repeatability of the image analysis based on 3 repeated measures (assessed as intraclass correlation coefficient – ICC) of total femoral torsion, ITT, femoral lateral and frontal bowing, tibial torsion, tibial lateral bowing, mechanical axis, and femoral mechanical-anatomical angle were excellent (all ICC > 0.9). Reliability of CT (ICC:0.843), tibial frontal bowing (ICC:0.768), acetabular version (ICC:0.859) and acetabular coverage (ICC:0.855) measures were good.

To measure the lateral and frontal femoral bowing, the centre of the shaft was identified at four landmarks; immediately distal to the lesser trochanter, 1/3 the length of the proximal-distal shaft of the femur; 2/3 of the length of the proximal-distal shaft (the shaft is located between the cuts “c” and “d” in Figure 24) and at the intercondylar femoral notch. Similarly, the lateral and frontal tibial bowing was defined using the centre of the shaft at the intercondylar notch, the proximal third of the tibia, the distal third of the tibia at the distal tibial plateau. The two lines defining the mechanical axis angle were those connecting the centre of the femoral head and the intercondylar notch, and the

intercondylar notch and the centre of the distal tibial epiphysis. The two lines defining the femoro-tibial angle were those connecting the centre of the femoral shaft at the distal third of the femur and the intercondylar notch, and the intercondylar notch and the proximal third of the tibia.

The acetabular version and coverage were evaluated in the cross-section where the femoral head was largest. It was defined as the angle between the anterior and posterior acetabular margins of the acetabulum and the sagittal plane (Figure 24). Acetabular coverage was assessed as the angle between the posterior and anterior edge of the acetabulum and the centre of the femoral head.

To calculate the relative angle λ in the frontal plane, the coordinates of the desired reference points were calculated using Equation 2:

$$\lambda = arctan\left(\frac{\frac{ay-by}{ax-bx} - \frac{cy-dy}{cx-dx}}{1+\frac{ay-by}{ax-bx} * \frac{cy-dy}{cx-dx}}\right)$$

Equation 2

where "a" and "b" represent the proximal and distal reference points of the proximal axis respectively and "c" and "d" the proximal and distal reference points of the distal axis. “B” and “c” overlap in the case of the mechanical axis and femoro-tibial angle (Figure 24). “Y” and “x” on the other hand are respectively the antero-posterior coordinates, and the medio-lateral coordinates.

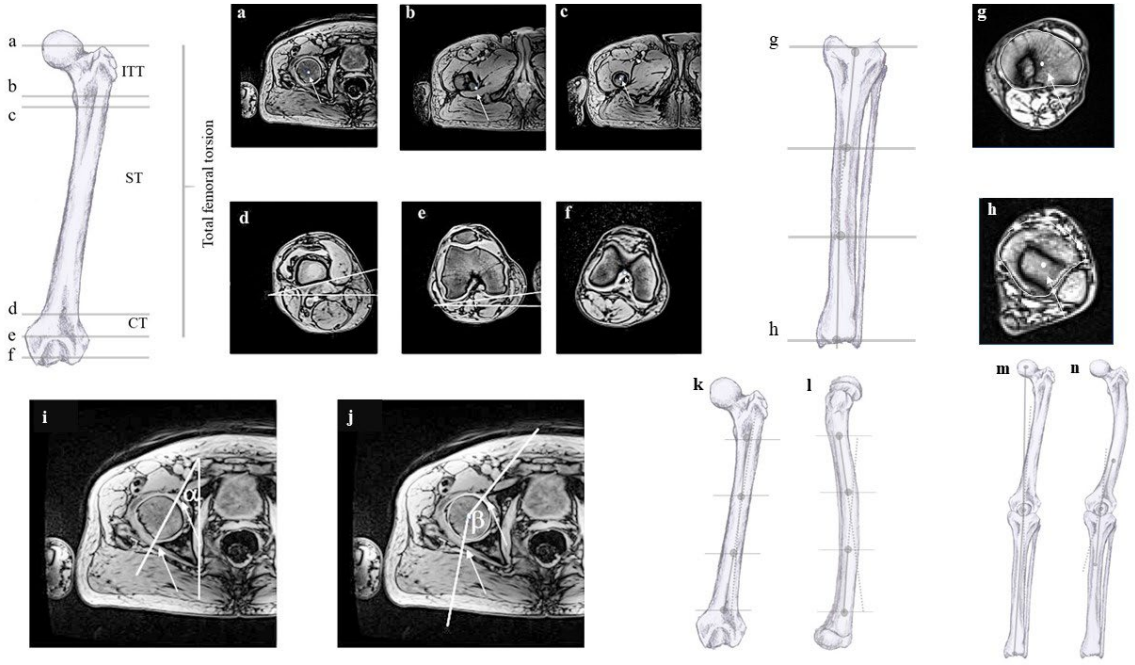

Figure 64 Angle definitions: a) femoral head centre, b) tip lesser trochanter, c) shaft centre, d) posterior distal shaft line, e) posterior condylar line, f) intercondylar notch. The angles measured in "d" and "e" have a horizontal line indicating the coronal plane as reference. Total femoral torsion is the angle between the line joining a and c and the reference in e. ITT is the angle connecting the landmarks in a-c and b-c, ST is the angle connecting c-b and the upper line in d, CT is the angle between d and c. g) and h) tibial lateral and frontal bowing landmarks. i) Acetabular version α and j) acetabular coverage β. The slice where the circumference of the femoral head was largest was chosen for analysis. The arrows show the rim of the acetabulum. k) femoral lateral bowing landmarks. l) femoral frontal bowing landmarks. m) mechanical axis landmarks. n) femoro-tibial angle landmarks. Figure adapted with permission from Scorcelletti and colleagues, illustrations by Xaali O'Reilly-Berkeley.

Functional performance

Total relative peak power and force were recorded during 3 countermovement jumps, multiple two-leg hopping, and multiple one leg hopping on a Leonardo Mechanograph® platform (Leonardo Mechanograph® v4.4b01.35). For the countermovement jumps, participants were asked to jump as high as possible, with limited aid from arms swing. For the hopping movements, participants were instructed to bounce on the ball of the foot with stiff knee and ankle joints. They initially began with lower intensity hops, and then over approximately 6-10 hops increased hop intensity until a plateau in peak force was evident. The countermovement jump with the greatest peak power was selected for

analysis, and the valid hop with the greater peak force was automatically selected by the software for analysis. Physical activity was assessed using the Freiburg questionnaire of physical activity (FrQ).

Statistical analysis

Data were examined using R studio (Version 1.4.1717 2009-2021 Rstudio, PBC, R kernel Version4.1.0). Multiple linear regression with age and training status as independent variables, as well as their interaction, was used to determine associations with femoral and tibial geometry, femoro-tibial alignment, and acetabular parameters (Mansournia et al., 2021). Alpha value for main effects was $p < 0.05$, and for interactions $p < 0.1$. Where interaction terms were not evident (beta value $p > 0.2$), the model was simplified to only include main effects. Linear mixed effects models with age and training status as random effects were used to determine main effects of bone geometry on jump and hop outcomes.

5.4 Results

Out of 43 male participants of the study, 22 were considered young (10 trained 24±2.2y, 12 sedentary 28.8±4.4y) and 21 old (10 Trained 65±4.1y, 11 Sedentary 66.9±5.3y). No differences were evident for height and weight between the 4 groups (Table 4).

		20-34 years old		**60-75 years old**		**Anova**
		10 Trained	*12 Sedentary*	*10 Trained*	*11 Sedentary*	*p-value*
Age (years)	*mean*	24	29	65	67	
	SD	2	4 (p=.005)	4	5 (p=.399)	
Height (cm)	*mean*	180.2	181.1	177.6	176.9	0.591
	SD	8.3	6.5	7.6	5.6	
Weight (Kg)	*mean*	77.4	73.6	84.8	79.9	0.655
	SD	14	13	33.8	8.9	
Activity level (MET)	*mean*	56.6	20.1	94.3	24.8	
	SD	21	42 (p=.595)	45.4	13.1 (p=.047)	
Relative jump power(W/kg)	*mean*	62.5	49.9	42.7	37.0	
	SD	6.5	10.0 (p=.003)	7.5	7.6(p=.115)	
Relative hop Force (N/kg)	*mean*	33.6	30.9	31.8	24.8	
	SD	4.9	3.3 (p=.170)	3.3	3.6 (p<.001)	
EFI %	*mean*	107.3	85.3	112.9	101.8	
	SD	8.9	18.0(p=.004)	16.6	20.3 (p=0.201)	

Table 4 Anthropometric data of the cohort. The activity level is based on the Freiburg questionnaire of physical activity. Age, activity level, relative to bodyweight power and force comparisons are done within the age group. The Esslinger Fitness Index (EFI) is an estimation of the physical fitness level normalized for sex and age, where 100% represents a typical value.

Information on self-reported metrics such as years of engagement in power disciplines, adherence to structured training regimens, and level of competition during youth have and self-reported personal best performance of the athletes been included (Table5 and 6)

	Subj ID	years competing in discipline	Weekly training hours	Years following structured training regimen	Competing at national level in Youth
Young trained 20-34 years old	1	15	18	12	Yes
	2	10	10	2	No
	3	8	10	8	No
	4	18	11	5	No
	5	5	10	8	No
	6	0	18	8	No
	7	8	11	8	Yes
	8	1	10	10	Yes
	9	5	9	8	Yes
	10	7	14	4	No
Older trained 60-75 years old	1	20	4	20	Yes
	2	52	7	45	Yes
	3	55	6	55	Yes
	4	5	10	5	Yes
	5	6	12	50	Yes
	6	30	8	40	No
	7	40	8	50	Yes
	8	10	14	5	Yes
	9	39	5	39	No
	10	6	6	8	Yes

Table 5 presents data pertaining to long-term exercise participation in two age groups: young (<35 years old) and old (60-75 years old) athletic individuals. Specifically, the table reports on the number of years that each participant has competed in their current best discipline, the number of weekly hours spent on training, the duration of following a structured training regimen, and whether the participant had engaged in sports at the national level during their youth, regardless of their current track and field discipline. The preliminary unpublished findings from the TaFMAC study. (https://www.dlr.de/me/en/desktopdefault.aspx/tabid-14088/), indicate that less than 20% of master athletes specialize in their latest discipline during their youth. Notably, in their youth, participants typically trained in team sports and achieved a good level of proficiency, as confirmed by the data in the last column of the table. This information serves to provide insight into the exercise habits of athletic individuals across different age groups.

Participant N.	**Young trained (20-34 years old)**			**Older trained (60-75 years old)**		
	Discipline	*Personal best performance*	AGP (%)	*Discipline*	*Personal best performance*	AGP (%)
1	100m Sprint	7.0sec. (60m)	91	200m Sprint	27.76sec.	88
2	100m Sprint	11.63sec.	84	200;400m Sprint	28.64sec.; 66.30sec.	90;89
3	100m Sprint	11.4sec.	86	400m Sprint	60.66sec.	89
4	100m Sprint	11.3sec	87	800m	2min.; 24sec.	91
5	100m Sprint	11.17sec	88	60m;100m Hurdles	9.86sec (60m)	92
6	100m Sprint	11.42sec.	86	Long jump	5.08m	108
7	100,200 m Sprint	NA	NA	Triple jump	11.82m	92
8	400m Sprint	50.7sec.	85	Triple jump	10.40m	79
9	Long jump	6.60m	74	Javelin	36m	65
10	Long jump	NA	NA	Pole vault	2.8m	78

Table 6 Discipline and self-reported personal best performances of the athletes. AGP – Age-graded performance, 100%+ world record, 90%+ world class, 80%+ national class,70%+ regional class, 60%+ local class. The percentages have been calculated according to 2010 world records.

Training status was associated with increased femoral frontal bowing with the trained group having 2° higher bowing (95%CI:(-3.8°) -(-0.6°); p=0.009) compared to the sedentary group. In addition, a training status by age interaction indicated a larger 4° (95%CI: (-7.1°)-(-1.4°); p=0.005) acetabular version in the athlete group only in young individuals. All other parameters were similar between groups (all p>0.13) (Table 7 and Figure 25).

Variable	p-value		
	Age	*Training*	*Interaction*
Total femoral torsion (°)	.204	.780	.713
ITT (°)	.360	.508	.449
ST (°)	.478	.839	.228
CT (°)	.454	.544	.638
Femoral lateral bowing (°)	**.005**	.063	.837
Femoral frontal bowing (°)	.695	**.009**	.475
Femoral mechanical anatomical angle (°)	.833	.502	.912
Tibial lateral bowing (°)	.957	.569	.694
Tibial frontal bowing (°)	.997	.917	.273
Mechanical axis (°)	.223	.622	.728
Femorotibial angle (°)	.178	.670	.817
Acetabular coverage angle (°)	.330	.134	.163
Acetabular version angle (°)	.847	**.005**	**.046**

Table 7 All p-values of the multiple linear regression with age and training status as independent variable. When the interaction was evident the p-value of the interaction is emboldened and the p-value for age and training of the interaction has been reported.

Ages showed an association with femoral lateral bowing with the older group having a 2.2° (95%CI:0.8-3.7°; p=0.01) higher lateral bowing compared to the younger group. Age had no association on all other studied parameters (p>0.17). Femoral and tibial geometry, and femoro-tibial alignment parameters were not associated with outcomes of countermovement squat jumps, two leg hopping and one leg hopping (Table 8).

Variables	**Relative peak power countermovement squat-jump**			**Relative peak force two leg hopping**			**Relative peak force one leg hopping**		
	Estimates	*CI*	*p*	*Estimates*	*CI*	*p*	*Estimates*	*CI*	*p*
Total femoral torsion (°)	-0.06	-0.31-0.19	.632	-0.22	-0.53 – 0.09	.161	-0.01	-0.13-0.11	.852
ITT (°)	-0.09	-0.32-0.15	.483	-0.21	-0.51 – 0.09	.167	-0.06	-0.18-0.05	.298
ST (°)	0.11	-0.14-0.36	.898	-0.9	-2.02 – 0.22	.110	0.04	-0.08-0.16	.496
CT (°)	0.20	-0.70-1.09	.670	0.15	-0.16 – 0.47	.325	-0.33	-0.75-0.09	.134
Femoral lateral bowing (°)	0.44	-0.69-1.57	.214	1.18	-0.19 – 2.56	.090	0.06	-0.48-0.61	.820
Femoral frontal bowing (°)	-0.54	-1.52-0.44	.290	-0.22	-1.48 – 1.03	.722	0.12	-0.36-0.60	.630
Tibial lateral bowing (°)	-1.14	-2.28-0.00	.058	-0.68	-2.21 – 0.85	.374	0.09	-0.49-0.67	.771
Tibial frontal bowing (°)	-0.01	-0.78-0.75	.974	0.02	-0.95 – 0.99	.971	0.14	-0.22-0.51	.447
Mechanical angle (°)	0.58	-0.47-1.64	.283	0.6	-0.76 – 1.96	.382	-0.04	-0.56-0.48	.879
Femorotibial angle (°)	-0.14	-1.17-0.88	.789	-0.6	-1.91 – 0.70	.355	0.02	-0.47-0.52	.932
Acetabular coverage angle (°)	-0.22	-0.48-0.17	.347	0.06	-0.86 – 0.99	.892	-0.07	-0.23-0.09	.338
Acetabular version angle (°)	-0.16	-0.99-0.55	.575	-0.15	-0.56 – 0.27	.474	0.18	-0.18-0.55	.377

Table 8 Associations between femoral and tibial geometrical parameters and measures of muscle function assessed in this study. In the table the estimates are presented as the unstandardised regression coefficients, confidence intervals of the regression coefficients (CI) and significance (p-value) of the linear mixed effects. The muscle function parameters have been normalised to the participants' body mass. Relative power has been considered for the countermovement squat jump. Relative peak force has been considered for the two hopping movements. Linear mixed effects model with age and training status as random effects was used to determine main effects of bone geometry on jump and hop outcome. Intertrochanteric Torsion (ITT), Shaft Torsion (ST), Condylar Torsion (CT).

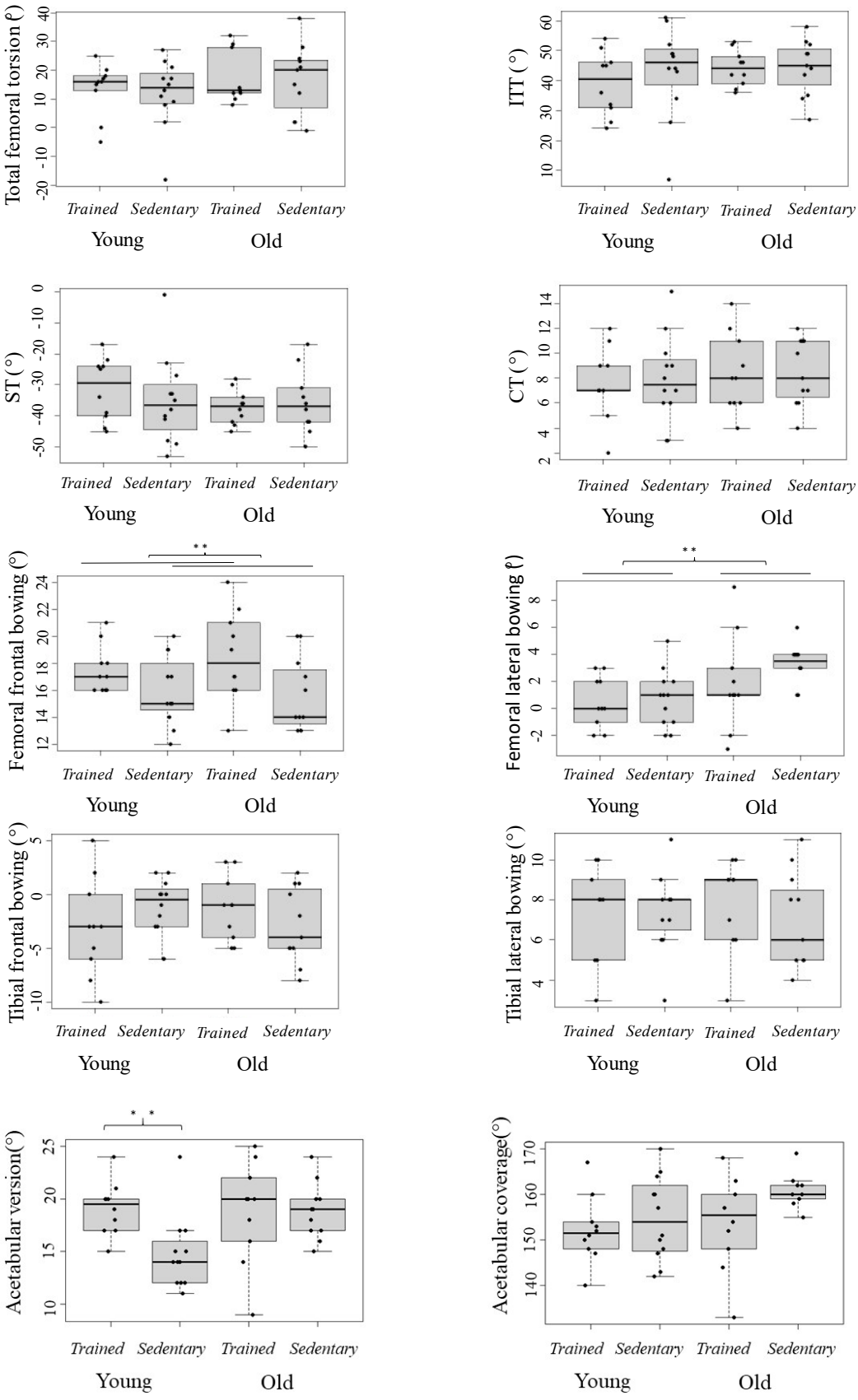

Figure 75 Box plots with interquartile range of femoral and tibial parameters grouped into relevant age and training status. ITT is the intertrochanteric torsion, ST the shaft torsion and CT the condylar torsion.

5.5 Discussion

This study measured acetabular and lower limb bone geometry, and lower limb alignment in in a cohort of young (>35y) and older (>65y) track and field power athletes and sedentary individuals. The primary aim was to identify associations between long-term participation in exercise and lower limb geometry in young and older adults. Being an elite track and field athlete was associated with 2° higher femoral frontal bowing regardless of age. In addition, participation in competitive track and field power events, was also associated with age-dependent associations for the acetabular version, with the athlete group having a 4° higher anteversion only in young adults. Age was also associated with femoral shape with the older group having 2.2° higher femoral lateral bowing. The secondary aim was to identify associations between lower limb geometry and peak power and force output during compound movements such as squat jump and vertical hopping.

A number of studies have identified differences in gross lower limb bone morphology between younger athletes and non-athletes, attributable to differences in exercise and associated loading throughout development. Professional ballet dancers had higher neck-shaft angles and lower acetabular version than non-athletes (Mayes et al., 2017). Similarly, elite young adult gymnasts had a greater neck-shaft angles than age-match controls (Papavasiliou et al., 2014). However, studies examining associations between participation in long-term exercise in adulthood and skeletal morphology are scarce. Previous work examining associations of work-related physical activity with femoral bowing found the same magnitude as the current study (Do et al., 2020).

Whilst several studies have characterised the dramatic changes in bone morphology which occur during childhood, changes in adulthood remain relatively unexplored. A large study in a Chinese population observed small differences of 1.6° greater neck-shaft angle and

lower acetabular version in younger adults (<60) compared to older adults (>60 years) (Jiang et al., 2015). However, details of mean age were not given so it is not possible to understand what time gap this association represents. Other studies suggest that femoral torsion decreases during adulthood (Waisbrod et al., 2017; Pierrepont et al., 2019). In contrast, another large study found no difference in neck-shaft angle with age (Gilligan et al., 2013), although this could be explained with variation introduced by the inclusion of samples from a variety of geographical regions and different historical periods. In accordance with these findings, a previous study observed similar age-related differences in femoral bowing (Do et al., 2020).

The absence of pronounced differences in lower limb bone morphology with age and exercise could be related to physeal closure. In previous work, it was demonstrated that the mechanoadaptive capacity of bone was markedly reduced when exercise was commenced following skeletal maturity compared to younger starters (Ireland et al., 2014a). In particular, epiphyseal regions seemed to be most affected which may explain the absence of differences in features such as FNA. In contrast, the diaphysis retained some ability to alter its geometry in response to loading which could account for the small differences in femoral bowing. Indeed, similar effects with age are supported by previous work showing continued reshaping of the periosteal and endocortical borders throughout adulthood (Riggs et al., 2004; Lauretani et al., 2008). This could explain the finding of age-associated differences in shaft bowing, which could arise from remodelling of the diaphyseal borders.

The physiological characteristics of master athletes have been well characterised, and it is clear that regular participation in athletic power events is associated with improved health and function (Tanaka et al., 2011). Further to that, recent longitudinal studies suggest that many of the advantages in indicators of musculoskeletal health such as bone strength and

lower limb power are maintained with age (Ireland et al., 2020). The current data suggest that any additional benefits to whole-bone geometry are limited. Whilst the higher femoral bowing evident in master athletes is associated with increased risk of rare, atypical femoral fractures (Haider et al., 2019), its relationship with overall fracture risk is unknown. However, importantly these data also do not indicate any negative effects which may negate advantages to other aspects of musculoskeletal health.

Previous literature reported associations between bone shape parameters, neuromuscular function, and biomechanics. For example, total femoral torsion was associated with differences between muscle activation patterns (Nyland et al., 2004), lever arms of the hip muscles (Scheys et al., 2008; Kim et al., 2012; Li et al., 2014) and disadvantageous kinematics during landing (Howard et al., 2011). However, in the current study I did not observe any associations between bone geometry and clinically relevant muscle function outcomes. Muscle function can adapt dramatically in response to physical activity and exercise even in older age (Borde et al., 2015), whereas the current study suggests that the potential for exercise-related adaptations in bone geometry during adulthood is very limited. Therefore, characteristics other than bone geometry may be more important determinants of muscle function in adulthood.

Research implications

Given the greater plasticity of the skeletal system during development, future work should assess associations between bone geometry and muscle function in children and adolescents.

Limitations

As a cross-sectional study, I was unable to attribute causality and it may be that minor associations observed result from differences in other, unmeasured characteristics. Given the evidence of skeletal adaptation to exercise during childhood it may be that differences in early life activity contributed to observed differences and such information would have been difficult to retrieve accurately. Nonetheless, to partially address this concern, self-reported metrics such as years of engagement in power disciplines, adherence to structured training regimens, and level of competition during youth were collected (Table5). However, they do not detail the type or intensity of training which may have also contributed to observed differences. In addition, the study was not powered to detect minor associations of exercise and age with measured geometrical parameters.

Conclusions

Modest differences in frontal bowing between athletes and non-athletes, and modest differences in acetabular version and femoral angle between young athletes and controls were observed. The site-specific nature of these differences may highlight some retained ability to adapt bone shaft geometry in adulthood whereas epiphyseal geometry is largely fixed. Therefore, the ability to alter skeletal geometry via exercise in adulthood appears limited reinforcing the importance of physical activity during development as a strategy to optimise life-long skeletal health. Conversely, skeletal geometry does not appear to be a determinant of muscle function in adulthood. This may in part explain why strategies to improve muscle function remain effective even into old age.

Chapter 6 General Discussion

The aim of the work within this thesis was to identify an appropriate method to assess femoral torsion in both children and adults. Thereafter, to examine key determinants of variation in femoral torsion and the consequences of altered torsion for health and function. I reviewed the literature to identify appropriate methods for a variety of purposes. I developed a novel technique theoretically suitable for children and infants which needs further improvements. Furthermore, I characterised lower limb skeletal geometry in individuals with XLH, and young and old track and field power athletes. Additionally, I explored to what extent hip, femoral and tibial shape parameters are interrelated.

Femoral torsion can vary greatly between subjects and has an effect on hip biomechanics, such as changing moment arm lengths and how the hip joint is loaded. Development of femoral torsion appears to be strongly influenced by mechanical forces experienced during everyday movements (Shefelbine and Carter, 2004). This is evidenced by large differences in femoral torsion in groups where movement is impaired, such as children born breech (Frysz et al., 2020) or individuals with neuromuscular conditions such as cerebral palsy (Bobroff et al., 1999a). Further studies have outlined that femoral torsion is the result of torsion occurring along the femur at regional level independently (Seitlinger et al., 2016; P. W. Ferlic et al., 2018; Archibald et al., 2019). Furthermore, it has been associated with other lower limb geometrical parameters including acetabular version (Akiyama et al., 2012), femoral lateral bowing (Liu et al., 2021), tibial torsion (Fabry et al., 1973b) and knee valgus alignment (Li et al., 2022).

6.1 Method identification

The first stage to achieving the original aim was to identify an accurate method. The literature review outlined several methods to assess femoral torsion. The chosen landmarks and the definition of total femoral torsion can result in discrepancies in measurements by up to 20° in the same participant. Furthermore, there is evidence that total femoral torsion occurs throughout the femur at the two epiphyses and diaphysis (Seitlinger et al., 2016; Waisbrod et al., 2017; Archibald et al., 2019).

CT, MRI, and ultrasound are commonly used to assess femoral torsion and they all have their strength and weaknesses. CT uses ionising radiation and is therefore not suited for screening or longitudinal assessment in children and infants especially when the whole three-dimensional lower limb needs to be imaged. However, X-ray attenuation is very different between mature bone and soft tissue and is therefore ideal for diagnosis of skeletal conditions. MRI uses magnetic fields and radio frequencies to generate images and is therefore free from ionising radiation, which makes this ideal for screening and longitudinal studies where multiple scans are needed for research purposes. However, MRI scanning of the whole lower limb has been reported to take up to 45 minutes if three-dimensional rendering of the femur is required (Botser et al., 2012) and is therefore not suited for scanning children and infants without sedation. At DLR scanning times were about 20 minutes with a slice thickness of 4mm and future improvements might decrease MRI scanning times. Whilst both radiation and the need for sedation present challenges even in clinical scanning, they present an additional ethical burden when proposed in non-clinical studies such as this. MRI is also often not available in all clinics due to its elevated costs of space, money, and qualified personnel. Therefore, MRI and CT were not ideal for application in these studies.

Ultrasound uses sound waves to generate images, and it does not permeate mature bone permitting only the identification of the surface of skeletal structures. Whilst ultrasound is relatively cheap compared to CT and MRI and image acquisition is fast, test-retest reliability is only moderate (Terjesen and Anda, 1987; Elke et al., 1991; Aamodt et al., 1995; Tomczak et al., 1997), not allowing the accurate detection of the yearly decrease in the order of 1.5° in total femoral torsion. Alternatively, when a coordinate system, such as motion caption, is added to track the ultrasound probe in three dimensions, the now "Free-hand" ultrasound has excellent reliability (Passmore et al., 2016a; Greatrex et al., 2017). Although, the equipment costs, set up time, image acquisition time and post processing time increase drastically. Therefore, I decided to investigate further development of these systems to make them more applicable in my planned studies..

6.2 Method development

Functional methods, where the participant is required to lay relaxed and an operator rotates the leg of the participant, such as the internal range of motion test and the trochanteric prominence angle test (TPAT) have shown good prediction of low, normal, and high femoral torsion (Muhamad et al., 2012; Chadayammuri et al., 2016; Uding et al., 2019) with an inter-observer ICC of 0.89 for the internal range of motion test, and 0.81 for the TPAT (Chung et al., 2010). However, the measurement of the total femoral torsion in scalar data and not in class data reveals a correlation regression coefficient with data yielded by a gold standard method, ranging from 0.12 to 0.85 (Chung et al., 2010; Sangeux et al., 2014; Uding et al., 2019) and is therefore not applicable for purposes investigating yearly developments in the order of ~1.5°.

Two exploratory measures were tested to increase the precision of functional tests. One involved coupling functional methods with motion capture (Vicon), with the aim to define

the whole sphere determined by the ROM of the hip. The second involved the combination of the TPAT and an ultrasound device: the palpation of the greater trochanter needed for the TPAT was substituted with the US imaging of the greater trochanter while rotating the participants leg on the longitudinal axis of the femur. Through this approach I was able to track the movement of the apex of the greater trochanter and define the circle it created considering the femoral head as the rotational centre (Figure 26). However, both of these exploratory measures were soon dismissed, as the poor precision of the approach meant that these measures would have not been suitable for the purposes of the PhD.

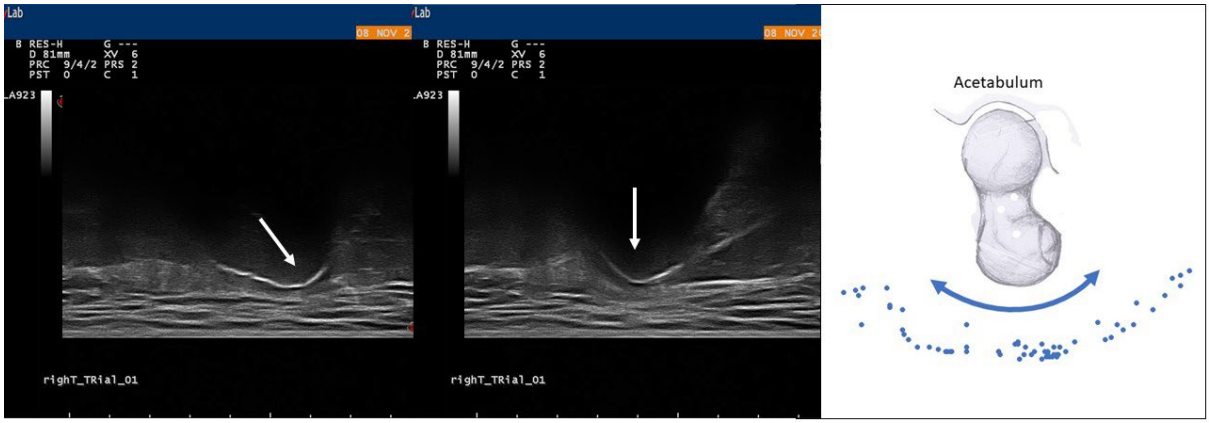

Figure 26 Left and middle panel are two separate frames of the US tracking of the apex of the greater trochanter. The arrows indicate the greater trochanter. Right panel: the blue dots represent the defined point on the greater trochanter identified and annotated manually. The same point was tracked through the range of motion of the internal and external rotation of the femur. On the X and Y-axis, the coordinates of the axial view are presented. The plane corresponds to the axial plane. The imaginary X being laterally to the thigh and Y frontally.

At this stage, the focus was directed towards 3D free hand ultrasound, coupling a standard ultrasound with a motion caption system. I contacted the leading researcher in this area which developed a system called Orthopilot. This commercial system composed of a regular ultrasound and a two infrared camera system tracking reflective markers on the US probe, which was able to measure total femoral torsion. However, an agreement with the company could not be found to access the software and obtain raw data which would allow deeper understanding of the femoral torsion measurements and allow broader assessment

of proximal femoral shape (i.e. regional torsion, femoral head size, femoral neck length, acetabular parameters) and the method was therefore discarded. A collaboration was arranged with the university of Sheffield working on a free hand US method, using a 10 infrared Vicon camera system (Greatrex, 2019). However, I soon recognised that the infrastructure needed for this method was too time-consuming to allow large-scale data collection, and not applicable in clinical settings.

Since the original aim of the PhD project was to develop a method which was viable in children and infants and the immature bone is transparent to ultrasound, I arranged a collaboration with the Kinderklinik (children's clinic) at the university hospital Cologne. In Germany, a routine test is done in infants to screen for hip dysplasia, and I was allowed to observe screening tests and collect various views of the infant's hip (Figure 27).

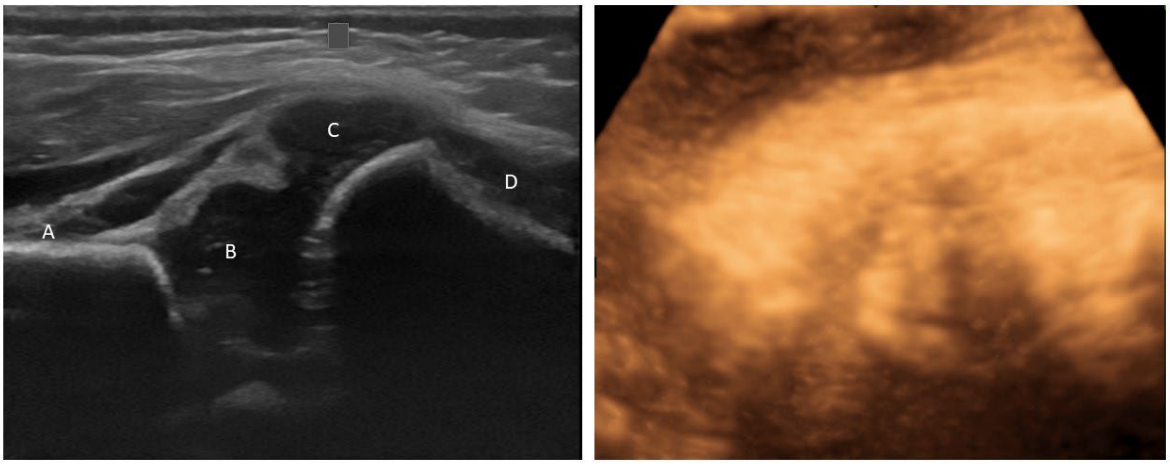

Figure 87 Left panel ultrasound of the femoral neck in the coronal plane. The probe surface is at the top of the image. Notice that you can see through the proximal femur. A: ilium; B: femoral head; C: trochanter; D: femoral shaft. The right panel shows the proximal femur with the current 3D imaging technology available in the US scanner. Notice the poor image quality in the right panel compared to that in the 2D image on the left.

After exploring the possibility to couple ultrasound methods with functional methods and motion caption systems, I identified FAROARM® as a coordinate measurement system

suitable for the purpose of locating features of the two-dimensional ultrasound scanner in a three-dimensional space.

The US-FAROARM® repeatability pilot study resulted in only moderate (ICC = 0.615) to poor (ICC= 0.329) reliability for femoral length and femoral torsion, respectively. Current three-dimensional ultrasound methods, although more expensive and time-consuming in their collection and analysis, yield excellent repeatability (ICC>0.90) (Passmore et al., 2016a; Greatrex et al., 2017). The theoretical combined spatial resolution of the US-FAROARM® is lower than 0.1 cm and does not justify a moderate to poor repeatability. The main source of error was the difficulty to identify the landmarks of interest during the analysis of the two-dimensional US video, without the context of the position of the probe relative to the body of the tested individual. This limiting factor can be solved in future studies by recording a trigger signal when the assessor has identified the landmark of interest. Alternatively, the reconstruction of a three-dimensional model by interpolating images would have allowed the contextualisation of the landmarks of interest relative to the individuals hip and femur. The second stage to achieving the original goal was to further develop the US-FAROARM®. I planned a validity study at DLR to examine the various definitions of femoral torsion using a three-dimensional reconstruction using US-FAROARM® and MRI data which is currently the gold standard for musculoskeletal imaging. The Medical Council of North Rhine did not grant us ethical approval to conduct the validity study as this was classed as a medical device development, with the obligation of following a separate ethical application involving external audits and sponsors. That would have required much more time and funding, both of which were not available in the PhD project. I therefore began to work on a more developed clinical validation study, but shortly after the rejected application Germany and the United Kingdom went into full lockdown and a contingency plan had to be put into place.

6.3 Lower limb bone geometry in adult individuals with X-linked hypophosphatemia: an observational study

The German Aerospace Agency in collaboration with the University of Wuerzburg was planning the collection of lower limb MRI data in individuals with XLH to evaluate muscle fatigue and physical performance in XLH vs healthy control. Specifically, individuals with XLH experience skeletal issues, including short stature, limb deformities, joint problems, and early onset of osteoarthritis (Francis et al., 1995; Carpenter et al., 2011; Lambert et al., 2019; Steele et al., 2020). Common deformities include bowing of the femoral shaft, varus, and valgus alignment (Horn et al., 2017) and abnormal tibial torsion (Steele et al., 2020). Objective characterisation of bone geometry in this cohort was not available in the literature at that time. Therefore, I established a collaboration to collect and analyse MRI data evaluating clinically-relevant aspects of lower limb and hip geometry, including femoral and tibial torsion, femoral and tibial shaft bowing, bone cross-sectional area CSA, acetabular version and coverage was put in place.

Large differences in clinically-relevant measures of tibia and particularly femur bone geometry were observed in individuals with XLH compared to controls. Specifically, individuals with XLH exhibited lower femoral torsion compared to healthy controls. Further analysis on regional femoral torsion, revealed that lower proximal, intertrochanteric torsion was the main contributor to the finding. Altered torsional parameters of the femur have shown to change the lever arms of hip muscles contributing to waddling gate (Horn et al., 2017), and increased risk of early onset of osteoarthritis commonly experienced in this cohort (Hardy et al., 1989; Skrinar et al., 2019). This is clinically important as femoral osteotomy is often considered in individuals with XLH (Sharkey et al., 2015), and to date, surgical protocols focus on frontal plane deformities (Carpenter et al., 2011; Gizard et al., 2017; Horn et al., 2017). Assessment of total and regional torsion should inform

development of future surgical guidelines. Additionally, femoral, and tibial bowing were greater in people with XLH despite all individuals but two, underwent at least one corrective surgery during their lifetime. These differences may plausibly contribute to clinical manifestations of XLH such as early onset osteoarthritis, pseudo fractures and altered gait and therefore should be considered when planning corrective surgeries.

6.4 Associations between long-term exercise participation and lower limb bone geometry in young and older adults

Whilst lower limb geometry changes significantly during childhood, including a yearly decrease in femoral torsion of ~1.5° (Tönnis and Heinecke, 1991a; Fabry et al., 1994) and varus bowing overcorrection of ~25° during the first years of life, little is known about lower limb geometry changes during adulthood. Evidence shows bone cross sectional area increasing by ~15% (Riggs et al., 2004; Lauretani et al., 2008) and femoral torsion decreasing by ~3° from 20 to 90 years of age (Waisbrod et al., 2017; Inamdar et al., 2019; Pierrepont et al., 2019). Mechanical loading in early life is a key determinant in bone shape development (Fabeck et al., 2002; Daly, 2007; Ireland et al., 2019) and bone composition (Janz et al., 2001; Daly, 2007). Studies in adult athletes have established a mechanoadaptive capacity even in the mature bone, including greater tibial and femoral bone cross sectional area in athletes compared to control, with larger adaptations in athletes participating in high impact events (Nikander et al., 2005; Wilks et al., 2009a). Whilst effect of physical activity during adulthood on bone cross sectional geometry is well explored, rather few studies have explored other clinically relevant parameters of lower limb geometry.

Therefore, an additional collaborative study was initiated with the German Aerospace Agency to assess skeletal geometry in young and master athletes and controls. I added a

three-dimensional analysis of whole lower limb MRI scans, including acetabular version and coverage, femoral and tibial total and regional torsion, femoral and tibial frontal and lateral bowing, and lower limb alignment. Additionally, I examined associations of lower limb geometry parameters and muscle function. Trained individuals had 2° higher femoral frontal bowing and older individuals had 2.2° higher lateral bowing. An age-by-training interaction indicated 4° greater acetabular version in trained individuals in the young group only. Lower limb geometry measures such as acetabular coverage and version, femoral torsion, femoral bowing, and leg alignment were not associated with peak power and force during a squat jump and single leg hopping. The ability to alter skeletal geometry via exercise in adulthood is limited. This reinforces the importance of exercise during development as a strategy to optimise life-long skeletal health. Furthermore, lower limb geometry does not appear to be associated with peak muscle function. This outcome is unexpected considering that a decreasing femoral torsion is associated with a longer lever arm for hip extensor muscles (Scheys et al., 2008). In addition, muscular activation patterns are affected by changing femoral torsion parameters (Nyland et al., 2004) and changes in femoral and hip shape leads to altered movement mechanics including during gait (Scheys et al., 2008; Uemura et al., 2018) and in landing kinematics (Howard et al., 2011), as well as affecting contact and shear forces of the femur (Pritchett and Perdue, 1988; Fishkin et al., 2006; Altai et al., 2021).

6.5 Femoral torsion vs broader description of geometry

Total femoral torsion clearly changes depending on the mechanical environment it develops in. During gestation femoral anteversion increases by 30° (Watanabe, 1974; Walker and Goldsmith, 1981) and more so when the foetus finds itself in a forced internally rotated position of the hip joint, such as in the case of breech presentation (Wilkinson,

1962). Total femoral anteversion decreases when loading is applied with the onset of walking by ~1.5° a year (Svenningsen et al., 1989; Tönnis and Heinecke, 1991a; Fabry et al., 1994), a greater decrease is seen in obese children (Galbraith et al., 1987) and little to no decrease is found in children with motor development disorders such as cerebral palsy (Fabry et al., 1994; Bobroff et al., 1999a). Femoral anteversion is greater also in other cohorts with conditions affecting neuromuscular development including Down syndrome (Shaw and Beals, 1992) and Charcot-Marie-Tooth disease (Novais et al., 2014). Interestingly, there is evidence of femoral torsion occurring throughout the femur independently, at the intertrochanteric level, through the diaphysis and at the condylar level (Seitlinger et al., 2016; Waisbrod et al., 2017; Archibald et al., 2019), thereof suggesting different aetiologies and distinct biomechanical relevance (Kim et al., 2012; Seitlinger et al., 2016). However, it is not clear to date what the mechanical determinants of a high rather than low femoral anteversion are, whether it is the reaction forces of gait during development as suggested by Fabeck (Fabeck et al., 2002), or the torque of hip muscles on the femur. In the first scenario, the reaction forces going through the femur are multifactorial and depend on other geometrical parameters from the hip down including acetabular geometry, femoral neck inclination and length, femoral lateral and frontal bowing, lower limb alignment and tibial torsion and bowing. For example, high femoral torsion has been suggested to be compensated by external tibial torsion (Fabry et al., 1973b) and is indirectly associated with valgus knee alignment during landing (Howard et al., 2011). Additionally, often, only few parameters are considered when planning surgery without considering the lower limb as an ensemble to name a few examples, regional torsion is not accounted for when doing derotational osteotomies (Seitlinger et al., 2016; Ferlic et al., 2018) and frontal plane deformities, such as those seen in individuals with XLH, are planned on frontal plane radiographs (Carpenter et al., 2011; Gizard et al., 2017; Horn

et al., 2017) without considering the sagittal and axial plane. Therefore, in these studies I comprehensively analysed lower limb shape parameters on the frontal, sagittal, and axial plane.

Lower limb geometry was characterised and is different across all three planes in individuals with XLH compared to healthy controls. This finding is in line with the current literature and with the soft bones of this clinical cohort. Interestingly, total femoral torsion is lower in the XLH cohort, suggesting a greater decrease than the ~1.5° yearly decrease in femoral torsion found in the literature for the healthy population. Intertrochanteric torsion seems to be the main contributor to this axial plane finding, suggesting a greater malleability of the femoral neck in individuals with XLH. I also comprehensively characterised lower limb bone geometry in young and old sedentary adults and young and old track and field power athletes to examine the associations of long-term exercise in adulthood on joint shape. Only relatively small differences across groups in the frontal and sagittal plane of the femur and acetabulum have been established. The magnitude of the associations of femoral frontal and lateral bowing with physical activity and age is consistent with the literature (Shimosawa et al., 2018; Do et al., 2020) and discussed in the next paragraphs. Although the present study did not find significant associations between geometrical parameters on the transverse plane, particularly femoral regional torsion parameters, and physical activity and age, it is important to consider the high level of variability of the measure and the limited statistical power of the study to detect minor associations. Moreover, this finding is not consistent with the current literature regarding age-related changes in femoral torsion (Inamdar et al., 2019; Pierrepont et al., 2019), and the relationship between physical activity and femoral torsion has not been explored yet. This observation is further expounded in the subsequent paragraphs.

Further analysis of the lower limb geometrical data of both studies did not identify any correlation of axial plane parameters with frontal or sagittal plane parameters *(p>0.2)* contrary to suggestions of the current literature that found a positive corelation of femoral anteversion with lateral femoral bowing on a cohort of 381 individuals (Liu et al., 2021), and a week association (r<0.13) of femoral lateral bowing with valgus femoro-tibial alignment on two sample sizes of 1538 and 143 limbs (Cho et al., 2018; Lu et al., 2019). Although this study did not find any inter-relationships between different geometric features, including acetabular version and coverage, femoral regional and tibial torsion, femoral and tibial lateral and front bowing, and femorotibial alignment, the sample size was too small to identify minor associations, and therefore it is not possible to draw any meaningful conclusions from it. However, it seems that the analysed clinically-relevant features of lower limb geometry may be independent of each other. This may suggest that differences in regional loading contribute to lower limb geometry, and surgical or other interventions should consider the independence of these features. Future studies with large cohorts should comprehensively analyse associations of multiple lower limb geometrical parameters to identify their possible biomechanical aetiologies.

6.6 Mechanoadaptation

The pattern of bone cross-sectional shape adaptations to mechanical loading in early life are well known (Fabeck et al., 2002; Janz et al., 2004; Daly, 2007; Ireland et al., 2019; Saunders et al., 2020). In contrast, childhood adaptation of whole bone shape is less well-explored; femoral torsion decreases by ~1.5° yearly (Fabry et al., 1973b; Svenningsen et al., 1989; Tönnis and Heinecke, 1991a) and varus alignment changes by 25° (Holt et al., 1954; Salenius and Vankka, 1975) from onset of walking until completion of growth. Individuals with conditions that do not permit normal motor development will often face abnormal

shape development including femoral and tibial torsion and limb misalignments (Staheli et al., 1968; Fabry et al., 1973b; Bobroff et al., 1999a; Ward et al., 2006). Modest changes can be seen after full skeletal maturity, including a decrease of ~3° in femoral torsion (Inamdar et al., 2019; Pierrepont et al., 2019) and an increase in femoral lateral bowing of a similar magnitude (Shimosawa et al., 2018). Whilst previous studies have explored the impact of physical activity on cross sectional geometry of bones (Nikander et al., 2005; Wilks et al., 2009a), its effect on whole lower limb geometry in adulthood remains unexplored.

No associations were observed on the axial plane for high impact exercise and age. I identified an association of high impact exercise with femoral frontal bowing of the magnitude of 2°, which is of a similar magnitude of that previously observed with low impact exercise (Do et al., 2020). I also found an association of age and femoral lateral bowing consistent with previous literature (Shimosawa et al., 2018).

Previous research demonstrated that the mechano-adaptive capacity of exercise is reduced after skeletal maturity (Ireland et al., 2014b). Particularly, bone outer geometry in epiphyseal regions appeared to become un-responsive to mechanoadaptation after skeletal maturity, which may explain why I observed no associations between exercise and intertrochanteric torsion. The diaphysis, however, retains the ability to modify its geometry as a result of loading, which may explain the small differences in femoral bowing. In fact, prior work has shown that the endocortical and periosteal borders continue to reshape throughout adulthood (Riggs et al., 2004; Lauretani et al., 2008). However, it does not seem that chronic high impact exercise has an effect on the diaphysis of greater magnitude than aging or low impact exercise.

6.7 Future research

MRI and CT scanners have clear limitations regarding the study of infants and children. Not only are they expensive and un-available in many settings, but they represent a barrier in scanning children and infants as MRI requires individuals to lay still in a claustrophobic space for a relatively long time, and CT exposes participants to radiation. Ultrasound methods, on the other hand, do not have the desired accuracy to reliably study bony adaptations of the magnitude of lower than 10°. Free-hand ultrasound systems provide promising reliability for three-dimensional measures, but the hardware needed for existing approaches is expensive and not employable in clinics. Furthermore, data collection and post-processing times are long. The optimisation of the US-FAROARM® is important for both, basic and clinical science research. The US-FAROARM® represents a quick and inexpensive device that necessitates of little post data-processing time. In the current thesis, the US-FAROARM® has been studied in its primordial state, selecting landmarks on a two-dimensional US B-mode video. Future studies will interpolate the frames of the video and use query generative networks to reconstruct a three-dimensional model of the scanned object.

There is a lack of understanding of the determinants of whole lower limb bone shape, which is clinically important given associations between these characteristics and important clinical outcomes such as osteoarthritis (Fujishiro et al., 2014; Matsumoto et al., 2015; Shimosawa et al., 2018; Inamdar et al., 2019; Do et al., 2020), atypical fractures (Gelberman et al., 1986; Shin et al., 2017) and hip dysplasia (Li et al., 2014; Lerch et al., 2018). Work presented in this thesis suggests that large changes in whole-bone shape happen only throughout skeletally immature individuals of and only irrelevant changes occur after skeletal maturity even with application of chronic high-impact exercise. Longitudinal imaging studies in the skeletal immature are needed to track whole lower limb bone shape

parameters, and explore associations with possible factors affecting skeletal lower limb shape including weight (Galbraith et al., 1987), movement analysis parameters (Fabeck et al., 2002) and muscle strain (Haike, 1964; Yadav et al., 2017) and physical activity level (Janz et al., 2004).

Additionally, although observed differences in lower limb skeletal geometry between sedentary and high impact discipline athletes were minimal, a further study should address differences of lower limb bone geometry in individuals exposed to long-term disuse or movement impairment such as spinal cord injury or cerebral palsy. Whilst the effects of disuse on bone composition and cross-sectional bone geometry have been extensively studied (Rittweger et al., 2006; Varzi et al., 2015; Abdelrahman et al., 2021), to our knowledge no studies have been conducted on three-dimensional shape analysis.

Overall, the work presented has considerable strengths. The novel whole-limb assessment of geometry allowed the objective description of three-dimensional bone shape in greater detail than previous studies. Furthermore, this allowed novel assessment of the relationships between different shape components to be performed. I also used detailed characterisation of multiple components of muscle function to assess their relationship with skeletal geometry. The XLH and athlete studies recruited well-characterised individuals for assessment. One of the weaknesses of these studies is the relatively small sample sizes, which only gave the study power to detect larger effect sizes. Whilst the imaging assessments used showed good reliability, some aspects have not been clinically validated either by our group or others.

6.8 Conclusions

The work presented in this thesis has developed novel insights into assessment of lower limb geometry, and to interrelationships between different aspects of geometry as well as

their consequences for physical function. In addition, it has provided new evidence as to the effects of long-term exercise in adulthood, and of impaired phosphate metabolism in XLH, on lower limb geometry.

Total femoral torsion is an important skeletal geometrical parameter, affecting hip biomechanics. Altered total femoral torsion is associated with hip dysplasia, hip and knee osteoarthritis, atypical fractures, and movement impairments. However, total femoral torsion appears to be a combination of intertrochanteric torsion, shaft torsion and condylar torsion developing independently and resulting in separate clinical outcomes. Furthermore, multiple other skeletal lower limb shape parameters affect the biomechanics of the lower limbs including femoral frontal and lateral bowing, lower limb alignment, and tibial torsion and bowing. In these studies, lower limb bone shape parameters seem not to be interrelated and need therefore to be considered individually on every participant. It is especially important to comprehensively characterise skeletal shape parameters on frontal, sagittal and axial plane when contemplating reconstructive surgical procedures. To ensure satisfactory surgical outcomes regional torsional parameters need to be considered to warrant subject specific advantageous muscular lever arms.

After skeletal maturity no adaptations were observed in epiphyseal regions even in chronically-trained power athletes. A small association, presumably as a result of loading at younger age, was observed in femoral frontal bowing, possibly due to endocortical and periosteal reshaping. These results reinforce the importance of physical activity and exercise during development, and also suggest that participation in long-term exercise in adulthood is not associated with any substantial deleterious effects on bone shape. The observations of large differences in multiple aspects of lower limb geometry in individuals with XLH suggest the need for comprehensive three-dimensional assessments of bone geometry in clinical populations. In addition, as these effects were evident despite most

participants having multiple previous lower limb surgeries to correct aberrant geometry highlights the need for effective pharmacological or physical therapies to improve bone and joint health.

Finally, I identified limitations of current methods of assessment of bone geometry in clinical and particularly basic science research, with studies in children proving most challenging. I developed a novel US-FAROARM® approach which appears promising but does not currently represent an alternative to established three-dimensional imaging devices. Its optimisation would represent a cost and time effective solution to current limitations in, basic and clinical science research.

References

Aamodt, A., Terjesen, T., Eine, J. and Kvistad, K. (1995) 'Femoral anteversion measured by ultrasound and CT: a comparative study.' *Skeletal radiology*, 24(2) pp. 105-109.

Abdelrahman, S., Ireland, A., Winter, E. M., Purcell, M. and Coupaud, S. (2021) 'Osteoporosis after spinal cord injury: Aetiology, effects and therapeutic approaches.' *Journal of Musculoskeletal & Neuronal Interactions*, 21(1) p. 26.

Aird, J., Hogg, A. and Rollinson, P. (2009) 'Femoral torsion in patients with Blount's disease: a previously unrecognised component.' *The Journal of bone and joint surgery. British volume*, 91(10) pp. 1388-1393.

Akiyama, M., Nakashima, Y., Fujii, M., Sato, T., Yamamoto, T., Mawatari, T., Motomura, G., Matsuda, S., et al. (2012) 'Femoral anteversion is correlated with acetabular version and coverage in Asian women with anterior and global deficient subgroups of hip dysplasia: a CT study.' *Skeletal radiology*, 41(11) pp. 1411-1418.

Akoglu, H. (2018) 'User's guide to correlation coefficients.' *Turkish Journal of Emergency Medicine*, 18(3) p. 91.

Allen, M. R. and Burr, D. B. (2019) 'Bone growth, modeling, and remodeling.' *In Basic and Applied Bone Biology*. Elsevier, pp. 85-100.

Allen, K.D., Thoma, L.M. and Golightly, Y.M., 2022. Epidemiology of osteoarthritis. *Osteoarthritis and Cartilage*, 30(2), pp.184-195.

Altai, Z., Montefiori, E., van Veen, B., A. Paggiosi, M., McCloskey, E. V., Viceconti, M., Mazzà, C. and Li, X. (2021) 'Femoral neck strain prediction during level walking using a combined musculoskeletal and finite element model approach.' *Plos one*, 16(2) p. e0245121.

Alvik, I. (1962) 'Increased anteversion of the femur as the only manifestation of dysplasia of the hip.' *Clinical orthopaedics*, 22 pp. 16-20.

Amraee, D., Alizadeh, M., Minoonejhad, H., Razi, M. and Amraee, G. (2017) 'Predictor factors for lower extremity malalignment and non-contact anterior cruciate ligament injuries in male athletes.' *Knee Surgery, Sports Traumatology, Arthroscopy*, 25(5) pp. 1625-1631.

Anda, S., Terjesen, T., Kvistad, K. A. and Svenningsen, S. (1991) 'Acetabular angles and femoral anteversion in dysplastic hips in adults: CT investigation.' *Journal of computer assisted tomography*, 15(1) pp. 115-120.

Archibald, H. D., Petro, K. F. and Liu, R. W. (2019) 'An anatomic study on whether femoral version originates in the neck or the shaft.' *Journal of Pediatric Orthopaedics*, 39(1) pp. e50-e53.

Arnold, A. S., Komallu, A. V. and Delp, S. L. (1997) 'Internal rotation gait: a compensatory mechanism to restore abduction capacity decreased by bone deformity?' *Developmental Medicine & Child Neurology*, 39(1) pp. 40-44.

Aronsson, D. D., Goldberg, M. J., Kling Jr, T. F. and Roy, D. R. (1994) 'Developmental dysplasia of the hip.' *Pediatrics*, 94(2) pp. 201-208.

Audenaert, E. A., Peeters, I., Vigneron, L., Baelde, N. and Pattyn, C. (2012) 'Hip morphological characteristics and range of internal rotation in femoroacetabular impingement.' *Am J Sports Med*, 40(6), Jun, 2012/04/05, pp. 1329-1336.

Aversa, R., Petrescu, F. I., Petrescu, R. V. and Apicella, A. (2016) 'Flexible stem trabecular prostheses.' *American Journal of Engineering and Applied Sciences*, 9(4)

Backman, S. (1957) 'The proximal end of the femur: investigations with special reference to the etiology of femoral neck fractures; anatomical studies; roentgen projections; theoretical stress calculations; experimental production of fractures.' *Acta radiologica. Supplementum*, (146) pp. 1-166.

Bagnall, K., Harris, P. and Jones, P. (1982) 'A radiographic study of the longitudinal growth of primary ossification centers in limb long bones of the human fetus.' *The Anatomical Record*, 203(2) pp. 293-299.

Ballock, R. T. and O'Keefe, R. J. (2003) 'Physiology and pathophysiology of the growth plate.' *Birth Defects Research Part C: Embryo Today: Reviews*, 69(2) pp. 123-143.

Bardeen, C. R. (1905) 'Studies of the development of the human skeleton.' *Am J Anat*, 4 pp. 265-302.

Bardeen, C. R. and Lewis, W. H. (1901) 'Development of the limbs, body-wall and back in man.' *American Journal of Anatomy*, 1(1) pp. 1-35.

Batailler, C., Weidner, J., Wyatt, M., Dalmay, F. and Beck, M. (2018) 'Position of the greater trochanter and functional femoral antetorsion: Which factors matter in the management of femoral antetorsion disorders?' *Bone Joint Journal*, 100(6) pp. 712-719.

Beals, R. K. (1969) 'Developmental changes in the femur and acetabulum in spastic paraplegia and diplegia.' *Developmental Medicine & Child Neurology*, 11(3), Jun, pp. 303-313.

Beck-Nielsen, S. S., Brock-Jacobsen, B., Gram, J., Brixen, K. and Jensen, T. K. (2009) 'Incidence and prevalence of nutritional and hereditary rickets in southern Denmark.' *Eur J Endocrinol*, 160(3), Mar, 2008/12/20, pp. 491-497.

Beck-Nielsen, S. S., Mughal, Z., Haffner, D., Nilsson, O., Levtchenko, E., Ariceta, G., de Lucas Collantes, C., Schnabel, D., et al. (2019) 'FGF23 and its role in X-linked hypophosphatemia-related morbidity.' *Orphanet J Rare Dis*, 14(1), Feb 26, 2019/02/28, p. 58.

Bedi, A., Dolan, M., Leunig, M. and Kelly, B. T. (2011) 'Static and dynamic mechanical causes of hip pain.' *Arthroscopy: The Journal of Arthroscopic & Related Surgery*, 27(2) pp. 235-251.

Beebe, M. J., Wylie, J. D., Bodine, B. G., Kapron, A. L., Maak, T. G., Mei-Dan, O. and Aoki, S. K. (2017) 'Accuracy and Reliability of Computed Tomography and Magnetic Resonance Imaging Compared With True Anatomic Femoral Version.' *Journal of Pediatric Orthopaedics*, 37(4), Jun, 2017/03/01, pp. e265-e270.

Berryman, F., Pynsent, P. and McBryde, C. (2014) 'A semi-automated method for measuring femoral shape to derive version and its comparison with existing methods.' *International journal for numerical methods in biomedical engineering*, 30(11) pp. 1314-1325.

Black, J. D., & Tadros, B. J. (2020). Bone structure: from cortical to calcium. *Orthopaedics and Trauma*, 34(3), 113-119.

Bobroff, E. D., Chambers, H. G., Sartoris, D. J., Wyatt, M. P. and Sutherland, D. H. (1999a) 'Femoral anteversion and neck-shaft angle in children with cerebral palsy.' *Clinical Orthopaedics and Related Research*, 364 pp. 194-204.

Bobroff, E. D., Chambers, H. G., Sartoris, D. J., Wyatt, M. P. and Sutherland, D. H. (1999b) 'Femoral anteversion and neck-shaft angle in children with cerebral palsy.' *Clinical Orthopaedics and Related Research®*, 364 pp. 194-204.

Bonewald, L. F. (2011) 'The amazing osteocyte.' *Journal of bone and mineral research*, 26(2) pp. 229-238.

Borde, R., Hortobágyi, T. and Granacher, U. (2015) 'Dose–response relationships of resistance training in healthy old adults: a systematic review and meta-analysis.' *Sports medicine*, 45(12) pp. 1693-1720.

Botser, I. B., Ozoude, G. C., Martin, D. E., Siddiqi, A. J., Kuppuswami, S. and Domb, B. G. (2012) 'Femoral anteversion in the hip: comparison of measurement by computed tomography, magnetic resonance imaging, and physical examination.' *Arthroscopy: The Journal of Arthroscopic & Related Surgery*, 28(5) pp. 619-627.

Bouziri, H., Descatha, A., Roquelaure, Y., Dab, W. and Jean, K. (2022) 'Can we distinguish the roles of demographic and temporal changes in the incidence and prevalence of musculoskeletal disorders? A systematic review.' *Scandinavian Journal of Work, Environment & Health*, 48(4) pp. 253-263.

Brandi, M. L. (2009) 'Microarchitecture, the key to bone quality.' *Rheumatology*, 48(suppl_4) pp. iv3-iv8.

Bråten, M., Terjesen, T. and Rossvoll, I. (1992) 'Femoral anteversion in normal adults. Ultrasound measurements in 50 men and 50 women.' *Acta Orthopaedica Scandinavica*, 63(1), Feb, pp. 29-32.

Brenner, D. J. and Hall, E. J. (2007) 'Computed tomography—an increasing source of radiation exposure.' *New England Journal of Medicine*, 357(22) pp. 2277-2284.

Bucay, N., Sarosi, I., Dunstan, C.R., Morony, S., Tarpley, J., Capparelli, C., Scully, S., Tan, H.L., Xu, W., Lacey, D.L. and Boyle, W.J., (1998). Osteoprotegerin-deficient mice develop early onset osteoporosis and arterial calcification. *Genes & development*, 12(9), pp.1260-1268.

Buck, F. M., Guggenberger, R., Koch, P. P. and Pfirrmann, C. W. (2012) 'Femoral and tibial torsion measurements with 3D models based on low-dose biplanar radiographs in comparison with standard CT measurements.' *American Journal of Roentgenology*, 199(5), Nov, 2012/10/26, pp. W607-612.

Buddenbrock, B., Wissing, H., Müller, R.-D. and John, V. (1997) 'Radiologische Rotationsfehlerbestimmung am Femur-Computertomographie, optimierte Messgenauigkeit und Expositionsdosis.' *Zeitschrift für Orthopädie und ihre Grenzgebiete*, 135(01) pp. 9-16.

Burr, D. B., & Allen, M. R. (Eds.). (2019). *Basic and applied bone biology*. Academic Press.

Byrd, J. W. T. (2005) *Operative hip arthroscopy.* Springer.

Caouette, C., Rauch, F., Villemure, I., Arnoux, P., Gdalevitch, M., Veilleux, L., Heng, J. and Aubin, C.-É. (2014) 'Biomechanical analysis of fracture risk associated with tibia deformity in children with osteogenesis imperfecta: a finite element analysis.' *J Musculoskelet Neuronal Interact*, 14(2) pp. 205-212.

Cameron, K. L., Hsiao, M. S., Owens, B. D., Burks, R., & Svoboda, S. J. (2011). Incidence of physician-diagnosed osteoarthritis among active duty United States military service members. *Arthritis & Rheumatism,* 63(10), 2974-2982.

Capelli, S., Donghi, V., Maruca, K., Vezzoli, G., Corbetta, S., Brandi, M. L., Mora, S. and Weber, G. (2015) 'Clinical and molecular heterogeneity in a large series of patients with hypophosphatemic rickets.' *Bone*, 79 pp. 143-149.

Carpenter, T. O. (1997) 'New perspectives on the biology and treatment of X-linked hypophosphatemic rickets.' *Pediatric Clinics*, 44(2) pp. 443-466.

Carpenter, T. O., Imel, E. A., Holm, I. A., Jan de Beur, S. M. and Insogna, K. L. (2011) 'A clinician's guide to X-linked hypophosphatemia.' *Journal of Bone and Mineral Research*, 26(7) pp. 1381-1388.

Carriero, A., Jonkers, I. and Shefelbine, S. J. (2011) 'Mechanobiological prediction of proximal femoral deformities in children with cerebral palsy.' *Computer methods in biomechanics and biomedical engineering*, 14(03) pp. 253-262.

Carter, D. R., Orr, T. E., Fyhrie, D. P. and Schurman, D. J. (1987) 'Influences of mechanical stress on prenatal and postnatal skeletal development.' *Clinical orthopaedics and related research*, (219) pp. 237-250.

Castaño-Betancourt, M. C., Van Meurs, J. B., Bierma-Zeinstra, S., Rivadeneira, F., Hofman, A., Weinans, H., Uitterlinden, A. G. and Waarsing, J. H. (2013) 'The contribution of hip geometry to the prediction of hip osteoarthritis.' *Osteoarthritis Cartilage*, 21(10), Oct, 2013/07/03, pp. 1530-1536.

Chadayammuri, V., Garabekyan, T., Bedi, A., Pascual-Garrido, C., Rhodes, J., O'hara, J. and Mei-Dan, O. (2016) 'Passive hip range of motion predicts femoral torsion and acetabular version.' *The Journal of bone and joint surgery. American volume*, 98(2) pp. 127-134.

Chaibi, Y., Cresson, T., Aubert, B., Hausselle, J., Neyret, P., Hauger, O., De Guise, J. and Skalli, W. (2012) 'Fast 3D reconstruction of the lower limb using a parametric model and statistical inferences and clinical measurements calculation from biplanar X-rays.' *Computer methods in biomechanics and biomedical engineering*, 15(5) pp. 457-466.

Cheema, J. I., Grissom, L. E. and Harcke, H. T. (2003) 'Radiographic characteristics of lower-extremity bowing in children.' *Radiographics*, 23(4) pp. 871-880.

Chen, L.-P., Chang, T.-K., Huang, T.-Y., Kwok, T.-G. and Lu, Y.-C. (2014) 'The correlation between lateral bowing angle of the femur and the location of atypical femur fractures.' *Calcified tissue international*, 95(3) pp. 240-247.

Cheng, X. G., Nicholson, P. H., Boonen, S., Brys, P., Lowet, G., Nijs, J. and Dequeker, J. (1997) 'Effects of anteversion on femoral bone mineral density and geometry measured by dual energy X-ray absorptiometry: a cadaver study.' *Bone*, 21(1), Jul, pp. 113-117.

Cho, M.-R., Lee, Y. S. and Choi, W.-K. (2018) 'Relationship between lateral femoral bowing and varus knee deformity based on two-dimensional assessment of side-to-side differences.' *Knee surgery & related research*, 30(1) p. 58.

Chung, C. Y., Lee, K. M., Park, M. S., Lee, S. H., Choi, I. H. and Cho, T. J. (2010) 'Validity and reliability of measuring femoral anteversion and neck-shaft angle in patients with cerebral palsy.' *The Journal of bone and joint surgery. American volume*, 92(5), May, 2010/05/05, pp. 1195-1205.

Cibulka, M. T. (2004) 'Determination and significance of femoral neck anteversion.' *Physical therapy*, 84(6) pp. 550-558.

Cieza, A., Causey, K., Kamenov, K., Hanson, S. W., Chatterji, S. and Vos, T. (2020) 'Global estimates of the need for rehabilitation based on the Global Burden of Disease study 2019: a systematic analysis for the Global Burden of Disease Study 2019.' *The Lancet*, 396(10267) pp. 2006-2017.

Clarac, J.-P., Pries, P., Laine, M., Richer, J.-P., Freychet, H., Goubault, F., Barret, D., HURMIS, A., et al. (1985) 'Mesure de l'antertorsion du col fémoral par échographie. Comparaison avec la tomodensitométrie.' *Revue de chirurgie orthopédique et réparatrice de l'appareil moteur*, 71(6) pp. 365-368.

Cyvín, K. B. (1977) 'A Follow-up Study of Children with Instability of the Hip Joint at Birth: Clinical and Radiological Investigations with Special Reference to the Anteversion of the Femoral Neck.' *Acta Orthopaedica Scandinavica*, 48(sup166) pp. 3-62.

Currey, J. (2008). The structure and mechanical properties of bone. *Bioceramics and their clinical applications* (pp. 3-27). Woodhead Publishing.D'Ambrosia, R. D. (2005) Epidemiology of osteoarthritis. Vol. 28, pp. S201-S205. SLACK Incorporated Thorofare, NJ.

D'Alessandro, M. and Dow, K. (2019) 'Investigating the need for routine ultrasound screening to detect developmental dysplasia of the hip in infants born with breech presentation.' *Paediatrics & child health*, 24(2) pp. e88-e93.

Dallek, M. and Jungbluth, K. (1984) 'Biodynamics of the epiphyseal plate.' *Unfallchirurgie*, 10(1) pp. 33-35.

Daly, R. M. (2007) 'The effect of exercise on bone mass and structural geometry during growth.' *Optimizing Bone Mass and Strength*, 51 pp. 33-49.

Dan, M., Parr, W., Broe, D., Cross, M., & Walsh, W. R. (2018). Biomechanics of the knee extensor mechanism and its relationship to patella tendinopathy: a review. *Journal of Orthopaedic Research®*, 36(12), 3105-3112.

Davids, J. R., Benfanti, P., Blackhurst, D. W. and Allen, B. L. (2002) 'Assessment of femoral anteversion in children with cerebral palsy: accuracy of the trochanteric prominence angle test.' *Journal of Pediatric Orthopaedics*, 22(2) pp. 173-178.

De Vries, J. and Fong, B. (2006) 'Normal fetal motility: an overview.' *Ultrasound in Obstetrics and Gynecology: The Official Journal of the International Society of Ultrasound in Obstetrics and Gynecology*, 27(6) pp. 701-711.

Decker, S., Suero, E. M., Hawi, N., Muller, C. W., Krettek, C. and Citak, M. (2013) 'The physiological range of femoral antetorsion.' *Skeletal radiology*, 42(11), Nov, 2013/07/17, pp. 1501-1505.

Dickenson, E., Wall, P. D., Robinson, B., Fernandez, M., Parsons, H., Buchbinder, R., & Griffin, D. R. (2016). Prevalence of cam hip shape morphology: a systematic review. *Osteoarthritis and Cartilage*, 24(6), 949-961.

Do, S., Lee, C. G., Kim, D. H., Lee, G., Kim, K. Y., Ryu, S. Y. and Song, H. (2020) 'Factors related to femoral bowing among Korean female farmers: a cross-sectional study.' *Annals of Occupational and Environmental Medicine*, 32

Dougall, W.C., Glaccum, M., Charrier, K., Rohrbach, K., Brasel, K., De Smedt, T., Daro, E., Smith, J., Tometsko, M.E., Maliszewski, C.R. and Armstrong, A., (1999). RANK is essential for osteoclast and lymph node development. *Genes & development*, 13(18), pp.2412-2424.
Doyle, A. J. and Winsor, S. (2011) 'Magnetic resonance imaging (MRI) lower limb length measurement.' *Journal of Medical Imaging and Radiation Oncology*, 55(2) pp. 191-194.

Dunlap, K., Shands, A. R., Hollister, L. C., Gaul, J. S. and Streit, H. A. (1953) 'A new method for determination of torsion of the femur.' *The Journal of bone and joint surgery. American volume*, 35-A(2), Apr, pp. 289-311.

Dunn, D. and Notley, B. (1952) 'Anteversion of the neck of the femur: a method of measurement.' *The Journal of bone and joint surgery. British volume*, 34(2) pp. 181-186.

Eckhoff, D. G., Jacofsky, D. J., Springer, B. D., Dunbar, M., Cherian, J. J., Elmallah, R. K., Mont, M. A. and Greene, K. A. (2016) 'Bilateral symmetrical comparison of femoral and tibial anatomic features.' *The Journal of arthroplasty*, 31(5) pp. 1083-1090.

Egund, N. and Palmer, J. (1984) 'Femoral anatomy described in cylindrical coordinates using computed tomography.' *Acta Radiologica. Diagnosis*, 25(3) pp. 209-215.

Ehrenstein, T., Rikli, D. A., Peine, R., Gutberlet, M., Mittlmeier, T., Banzer, D., Mäurer, J. and Felix, R. (1999) 'A new ultrasound-based method for the assessment of torsional

differences following closed intramedullary nailing of femoral fractures.' *Skeletal radiology*, 28(6) pp. 336-341.

Elke, R., Ebneter, A., Dick, W., Fliegel, C. and Morscher, E. (1991) 'Die sonographische Messung der Schenkelhalsantetorsion.' *Zeitschrift für Orthopädie und ihre Grenzgebiete*, 129(02) pp. 156-163.

Eriksen, E. F., Eghbali-Fatourechi, G. Z., & Khosla, S. (2007). Remodeling and vascular spaces in bone. *Journal of bone and mineral research*, 22(1), 1-6.

Escott, B. G., Ravi, B., Weathermon, A. C., Acharya, J., Gordon, C. L., Babyn, P. S., Kelley, S. P. and Narayanan, U. G. (2013) 'EOS low-dose radiography: a reliable and accurate upright assessment of lower-limb lengths.' *JBJS*, 95(23) p. e183.

Fabeck, L., Tolley, M., Rooze, M. and Burny, F. (2002) 'Theoretical study of the decrease in the femoral neck anteversion during growth.' *Cells Tissues Organs*, 171(4) pp. 269-275.

Fabry, G., Macewen, G. D. and Shands Jr, A. (1973a) 'Torsion of the Femur: A Follow-up Study In Normal And Abnormal Conditions.' *JBJS*, 55(8) pp. 1726-1738.

Fabry, G., Macewen, G. D. and Shands Jr, A. (1973b) 'Torsion of the Femur: A Follow-up Study In Normal And Abnormal Conditions.' *Journal of bone and joint surgery* 55(8) pp. 1726-1738.

Fabry, G., Cheng, L. X. and Molenaers, G. (1994) 'Normal and abnormal torsional development in children.' *Clinical Orthopaedics and Related Research*, 302 pp. 22-26.

Fajar, J. K., Taufan, T., Syarif, M., & Azharuddin, A. (2018). Hip geometry and femoral neck fractures: A meta-analysis. *Journal of orthopaedic translation*, 13, 1-6.

Falchi, M. and Rollandi, G. A. (2004) 'CT of pelvic fractures.' *European journal of radiology*, 50(1) pp. 96-105.

Ferlic, P. W., Runer, A., Seeber, C., Thöni, M., Seitlinger, G. and Liebensteiner, M. C. (2018) 'Segmental torsion assessment is a reliable method for in-depth analysis of femoral alignment in computer tomography.' *International orthopaedics*, 42(6) pp. 1227-1231.

Ferlic, P. W., Runer, A., Seeber, C., Thoni, M., Seitlinger, G. and Liebensteiner, M. C. (2018) 'Segmental torsion assessment is a reliable method for in-depth analysis of femoral alignment in Computer Tomography.' *Int Orthop*, 42(6), Jun, 2017/08/16, pp. 1227-1231.

Fishkin, Z., Armstrong, D. G., Shah, H., Patra, A. and Mihalko, W. M. (2006) 'Proximal femoral physis shear in slipped capital femoral epiphysis-a finite element study.' *Journal of Pediatric Orthopaedics*, 26(3) pp. 291-294.

Florkow, M. C., Willemsen, K., Mascarenhas, V. V., Oei, E. H., van Stralen, M., & Seevinck, P. R. (2022). Magnetic Resonance Imaging Versus Computed Tomography for Three-Dimensional Bone Imaging of Musculoskeletal Pathologies: A Review. *Journal of Magnetic Resonance Imaging*, 56(1), 11-34.

Forlino, A., Cabral, W. A., Barnes, A. M. and Marini, J. C. (2011) 'New perspectives on osteogenesis imperfecta.' *Nat Rev Endocrinol*, 7(9), Jun 14, 2011/06/15, pp. 540-557.

Francis, F., Hennig, S., Korn, B., Reinhardt, R., De Jong, P., Poustka, A., Lehrach, H., Rowe, P., et al. (1995) 'A gene (PEX) with homologies to endopeptidases is mutated in patients with X–linked hypophosphatemic rickets.' *Nature genetics*, 11(2) pp. 130-136.

Frost, H. M. (1987) 'Bone "mass" and the "mechanostat": a proposal.' *The anatomical record*, 219(1) pp. 1-9.

Frost, H. M. (1990). Skeletal structural adaptations to mechanical usage (SATMU): 1. Redefining Wolff's law: the bone modeling problem. *The Anatomical Record*, 226(4), 403-413.

Frysz, M., Tobias, J. H., Lawlor, D. A., Aspden, R. M., Gregory, J. S. and Ireland, A. (2020) 'Associations between prenatal indicators of mechanical loading and proximal femur shape: findings from a population-based study in ALSPAC offspring.' *Journal of musculoskeletal & neuronal interactions*, 20(3) p. 301.

Fujii, M., Nakashima, Y., Yamamoto, T., Mawatari, T., Motomura, G., Matsushita, A., Matsuda, S., Jingushi, S., et al. (2010) 'Acetabular retroversion in developmental dysplasia of the hip.' *JBJS*, 92(4) pp. 895-903.

Fujishiro, T., Hayashi, S., Kanzaki, N., Hashimoto, S., Kurosaka, M., Kanno, T. and Masuda, T. (2014) 'Computed tomographic measurement of acetabular and femoral component version in total hip arthroplasty.' *International orthopaedics*, 38(5) pp. 941-946.

Galbraith, R. T., Gelberman, R. H., Hajek, P. C., Baker, L. A., Sartoris, D. J., Rab, G. T., Cohen, M. S. and Griffin, P. P. (1987) 'Obesity and decreased femoral anteversion in adolescence.' *Journal of Orthopaedic Research*, 5(4) pp. 523-528.

Gasser, J. A. and Kneissel, M. (2017) 'Bone physiology and biology.' *In Bone toxicology*. Springer, pp. 27-94.

Gaucher, C., Walrant-Debray, O., Nguyen, T. M., Esterle, L., Garabedian, M. and Jehan, F. (2009) 'PHEX analysis in 118 pedigrees reveals new genetic clues in hypophosphatemic rickets.' *Hum Genet*, 125(4), May, 2009/02/17, pp. 401-411.

Gelberman, R., Cohen, M., Shaw, B., Kasser, J., Griffin, P. and Wilkinson, R. (1986) 'Slipped capital femoral epiphysis: the influence of femoral retroversion.' *J Bone Joint Surg [Am]*, 68 pp. 1000-1007.

Gelberman, R. H., Cohen, M. S., Shaw, B. A., Kasser, J. R., Griffin, P. P. and Wilkinson, R. H. (1986) 'The association of femoral retroversion with slipped capital femoral epiphysis.' *Journal of Bone and Joint Surgery - Series A*, 68(7) pp. 1000-1007.

Gelberman, R. H., Cohen, M. S., Desai, S. S., Griffin, P. P., Salamon, P. B. and O'Brien, T. M. (1987) 'Femoral anteversion. A clinical assessment of idiopathic intoeing gait in children.' *The Journal of bone and joint surgery. British volume*, 69(1) pp. 75-79.

Genest, F. and Seefried, L. (2018) 'Subtrochanteric and diaphyseal femoral fractures in hypophosphatasia—not atypical at all.' *Osteoporosis international*, 29(8) pp. 1815-1825.

Gibson, R. (1967) 'Anteversion of the Femoral Neck: A Method of Measurement.' *Australasian radiology*, 11(2) pp. 163-169.

Gilligan, I., Chandraphak, S. and Mahakkanukrauh, P. (2013) 'Femoral neck-shaft angle in humans: variation relating to climate, clothing, lifestyle, sex, age and side.' *Journal of anatomy*, 223(2) pp. 133-151.

Gizard, A., Rothenbuhler, A., Pejin, Z., Finidori, G., Glorion, C., de Billy, B., Linglart, A. and Wicart, P. (2017) 'Outcomes of orthopedic surgery in a cohort of 49 patients with X-linked hypophosphatemic rickets (XLHR).' *Endocrine connections*, 6(8) pp. 566-573.

Gnudi, S., Ripamonti, C., Lisi, L., Fini, M., Giardino, R. and Giavaresi, G. (2002) 'Proximal femur geometry to detect and distinguish femoral neck fractures from trochanteric fractures in postmenopausal women.' *Osteoporosis International*, 13(1) pp. 69-73.

Gómez-Hoyos, J., Schröder, R., Reddy, M., Palmer, I. J. and Martin, H. D. (2016) 'Femoral neck anteversion and lesser trochanteric retroversion in patients with ischiofemoral impingement: A case-control magnetic resonance imaging study.' *Arthroscopy: The Journal of Arthroscopic & Related Surgery*, 32(1) pp. 13-18.

Gose, S., Sakai, T., Shibata, T., Murase, T., Yoshikawa, H. and Sugamoto, K. (2010) 'Morphometric analysis of the femur in cerebral palsy: 3-dimensional CT study.' *Journal of Pediatric Orthopaedics*, 30(6) pp. 568-574.

Greatrex, F. (2019) *Ultrasound and motion capture analysis for pre-operative planning in lower limb joint replacement surgeries.* University of Sheffield.

Greatrex, F., Montefiori, E., Grupp, T., Kozak, J. and Mazzà, C. (2017) 'Reliability of an Integrated Ultrasound and Stereophotogrammetric System for Lower Limb Anatomical Characterisation.' *Applied bionics and biomechanics*, 2017 pp. 4370649-4370649.

Grimston, S. K., Willows, N. D. and Hanley, D. A. (1993) 'Mechanical loading regime and its relationship to bone mineral density in children.' *Medicine and science in sports and exercise*, 25(11) pp. 1203-1210.

Grumbach, M. M. (1992) 'Puberty: ontogeny, neuroendocrinology, physiology, and disorders.' *In Williams textbook of endocrinology*. 10th ed., Vol. 9. pp. 1115-1626.

Günther, K., Kessler, S., Tomczak, R., Pfeifer, P. and Puhl, W. (1996) 'Femorale antetorsion: Stellenwert klinischer und bildgebender Untersuchungsverfahren bei Kindern und Jugendlichen.' *Zeitschrift für Orthopädie und ihre Grenzgebiete*, 134(04) pp. 295-301.

Hadjab, I., Farlay, D., Crozier, P., Douillard, T., Boivin, G., Chevalier, J., Meille, S. and Follet, H. (2021) 'Intrinsic properties of osteomalacia bone evaluated by nanoindentation and FTIRM analysis.' *Journal of Biomechanics*, 117 p. 110247.

Haffner, D., Emma, F., Eastwood, D. M., Duplan, M. B., Bacchetta, J., Schnabel, D., Wicart, P., Bockenhauer, D., et al. (2019) 'Clinical practice recommendations for the diagnosis and management of X-linked hypophosphataemia.' *Nature Reviews Nephrology*, 15(7) pp. 435-455.

Haider, I. T., Schneider, P. S. and Edwards, W. B. (2019) 'The role of lower-limb geometry in the pathophysiology of atypical femoral fracture.' *Current osteoporosis reports*, 17(5) pp. 281-290.

Haike, H.-J. (1964) *Tierexperimentelle Untersuchungen zur Frage der Entstehung der Osteochondrose des Schenkelkopfes, der Coxa vara und valga, sowie der pathologischen Antetorsion des koxalen Femurendes: Mit 18 Abb.* Verlag nicht ermittelbar.

Halpern, A. A., Tanner, J. and Rinsky, L. (1979) 'Does persistent fetal femoral anteversion contribute to osteoarthritis? A preliminary report.' *Clinical orthopaedics and related research*, (145) pp. 213-216.

Hardy, D., Murphy, W., Siegel, B., Reid, I. and Whyte, M. (1989) 'X-linked hypophosphatemia in adults: prevalence of skeletal radiographic and scintigraphic features.' *Radiology*, 171(2) pp. 403-414.

Harrison, T. (1961) 'The influence of the femoral head on pelvic growth and acetabular form in the rat.' *Journal of anatomy*, 95(Pt 1) pp. 12-24.

Hauge, E. M., Qvesel, D., Eriksen, E. F., Mosekilde, L., & Melsen, F. (2001). Cancellous bone remodeling occurs in specialized compartments lined by cells expressing osteoblastic markers. *Journal of bone and mineral research*, 16(9), 1575-1582.

Hayashi, S., Hashimoto, S., Matsumoto, T., Takayama, K., Shibanuma, N., Ishida, K., Niikura, T., Nishida, K., et al. (2021) 'Postoperative excessive anterior acetabular coverage is associated with decrease in range of motion after periacetabular osteotomy.' *HIP International*, 31(5) pp. 669-675.

Heller, M. O., Bergmann, G., Deuretzbacher, G., Claes, L., Haas, N. P. and Duda, G. N. (2001) 'Influence of femoral anteversion on proximal femoral loading: measurement and simulation in four patients.' *Clinical biomechanics*, 16(8) pp. 644-649.

Hermann, K. L. and Egund, N. (1997) 'CT measurement of anteversion in the femoral neck: the influence of femur positioning.' *Acta radiologica*, 38(4) pp. 527-532.

Hernandez, R. J., Tachdjian, M. O., Poznanski, A. K. and Dias, L. S. (1981) 'CT determination of femoral torsion.' *American Journal of Roentgenology*, 137(1) pp. 97-101.

Hinderaker, T., Uden, A. and Reikerås, O. (1994) 'Direct ultrasonographic measurement of femoral anteversion in newborns.' *Skeletal Radiology*, 23(2), Feb, pp. 133-135.

Hoffer, M. M., Prietto, C. and Koffman, M. (1981) 'Supracondylar derotational osteotomy of the femur for internal rotation of the thigh in the cerebral palsied child.' *The Journal of bone and joint surgery. American volume*, 63(3) pp. 389-393.

Hogervorst, T., Eilander, W., Fikkers, J. T. and Meulenbelt, I. (2012) 'Hip ontogenesis: how evolution, genes, and load history shape hip morphotype and cartilotype.' *Clinical Orthopaedics and Related Research*, 470(12) pp. 3284-3296.

Holt, J. F., Latourette, H. B. and Watson, E. H. (1954) 'Physiological bowing of the legs in young children.' *Journal of the American Medical Association*, 154(5) pp. 390-394.

Horn, A., Wright, J., Bockenhauer, D., Van't Hoff, W. and Eastwood, D. (2017) 'The orthopaedic management of lower limb deformity in hypophosphataemic rickets.' *Journal of children's orthopaedics*, 11(4) pp. 298-305.

Howard, J. S., Fazio, M. A., Mattacola, C. G., Uhl, T. L. and Jacobs, C. A. (2011) 'Structure, sex, and strength and knee and hip kinematics during landing.' *Journal of Athletic Training*, 46(4(p. 376.

Hunziker, E. B. (1994) 'Mechanism of longitudinal bone growth and its regulation by growth plate chondrocytes.' *Microscopy research and technique*, 28(6) pp. 505-519.

Imhoff, F. B., Cotic, M., Liska, F., Dyrna, F. G., Beitzel, K., Imhoff, A. B. and Herbst, E. (2019) 'Derotational osteotomy at the distal femur is effective to treat patients with patellar instability.' *Knee Surgery, Sports Traumatology, Arthroscopy*, 27(2) pp. 652-658.

Inamdar, G., Pedoia, V., Rossi-Devries, J., Samaan, M. A., Link, T. M., Souza, R. B. and Majumdar, S. (2019) 'MR study of longitudinal variations in proximal femur 3D morphological shape and associations with cartilage health in hip osteoarthritis.' *Journal of Orthopaedic Research*, 37(1) pp. 161-170.

Insogna, K. L., Briot, K., Imel, E. A., Kamenický, P., Ruppe, M. D., Portale, A. A., Weber, T., Pitukcheewanont, P., et al. (2018) 'A randomized, double-blind, placebo-controlled, phase 3 trial evaluating the efficacy of burosumab, an anti-FGF23 antibody, in adults with X-linked hypophosphatemia: week 24 primary analysis.' *Journal of Bone and Mineral Research*, 33(8) pp. 1383-1393.

Ireland, A., Maden-Wilkinson, T., Ganse, B., Degens, H. and Rittweger, J. (2014a) 'Effects of age and starting age upon side asymmetry in the arms of veteran tennis players: a cross-sectional study.' *Osteoporosis International*, 25(4) pp. 1389-1400.

Ireland, A., Rittweger, J., Schönau, E., Lamberg-Allardt, C. and Viljakainen, H. (2014b) 'Time since onset of walking predicts tibial bone strength in early childhood.' *Bone*, 68 pp. 76-84.

Ireland, A., Saunders, F. R., Muthuri, S. G., Pavlova, A. V., Hardy, R. J., Martin, K. R., Barr, R. J., Adams, J. E., et al. (2019) 'Age at onset of walking in infancy is associated with hip shape in early old age.' *Journal of Bone and Mineral Research*, 34(3) pp. 455-463.

Ireland, A., Mittag, U., Degens, H., Felsenberg, D., Ferretti, J. L., Heinonen, A., Koltai, E., Korhonen, M. T., et al. (2020) 'Greater maintenance of bone mineral content in male than female athletes and in sprinting and jumping than endurance athletes: a longitudinal study of bone strength in elite masters athletes.' *Archives of osteoporosis*, 15(1) pp. 1-10.

Jacobs, C. R., Temiyasathit, S. and Castillo, A. B. (2010) 'Osteocyte mechanobiology and pericellular mechanics.' *Annual review of biomedical engineering*, 12 pp. 369-400.

Janz, K. F., Letuchy, E. M., Burns, T. L., Gilmore, J. M. E., Torner, J. C. and Levy, S. M. (2014) 'Objectively measured physical activity trajectories predict adolescent bone strength: Iowa Bone Development Study.' *British journal of sports medicine*, 48(13) pp. 1032-1036.

Janz, K. F., Burns, T. L., Torner, J. C., Levy, S. M., Paulos, R., Willing, M. C. and Warren, J. J. (2001) 'Physical activity and bone measures in young children: the Iowa bone development study.' *Pediatrics*, 107(6) pp. 1387-1393.

Janz, K. F., Burns, T. L., Levy, S. M., Torner, J. C., Willing, M. C., Beck, T. J., Gilmore, J. M. and Marshall, T. A. (2004) 'Everyday activity predicts bone geometry in children: the iowa bone development study.' *Medicine and science in sports and exercise*, 36(7) pp. 1124-1131.

Jarrett, D. Y., Oliveira, A. M., Zou, K. H., Snyder, B. D. and Kleinman, P. K. (2010) 'Axial oblique CT to assess femoral anteversion.' *American Journal of Roentgenology*, 194(5) pp. 1230-1233.

Jend, H. (1986) 'Computed tomographic determination of the anteversion angle. Premises and possibilities.' *RoFo: Fortschritte auf dem Gebiete der Rontgenstrahlen und der Nuklearmedizin*, 144(4) pp. 447-452.

Jiang, N., Peng, L., Al-Qwbani, M., Xie, G.-P., Yang, Q.-M., Chai, Y., Zhang, Q. and Yu, B. (2015) 'Femoral version, neck-shaft angle, and acetabular anteversion in Chinese Han population: a retrospective analysis of 466 healthy adults.' *Medicine*, 94(21)

Jouve, J.-L., Glard, Y., Garron, E., Piercecchi, M.-D., Dutour, O., Tardieu, C. and Bollini, G. (2005) 'Anatomical study of the proximal femur in the fetus.' *Journal of Pediatric Orthopaedics B*, 14(2) pp. 105-110.

Junk, S., Terjesen, T., Rossvoll, I. and Bra, M. (1992) 'Leg length inequality measured by ultrasound and clinical methods.' *European journal of radiology*, 14(3) pp. 185-188.

Kaiser, P., Schmoelz, W., Schoettle, P., Zwierzina, M., Heinrichs, C. and Attal, R. (2017) 'Increased internal femoral torsion can be regarded as a risk factor for patellar instability—A biomechanical study.' *Clinical Biomechanics*, 47 pp. 103-109.

Kaiser, P., Attal, R., Kammerer, M., Thauerer, M., Hamberger, L., Mayr, R. and Schmoelz, W. (2016a) 'Significant differences in femoral torsion values depending on the CT measurement technique.' *Archives of orthopaedic and trauma surgery*, 136(9), Sep, 2016/08/10, pp. 1259-1264.

Kaiser, P., Attal, R., Kammerer, M., Thauerer, M., Hamberger, L., Mayr, R. and Schmoelz, W. (2016b) 'Significant differences in femoral torsion values depending on the CT measurement technique.' *Arch Orthop Trauma Surg*, 136(9), Sep, 2016/08/10, pp. 1259-1264.

Kalifa, G., Charpak, Y., Maccia, C., Fery-Lemonnier, E., Bloch, J., Boussard, J.-M., Attal, M., Dubousset, J., et al. (1998) 'Evaluation of a new low-dose digital x-ray device: first dosimetric and clinical results in children.' *Pediatric radiology*, 28(7) pp. 557-561.

Kandzierski, G., Matuszewski, Ł. and Wójcik, A. (2012) 'Shape of growth plate of proximal femur in children and its significance in the aetiology of slipped capital femoral epiphysis.' *International orthopaedics*, 36(12) pp. 2513-2520.

Kang, D., Kim, Y.-K., Kim, E.-A., Kim, D. H., Kim, I., Kim, H.-R., Min, K.-B., Jung-Choi, K., et al. (2014) Prevention of work-related musculoskeletal disorders. Vol. 26, pp. 1-2. Springer.

Karsdal, M. A., Larsen, L., Engsig, M. T., Lou, H., Ferreras, M., Lochter, A., ... & Foged, N. T. (2002). Matrix metalloproteinase-dependent activation of latent transforming growth factor-β controls the conversion of osteoblasts into osteocytes by blocking osteoblast apoptosis. *Journal of Biological Chemistry*, 277(46), 44061-44067.

Kelly, B. T., Bedi, A., Robertson, C. M., Dela Torre, K., Giveans, M. R. and Larson, C. M. (2012) 'Alterations in internal rotation and alpha angles are associated with arthroscopic cam decompression in the hip.' *The American journal of sports medicine*, 40(5) pp. 1107-1112.

Keppler, P., Strecker, W., Kinzl, L., Simmnacher, M. and Claes, L. (1999) 'Die sonographische bestimmung der beingeometrie.' *Orthopade*, 28(12) pp. 1015-1022.

Keppler, P., Krysztoforski, K., Swiatek, E., Krowicki, P., Kozak, J., Gebhard, F. and Pinzuti, J. (2007) 'A new experimental measurement and planning tool for sonographic-assisted navigation.' *Orthopedics*, 30(10) p. S144.

Khan, F. A., Koff, M. F., Noiseux, N. O., Bernhardt, K. A., O'Byrne, M. M., Larson, D. R., Amrami, K. K. and Kaufman, K. R. (2008) 'Effect of local alignment on compartmental patterns of knee osteoarthritis.' *The Journal of Bone and Joint Surgery. American volume.*, 90(9) p. 1961.

Khosla, S., Westendorf, J. J., & Oursler, M. J. (2008). Building bone to reverse osteoporosis and repair fractures. *The Journal of clinical investigation*, 118(2), 421-428.

Kim, H. Y., Lee, S. K., Lee, N. K. and Choy, W. S. (2012) 'An anatomical measurement of medial femoral torsion.' *Journal of Pediatric Orthopaedics B*, 21(6) pp. 552-557.

Kim, J., Park, T., Park, S. and Kim, S. (2000) 'Measurement of femoral neck anteversion in 3D. Part 2: 3D modelling method.' *Medical and Biological Engineering and Computing*, 38(6) pp. 610-616.

Kim, J. S., Park, T. S., Park, S. B., Kim, J. S., Kim, I. Y. and Kim, S. I. (2000) 'Measurement of femoral neck anteversion in 3D. Part 1: 3D imaging method.' *Medical and Biological Engineering and Computing*, 38(6), Nov, 2001/02/24, pp. 603-609.

Kingsley, P. C. and Olmsted, K. (1948) 'A study to determine the angle of anteversion of the neck of the femur.' *The Journal of bone and joint surgery. American volume*, 30(3) pp. 745-751.

Knittel, G. and Staheli, L. (1976) 'The effectiveness of shoe modifications for intoeing.' *The Orthopedic clinics of North America*, 7(4) p. 1019.

Koenig, J. K., Pring, M. E. and Dwek, J. R. (2012) 'MR evaluation of femoral neck version and tibial torsion.' *Pediatric radiology*, 42(1), Jan, 2011/08/16, pp. 113-115.

Koerner, J. D., Patel, N. M., Yoon, R. S., Sirkin, M. S., Reilly, M. C. and Liporace, F. A. (2013) 'Femoral version of the general population: does "normal" vary by gender or ethnicity?' *Journal of orthopaedic trauma*, 27(6), Jun, 2012/10/04, pp. 308-311.

Koo, T. K. and Li, M. Y. (2016) 'A guideline of selecting and reporting intraclass correlation coefficients for reliability research.' *Journal of chiropractic medicine*, 15(2) pp. 155-163.

Kulig, K., Harper-Hanigan, K., Souza, R. B. and Powers, C. M. (2010a) 'Measurement of femoral torsion by ultrasound and magnetic resonance imaging: concurrent validity.' *Phys Ther*, 90(11), Nov, 2010/08/21, pp. 1641-1648.

Kulig, K., Harper-Hanigan, K., Souza, R. B. and Powers, C. M. (2010b) 'Measurement of femoral torsion by ultrasound and magnetic resonance imaging: concurrent validity.' *Physical Therapy*, 90(11), Nov, 2010/08/21, pp. 1641-1648.

Kuo, T. Y., Skedros, J. G. and Bloebaum, R. D. (2003) 'Measurement of femoral anteversion by biplane radiography and computed tomography imaging: comparison with an anatomic reference.' *Investigative radiology*, 38(4) pp. 221-229.

Lambeek, A., De Hundt, M., Vlemmix, F., Akerboom, B., Bais, J., Papatsonis, D., Mol, B. and Kok, M. (2013) 'Risk of developmental dysplasia of the hip in breech presentation: the effect of successful external cephalic version.' *BJOG: An International Journal of Obstetrics & Gynaecology*, 120(5) pp. 607-612.

Lambert, A. S., Zhukouskaya, V., Rothenbuhler, A. and Linglart, A. (2019) 'X-linked hypophosphatemia: Management and treatment prospects.' *Joint Bone Spine*, 86(6), Nov, 2019/02/04, pp. 731-738.

Laplaza, F. J. and Root, L. (1994) 'Femoral anteversion and neck-shaft angles in hip instability in cerebral palsy.' *Journal of pediatric orthopedics*, 14(6) pp. 719-723.

Lauretani, F., Bandinelli, S., Griswold, M. E., Maggio, M., Semba, R., Guralnik, J. M. and Ferrucci, L. (2008) 'Longitudinal changes in BMD and bone geometry in a population-based study.' *Journal of Bone and Mineral research*, 23(3) pp. 400-408.

LeBlanc, A. D., Spector, E. R., Evans, H. J. and Sibonga, J. D. (2007) 'Skeletal responses to space flight and the bed rest analog: a review.' *Journal of Musculoskeletal and Neuronal Interactions*, 7(1) p. 33.

Lee, D., Lee, C. and Cho, T. (1992) 'A new method for measurement of femoral anteversion.' *International orthopaedics*, 16(3) pp. 277-281.

Lee, S., Kwon, Y., Lee, N., Bae, K. J., Park, S., Kim, Y. H., & Cho, K. H. (2019). The prevalence of osteoarthritis and risk factors in the Korean population: The Sixth Korea National Health and Nutrition Examination Survey (VI-1, 2013). *Korean Journal of Family Medicine*, 40(3), 171.

Lee, T. Q., Anzel, S. H., Bennett, K. A., Pang, D. and Kim, W. C. (1994) 'The influence of fixed rotational deformities of the femur on the patellofemoral contact pressures in human cadaver knees.' *Clinical orthopaedics and related research*, (302) pp. 69-74.

Lee, Y. S., Oh, S. H., Seon, J. K., Song, E. K. and Yoon, T. R. (2006) '3D femoral neck anteversion measurements based on the posterior femoral plane in ORTHODOC system.' *Med Biol Eng Comput*, 44(10), Oct, 2006/09/30, pp. 895-906.

Leitzes, A. H., Potter, H. G., Amaral, T., Marx, R. G., Lyman, S. and Widmann, R. F. (2005) 'Reliability and accuracy of MRI scanogram in the evaluation of limb length discrepancy.' *Journal of Pediatric Orthopaedics*, 25(6) pp. 747-749.

León-Muñoz, V. J., Manca, S., López-López, M., Martínez-Martínez, F. and Santonja-Medina, F. (2021) 'Coronal and axial alignment relationship in Caucasian patients with osteoarthritis of the knee.' *Scientific Reports*, 11(1) pp. 1-8.

Leonardi, F., Rivera, F., Zorzan, A. and Ali, S. M. (2014) 'Bilateral double osteotomy in severe torsional malalignment syndrome: 16 years follow-up.' *Journal of Orthopaedics and Traumatology*, 15(2) pp. 131-136.

Lerch, T. D., Todorski, I. A., Steppacher, S. D., Schmaranzer, F., Werlen, S. F., Siebenrock, K. A. and Tannast, M. (2018) 'Prevalence of femoral and acetabular version abnormalities in patients with symptomatic hip disease: a controlled study of 538 hips.' *The American journal of sports medicine*, 46(1) pp. 122-134.

Lewis, C. L., Laudicina, N. M., Khuu, A. and Loverro, K. L. (2017) 'The human pelvis: variation in structure and function during gait.' *The Anatomical Record*, 300(4) pp. 633-642.

Li, C., Ye, Y., He, S., Xu, D. and He, P. (2022) 'High femoral anteversion in osteoarthritic knees, particularly for severe valgus deformity.' *Journal of Orthopaedics and Traumatology*, 23(1) pp. 1-9.

Li, D. T., Cui, J. J., Henry, H. T. and Cooperman, D. R. (2019) 'Changes in proximal femoral shape during fetal development.' *Journal of Pediatric Orthopedics*, 39(3) p. e173.

Li, H., Wang, Y., Oni, J., Qu, X., Li, T., Zeng, Y., Liu, F. and Zhu, Z. (2014) 'The role of femoral neck anteversion in the development of osteoarthritis in dysplastic hips.' *The bone & joint journal*, 96(12) pp. 1586-1593.

Liebensteiner, M. C., Ressler, J., Seitlinger, G., Djurdjevic, T., El Attal, R. and Ferlic, P. W. (2016) 'High Femoral Anteversion Is Related to Femoral Trochlea Dysplasia.' *Arthroscopy: the Journal of Arthroscopic & Related Surgery*, 11(32) pp. 2295-2299.

Linglart, A., Biosse-Duplan, M., Briot, K., Chaussain, C., Esterle, L., Guillaume-Czitrom, S., Kamenicky, P., Nevoux, J., et al. (2014) 'Therapeutic management of hypophosphatemic rickets from infancy to adulthood.' *Endocrine connections*, 3(1) pp. R13-R30.

Liu, L., Lei, K., Chen, X., Fu, D., Yang, P., Yang, L. and Guo, L. (2021) 'Proximal external femoral torsion increases lateral femoral shaft bowing: a study based on 3D CT reconstruction models.' *Knee Surgery, Sports Traumatology, Arthroscopy*, pp. 1-9.

Lovejoy, C. O. (1988) 'Evolution of human walking.' *Scientific American*, 259(5) pp. 118-125.

Lovejoy, C. O. (2005a) 'The natural history of human gait and posture: Part 2. Hip and thigh.' *Gait & posture*, 21(1) pp. 113-124.

Lovejoy, C. O. (2005b) 'The natural history of human gait and posture: Part 1. Spine and pelvis.' *Gait & posture*, 21(1) pp. 95-112.

Lu, Y., Zheng, Z., Chen, W., Lv, H., Lv, J. and Zhang, Y. (2019) 'Dynamic deformation of femur during medial compartment knee osteoarthritis.' *Plos one*, 14(12) p. e0226795.

Magilligan, D. J. (1956) 'Calculation of the angle of anteversion by means of horizontal lateral roentgenography.' *Journal of Bone and Joint Surgery*, 38(6) pp. 1231-1246.

Mansournia, M. A., Collins, G. S., Nielsen, R. O., Nazemipour, M., Jewell, N. P., Altman, D. G. and Campbell, M. J. (2021) 'A CHecklist for statistical Assessment of Medical Papers (the CHAMP statement): explanation and elaboration.' *British journal of sports medicine*, 55(18) pp. 1009-1017.

Marr, C., Seasman, A. and Bishop, N. (2017) 'Managing the patient with osteogenesis imperfecta: a multidisciplinary approach.' *J Multidiscip Healthc*, 10 2017/04/25, pp. 145-155.

Matic, I., Matthews, B. G., Wang, X., Dyment, N. A., Worthley, D. L., Rowe, D. W., Grcevic, D. and Kalajzic, I. (2016) 'Quiescent bone lining cells are a major source of osteoblasts during adulthood.' *Stem cells*, 34(12) pp. 2930-2942.

Matsumoto, T., Hashimura, M., Takayama, K., Ishida, K., Kawakami, Y., Matsuzaki, T., Nakano, N., Matsushita, T., et al. (2015) 'A radiographic analysis of alignment of the lower extremities–initiation and progression of varus-type knee osteoarthritis.' *Osteoarthritis and cartilage*, 23(2) pp. 217-223.

Matsuo, K., & Irie, N. (2008). Osteoclast–osteoblast communication. *Archives of biochemistry and biophysics*, 473(2), 201-209.

Mayes, S., Ferris, A.-R., Smith, P., Garnham, A. and Cook, J. (2017) 'Bony morphology of the hip in professional ballet dancers compared to athletes.' *European radiology*, 27(7) pp. 3042-3049.

McSweeny, A. (1971) 'A study of femoral torsion in children.' *Journal of Bone and Joint Surgery, British volume*, 53(1), Feb, pp. 90-95.

Miller, M. E. and Hangartner, T. N. (1999) 'Temporary brittle bone disease: association with decreased fetal movement and osteopenia.' *Calcified tissue international*, 64(2) pp. 137-143.

Mindler, G. T., Kranzl, A., Stauffer, A., Haeusler, G., Ganger, R. and Raimann, A. (2020) 'Disease-specific gait deviations in pediatric patients with X-linked hypophosphatemia.' *Gait & Posture*, 81 pp. 78-84.

Mindler, G. T., Kranzl, A., Stauffer, A., Kocijan, R., Ganger, R., Radler, C., ... & Raimann, A. (2021). Lower limb deformity and gait deviations among adolescents and adults with X-linked hypophosphatemia. *Frontiers in Endocrinology*, 12, 754084.

Mohajer, B., Kwee, R. M., Guermazi, A., Berenbaum, F., Wan, M., Zhen, G., ... & Demehri, S. (2021). Metabolic syndrome and osteoarthritis distribution in the hand joints: a propensity score matching analysis from the osteoarthritis initiative. *The Journal of Rheumatology*, 48(10), 1608-1615.

Monazzam, S., Bomar, J., Dwek, J., Hosalkar, H. and Pennock, A. (2013) 'Development and prevalence of femoroacetabular impingement-associated morphology in a paediatric and adolescent population: a CT study of 225 patients.' *The Bone & Joint Journal*, 95(5) pp. 598-604.

Moore, K. L., Dalley, A. F. and Agur, A. M. (2013) *Clinically oriented anatomy.* Lippincott Williams & Wilkins.

Moulton, A. and Upadhyay, S. (1982) 'A direct method of measuring femoral anteversion using ultrasound.' *The Journal of bone and joint surgery. British volume*, 64(4) pp. 469-472.

Muhamad, A. R., Freitas, J. M., Bomar, J. D., Dwek, J. and Hosalkar, H. S. (2012) 'CT and MRI lower extremity torsional profile studies: measurement reproducibility.' *Journal of Children's Orthopaedics*, 6(5), Oct, 2013/10/02, pp. 391-396.

Murphy, S. B., Simon, S. R., Kijewski, P. K., Wilkinson, R. H. and Griscom, N. T. (1987) 'Femoral anteversion.' *The Journal of bone and joint surgery. American volume*, 69(8), Oct, 1987/10/01, pp. 1169-1176.

Nelitz, M. (2018) 'Femoral Derotational Osteotomies.' *Current reviews in musculoskeletal medicine*, 11(2), Jun, 2018/04/27, pp. 272-279.

Nelitz, M., Dreyhaupt, J., Williams, S. R. M. and Dornacher, D. (2015) 'Combined supracondylar femoral derotation osteotomy and patellofemoral ligament reconstruction for recurrent patellar dislocation and severe femoral anteversion syndrome: surgical technique and clinical outcome.' *International orthopaedics*, 39(12) pp. 2355-2362.

Nikander, R., Sievänen, H., Heinonen, A. and Kannus, P. (2005) 'Femoral neck structure in adult female athletes subjected to different loading modalities.' *Journal of Bone and Mineral Research*, 20(3) pp. 520-528.

Nilsson, O., Marino, R., De Luca, F., Phillip, M. and Baron, J. (2005) 'Endocrine regulation of the growth plate.' *Hormone research in paediatrics*, 64(4) pp. 157-165.

Novais, E. N., Bixby, S. D., Rennick, J., Carry, P. M., Kim, Y.-J. and Millis, M. B. (2014) 'Hip dysplasia is more severe in Charcot-Marie-Tooth disease than in developmental dysplasia of the hip.' *Clinical Orthopaedics and Related Research*, 472(2) pp. 665-673.

Nyland, J., Kuzemchek, S., Parks, M. and Caborn, D. (2004) 'Femoral anteversion influences vastus medialis and gluteus medius EMG amplitude: composite hip abductor EMG amplitude ratios during isometric combined hip abduction-external rotation.' *Journal of electromyography and kinesiology*, 14(2) pp. 255-261.

Ogata, K. and Goldsand, E. M. (1979) 'A simple biplanar method of measuring femoral anteversion and neck-shaft angle.' *The Journal of bone and joint surgery. American volume*, 61(6A) pp. 846-851.

Ott, S. M. (2018). Cortical or trabecular bone: what's the difference?. *American journal of nephrology*, 47(6), 373-376.

Papavasiliou, A., Siatras, T., Bintoudi, A., Milosis, D., Lallas, V., Sykaras, E. and Karantanas, A. (2014) 'The gymnasts' hip and groin: a magnetic resonance imaging study in asymptomatic elite athletes.' *Skeletal radiology*, 43(8) pp. 1071-1077.

Parfitt, A. M. (2002). Targeted and nontargeted bone remodeling: relationship to basic multicellular unit origination and progression. *Bone*, 30(1), 5-7.

Parfitt, A. M. (2003). Renal bone disease: a new conceptual framework for the interpretation of bone histomorphometry. *Current opinion in nephrology and hypertension*, 12(4), 387-403.

Parfitt, A. M. (2006). Misconceptions V--Activation of osteoclasts is the first step in the bone remodeling cycle. *Bone*, 39(6), 1170-1172.

Park, K.-W., Garcia, R.-a. N., Rejuso, C. A., Choi, J.-W. and Song, H.-R. (2015) 'Limb lengthening in patients with achondroplasia.' *Yonsei Medical Journal*, 56(6) pp. 1656-1662.

Parker, L., Nazarian, L. N., Carrino, J. A., Morrison, W. B., Grimaldi, G., Frangos, A. J., Levin, D. C. and Rao, V. M. (2008) 'Musculoskeletal imaging: medicare use, costs, and potential for cost substitution.' *Journal of the American College of Radiology*, 5(3) pp. 182-188.

Parvaresh, K. C., Pennock, A. T., Bomar, J. D., Wenger, D. R. and Upasani, V. V. (2018) 'Analysis of acetabular ossification from the triradiate cartilage and secondary centers.' *Journal of Pediatric Orthopaedics*, 38(3) pp. e145-e150.

Passmore, E. and Sangeux, M. (2016) 'Defining the medial-lateral axis of an anatomical femur coordinate system using freehand 3D ultrasound imaging.' *Gait Posture*, 45, Mar, 2016/03/17, pp. 211-216.

Passmore, E., Pandy, M. G., Graham, H. K. and Sangeux, M. (2016a) 'Measuring Femoral Torsion In Vivo Using Freehand 3-D Ultrasound Imaging.' *Ultrasound in Medicine and Biology*, 42(2), Feb, 2015/12/08, pp. 619-623.

Passmore, E., Graham, H. K., Pandy, M. G. and Sangeux, M. (2018) 'Hip- and patellofemoral-joint loading during gait are increased in children with idiopathic torsional deformities.' *Gait Posture*, 63, Jun, 2018/05/19, pp. 228-235.

Pauwels, F. and Maquet, P. G. (1979) *Biomécanique de l'appareil moteur: contributions à l'étude de l'anatomie fonctionnelle; traduit de l'allemand, entièrement revu et compl., comprenant 7 nouveaux chapitres.* Springer.

Payne, L. Z. and DeLuca, P. A. (1994) 'Intertrochanteric versus supracondylar osteotomy for severe femoral anteversion.' *Journal of pediatric orthopedics*, 14(1) pp. 39-44.

Phillips, H. O., Greene, W. B., Guilford, W. B., Mittelstaedt, C. A., Gaisie, G., Vincent, L. M. and Durell, C. (1985) 'Measurement of femoral torsion: comparison of standard roentgenographic techniques with ultrasound.' *Journal of pediatric orthopedics*, 5(5) pp. 546-549.

Piazzolla, A., Solarino, G., Bizzoca, D., Montemurro, V., Berjano, P., Lamartina, C., Martini, C. and Moretti, B. (2018) 'Spinopelvic parameter changes and low back pain improvement due to femoral neck anteversion in patients with severe unilateral primary hip osteoarthritis undergoing total hip replacement.' *European Spine Journal*, 27(1) pp. 125-134.

Pierrepont, J. W., Marel, E., Baré, J. V., Walter, L. R., Stambouzou, C. Z., Solomon, M. I., McMahon, S. and Shimmin, A. J. (2019) 'Variation in femoral anteversion in patients requiring total hip replacement.' *HIP International*, p. 1120700019848088.

Ponseti, I. (1978) 'Growth and development of the acetabulum in the normal child. Anatomical, histological, and roentgenographic studies.' *The Journal of bone and joint surgery. American volume*, 60(5) pp. 575-585.

Portale, A. A., Carpenter, T. O., Brandi, M. L., Briot, K., Cheong, H. I., Cohen-Solal, M., Crowley, R., Jan De Beur, S., et al. (2019) 'Continued Beneficial Effects of Burosumab in Adults with X-Linked Hypophosphatemia: Results from a 24-Week Treatment Continuation Period After a 24-Week Double-Blind Placebo-Controlled Period.' *Calcif Tissue Int*, 105(3), Sep, 2019/06/06, pp. 271-284.

Pritchett, J. W. and Perdue, K. D. (1988) 'Mechanical factors in slipped capital femoral epiphysis.' *Journal of pediatric orthopedics*, 8(4) pp. 385-388.

Qin, L., Liu, W., Cao, H. and Xiao, G. (2020) 'Molecular mechanosensors in osteocytes.' *Bone research*, 8(1) pp. 1-24.

Ráliš, Z. and McKibbin, B. (1973) 'Changes in shape of the human hip joint during its development and their relation to its stability.' *The Journal of Bone and Joint Surgery. British volume*, 55(4) pp. 780-785.

Rauch, F. (2005) 'Bone growth in length and width: the Yin and Yang of bone stability.' *Journal of musculoskeletal and neuronal interactions*, 5(3) p. 194.

Rauch, F. and Glorieux, F. H. (2004) 'Osteogenesis imperfecta.' *The Lancet*, 363(9418), 2004/04/24/, pp. 1377-1385.

Rauch, F. (2006). Watching bone cells at work: what we can see from bone biopsies. *Pediatric Nephrology*, 21, 457-462.

Reikerås, O. (1992) 'Patellofemoral characteristics in patients with increased femoral anteversion.' *Skeletal radiology*, 21(5) pp. 311-313.

Reikerås, O. and Høiseth, A. (1982) 'Femoral neck angles in osteoarthritis of the hip.' *Acta orthopaedica Scandinavica*, 53(5) pp. 781-784.

Reikerås, O., Bjerkreim, I. and Kolbenstvedt, A. (1983a) 'Anteversion of the acetabulum and femoral neck in normals and in patients with osteoarthritis of the hip.' *Acta Orthop Scand*, 54(1), Feb, pp. 18-23.

Reikerås, O., Bjerkreim, I. and Kolbenstvedt, A. (1983b) 'Anteversion of the acetabulum and femoral neck in normals and in patients with osteoarthritis of the hip.' *Acta orthopaedica Scandinavica*, 54(1), Feb, pp. 18-23.

Reyes, C., Garcia-Gil, M., Elorza, J. M., Mendez-Boo, L., Hermosilla, E., Javaid, M. K., ... & Prieto-Alhambra, D. (2015). Socio-economic status and the risk of developing hand, hip or knee osteoarthritis: a region-wide ecological study. *Osteoarthritis and cartilage*, 23(8), 1323-1329.

Reznikov, N., Shahar, R., & Weiner, S. (2014). Bone hierarchical structure in three dimensions. *Acta biomaterialia*, 10(9), 3815-3826.

Riggs, B. L., Melton III, L. J., Robb, R. A., Camp, J. J., Atkinson, E. J., Peterson, J. M., Rouleau, P. A., McCollough, C. H., et al. (2004) 'Population-based study of age and sex differences in bone volumetric density, size, geometry, and structure at different skeletal sites.' *Journal of Bone and Mineral Research*, 19(12) pp. 1945-1954.

Rippstein, J. (1955) 'Determination of the antetorsion of the femur neck by means of two x-ray pictures.' *Zeitschrift fur Orthopadie und ihre Grenzgebiete*, 86(3) pp. 345-360.

Rittweger, J. (2008) 'Ten years muscle-bone hypothesis: What have we learned so far?-Almost a Festschrift.' *J Musculoskelet Neuronal Interact*, 8(2) pp. 174-178.

Rittweger, J., Gerrits, K. H., Altenburg, T. M., Reeves, N. D., Maganaris, C. N. and Haan, A. d. (2006) 'Bone adaptation to altered loading after spinal cord injury: a study of bone and muscle strength.'

Rittweger, J., Frost, H. M., Schiessl, H., Ohshima, H., Alkner, B., Tesch, P. and Felsenberg, D. (2005) 'Muscle atrophy and bone loss after 90 days' bed rest and the effects of flywheel

resistive exercise and pamidronate: results from the LTBR study.' *Bone*, 36(6) pp. 1019-1029.

Rodríguez, J. I., Garcia-Alix, A., Palacios, J. and Paniagua, R. (1988) 'Changes in the long bones due to fetal immobility caused by neuromuscular disease. A radiographic and histological study.' *JBJS*, 70(7) pp. 1052-1060.

Ross, J. R., Nepple, J. J., Philippon, M. J., Kelly, B. T., Larson, C. M. and Bedi, A. (2014) 'Effect of changes in pelvic tilt on range of motion to impingement and radiographic parameters of acetabular morphologic characteristics.' *The American journal of sports medicine*, 42(10) pp. 2402-2409.

Rosskopf, A. B., Buck, F. M., Pfirrmann, C. W. and Ramseier, L. E. (2017a) 'Femoral and tibial torsion measurements in children and adolescents: comparison of MRI and 3D models based on low-dose biplanar radiographs.' *Skeletal Radiol*, 46(4), Apr, 2017/02/06, pp. 469-476.

Rosskopf, A. B., Ramseier, L. E., Sutter, R., Pfirrmann, C. W. and Buck, F. M. (2014) 'Femoral and tibial torsion measurement in children and adolescents: comparison of 3D models based on low-dose biplanar radiography and low-dose CT.' *American Journal of Roentgenology*, 202(3), Mar, 2014/02/22, pp. W285-291.

Rosskopf, A. B., Agten, C. A., Ramseier, L. E., Pfirrmann, C. W. A. and Buck, F. M. (2017b) 'Femoral torsion assessment with MRI in children: Should we use the bony or cartilaginous contours?' *European journal of radiology*, 92, Jul, 2017/06/19, pp. 153-158.

Ruby, L., Mital, M. A., O'Connor, J. and Patel, U. (1979) 'Anteversion of the femoral neck.' *Journal of Bone and Joint Surgery. American volume*, 61(1), Jan, 1979/01/01, pp. 46-51.

Ruwe, P. A., Gage, J. R., Ozonoff, M. and DeLuca, P. (1992) 'Clinical determination of femoral anteversion. A comparison with established techniques.' *The Journal of bone and joint surgery. American volume*, 74(6) pp. 820-830.

Ryder, C. T. and Crane, L. (1953) 'Measuring femoral anteversion: the problem and a method.' *The Journal of bone and joint surgery. American volume*, 35(2) pp. 321-328.

Sacchetti, B., Funari, A., Michienzi, S., Di Cesare, S., Piersanti, S., Saggio, I., Tagliafico, E., Ferrari, S., Robey, P.G., Riminucci, M. and Bianco, P., (2007). Self-renewing osteoprogenitors in bone marrow sinusoids can organize a hematopoietic microenvironment. *Cell*, 131(2), pp.324-336..

Saglam, Y., Akalan, N. E., Temelli, Y. and Kuchimov, S. (2016) 'Femoral derotation osteotomy with multi-level soft tissue procedures in children with cerebral palsy: Does it improve gait quality?' *Journal of children's orthopaedics*, 10(1) pp. 41-48.

Salenius, P. and Vankka, E. (1975) 'The development of the tibiofemoral angle in children.' *JBJS*, 57(2) pp. 259-261.

Sangeux, M., Mahy, J. and Graham, H. K. (2014) 'Do physical examination and CT-scan measures of femoral neck anteversion and tibial torsion relate to each other?' *Gait & posture*, 39(1) pp. 12-16.

Sangeux, M., Pascoe, J., Graham, H. K., Ramanauskas, F. and Cain, T. (2015) 'Three-dimensional measurement of femoral neck anteversion and neck shaft angle.' *Journal of computer assisted tomography*, 39(1) pp. 83-85.

Sasaki, S., Miyakoshi, N., Hongo, M., Kasukawa, Y. and Shimada, Y. (2012) 'Low-energy diaphyseal femoral fractures associated with bisphosphonate use and severe curved femur: a case series.' *Journal of bone and mineral metabolism*, 30(5) pp. 561-567.

Satpathy, J., Kannan, A., Owen, J. R., Wayne, J. S., Hull, J. R. and Jiranek, W. A. (2015) 'Hip contact stress and femoral neck retroversion: a biomechanical study to evaluate implication of femoroacetabular impingement.' *Journal of Hip Preservation Surgery*, 2(3) pp. 287-294.

Saunders, F. R., Gregory, J. S., Pavlova, A. V., Muthuri, S. G., Hardy, R. J., Martin, K. R., Barr, R. J., Adams, J. E., et al. (2020) 'Motor development in infancy and spine shape in early old age: Findings from a British birth cohort study.' *Journal of Orthopaedic Research®*, 38(12) pp. 2740-2748.

Scheys, L., Van Campenhout, A., Spaepen, A., Suetens, P. and Jonkers, I. (2008) 'Personalized MR-based musculoskeletal models compared to rescaled generic models in the presence of increased femoral anteversion: effect on hip moment arm lengths.' *Gait Posture*, 28(3), Oct, 2008/06/24, pp. 358-365.

Schmaranzer, F., Lerch, T. D., Siebenrock, K. A., Tannast, M. and Steppacher, S. D. (2019) 'Differences in femoral torsion among various measurement methods increase in hips with excessive femoral torsion.' *Clinical Orthopaedics and Related Research*, 477(5) pp. 1073-1083.

Schneider, B., Laubenberger, J., Jemlich, S., Groene, K., Weber, H. and Langer, M. (1997) 'Measurement of femoral antetorsion and tibial torsion by magnetic resonance imaging.' *The British journal of radiology*, 70(834) pp. 575-579.

Scorcelletti, M., Reeves, N. D., Rittweger, J. and Ireland, A. (2020) 'Femoral anteversion: significance and measurement.' *Journal of Anatomy*, 237(5) pp. 811-826.

Scorcelletti, M., Kara, S., Zange, J., Jordan, J., Semler, O., Schönau, E., Rittweger, J., Ireland, A., et al. (2022) 'Lower limb bone geometry in adult individuals with X-linked hypophosphatemia: an observational study.' *Osteoporosis International*, pp. 1-11.

Seefried, L., Dahir, K., Petryk, A., Högler, W., Linglart, A., Martos-Moreno, G. Á., Ozono, K., Fang, S., et al. (2020) 'Burden of illness in adults with hypophosphatasia: data from the global hypophosphatasia patient registry.' *Journal of Bone and Mineral Research*, 35(11) pp. 2171-2178.

Seitlinger, G., Moroder, P., Scheurecker, G., Hofmann, S. and Grelsamer, R. P. (2016) 'The Contribution of Different Femur Segments to Overall Femoral Torsion.' *The American journal of sports medicine*, 44(7), Jul, 2016/05/10, pp. 1796-1800.

Setiawati, R., & Rahardjo, P. (2019). Bone development and growth. *Osteogenesis and bone regeneration*, 10.

Shands Jr, A. and Steele, M. K. (1958) 'Torsion of the femur: a follow-up report on the use of the Dunlap method for its determination.' *JBJS*, 40(4) pp. 803-816.

Sharkey, M. S., Grunseich, K. and Carpenter, T. O. (2015) 'Contemporary medical and surgical management of X-linked hypophosphatemic rickets.' *JAAOS-Journal of the American Academy of Orthopaedic Surgeons*, 23(7) pp. 433-442.

Shaw, E. D. and Beals, R. K. (1992) 'The hip joint in Down's syndrome. A study of its structure and associated disease.' *Clinical orthopaedics and related research*, (278) pp. 101-107.

Shea, C., Rolfe, R. and Murphy, P. (2015) 'The importance of foetal movement for co-ordinated cartilage and bone development in utero: clinical consequences and potential for therapy.' *Bone & joint research*, 4(7) pp. 105-116.

Shefelbine, S. J. and Carter, D. R. (2004) 'Mechanobiological predictions of femoral anteversion in cerebral palsy.' *Annals of biomedical engineering*, 32(2) pp. 297-305.

Shimosawa, H., Nagura, T., Kobayashi, S., Harato, K., Nakamura, M., Matsumoto, M. and Niki, Y. (2018) 'Severe knee osteoarthritis patients show more femoral coronal bowing than moderate knee osteoarthritis patients–a study using three dimensional computed tomography.' *Osteoarthritis and Cartilage*, 26 pp. S444-S445.

Shin, W., Moon, N., Jang, J., Park, K. and Suh, K. (2017) 'Anterolateral femoral bowing and loss of thigh muscle are associated with occurrence of atypical femoral fracture: effect of failed tension band mechanism in mid-thigh.' *Journal of Orthopaedic Science*, 22(1) pp. 99-104.

Shultz, S. J., Nguyen, A.-D. and Schmitz, R. J. (2008) 'Differences in lower extremity anatomical and postural characteristics in males and females between maturation groups.' *Journal of orthopaedic & sports physical therapy*, 38(3) pp. 137-149.

Sims, N. A., & Gooi, J. H. (2008, October). Bone remodeling: Multiple cellular interactions required for coupling of bone formation and resorption. In Seminars in cell & developmental biology (Vol. 19, No. 5, pp. 444-451). Academic Press.

Singleton, M. C., & LeVeau, B. F. (1975). The hip joint: Structure, stability, and stress: A review. *Physical therapy*, 55(9), 957-973.

Skalski, M. (2022) *Radiology Quiz 19963 | Radiopaedia.org*. ID: 19963. Radiopaedia.org. [Online] [Accessed on 16/09/2022] https://radiopaedia.org/cases/19963/studies/19994?lang=gb

Skrinar, A., Dvorak-Ewell, M., Evins, A., Macica, C., Linglart, A., Imel, E. A., Theodore-Oklota, C. and San Martin, J. (2019) 'The lifelong impact of X-linked hypophosphatemia: results from a burden of disease survey.' *Journal of the Endocrine Society*, 3(7) pp. 1321-1334.

Smith, W. S., Ireton, R. J. and Coleman, C. R. (1958) 'Sequelae of experimental dislocation of a weight-bearing ball-and-socket joint in a young growing animal: gross alterations in bone and cartilage.' *JBJS*, 40(5) pp. 1121-1127.

Snow, M. (2021) 'Tibial torsion and patellofemoral pain and instability in the adult population: current concept review.' *Current Reviews in Musculoskeletal Medicine*, 14(1) pp. 67-75.

Song, H.-R., Choonia, A.-T., Hong, S. J., Lee, S.-H., Suh, S.-W., Cha, I. H. and Park, J.-T. (2006) 'Rotational profile of the lower extremity in achondroplasia: computed tomographic examination of 25 patients.' *Skeletal Radiology*, 35(12), December 01, pp. 929-934.

Staheli, L. T. (1993) 'Rotational problems in children.' *Journal of bone and joint surgery. American volume*, 75(6) pp. 939-949.

Staheli, L. T., Duncan, W. R. and Schaefer, E. (1968) 'Growth alterations in the hemiplegic child. A study of femoral anteversion, neck-shaft angle, hip rotation, C.E. angle, limb length and circumference in 50 hemiplegic children.' *Clinical Orthopaedics and Related Research*, 60, 1968 Sep-Oct, pp. 205-212.

Starker, M., Hanusek, S., Rittmeister, M. and Thoma, W. (1998) 'Validierung computertomographisch gemessener Antetorisonswinkel am Femur.' *Zeitschrift für Orthopädie und ihre Grenzgebiete*, 136(05) pp. 420-427.

Steele, A., Gonzalez, R., Garbalosa, J. C., Steigbigel, K., Grgurich, T., Parisi, E. J., Feinn, R. S., Tommasini, S. M., et al. (2020) 'Osteoarthritis, osteophytes, and enthesophytes affect biomechanical function in adults with X-linked hypophosphatemia.' *The Journal of Clinical Endocrinology & Metabolism*, 105(4) pp. e1798-e1814.

Strayer Jr, L. M. (1971) 'Embryology of the human hip joint.' *Clinical Orthopaedics and Related Research®*, 74 pp. 221-240.

Suda, T., Takahashi, N., Udagawa, N., Jimi, E., Gillespie, M. T., & Martin, T. J. (1999). Modulation of osteoclast differentiation and function by the new members of the tumor necrosis factor receptor and ligand families. *Endocrine reviews*, 20(3), 345-357.

Sugano, N., Noble, P. C. and Kamaric, E. (1998a) 'A comparison of alternative methods of measuring femoral anteversion.' *Journal of computer assisted tomography*, 22(4) pp. 610-614.

Sugano, N., Noble, P. C., Kamaric, E., Salama, J. K., Ochi, T. and Tullos, H. S. (1998b) 'The morphology of the femur in developmental dysplasia of the hip.' *The Journal of bone and joint surgery. British volume*, 80(4) pp. 711-719.

Sung, K. H., Kwon, S.-S., Chung, C. Y., Lee, K. M., Cho, G. H. and Park, M. S. (2018) 'Long-term outcomes over 10 years after femoral derotation osteotomy in ambulatory children with cerebral palsy.' *Gait & posture*, 64 pp. 119-125.

Sutter, R., Dietrich, T. J., Zingg, P. O. and Pfirrmann, C. W. (2015) 'Assessment of femoral antetorsion with MRI: comparison of oblique measurements to standard transverse measurements.' *American Journal of Roentgenology*, 205(1) pp. 130-135.

Suzuki, Y., Matsubayashi, J., Ji, X., Yamada, S., Yoneyama, A., Imai, H., Matsuda, T., Aoyama, T., et al. (2019) 'Morphogenesis of the femur at different stages of normal human development.' *PloS one*, 14(8) p. e0221569.

Svenningsen, S., Terjesen, T., Auflem, M. and Berg, V. (1989) 'Hip motion related to age and sex.' *Acta Orthopaedica Scandinavica*, 60(1) pp. 97-100.

Svenningsen, S., Apalset, K., Terjesen, T. and Anda, S. (1989) 'Regression of femoral anteversion. A prospective study of intoeing children.' *Acta Orthopaedica Scandinavica*, 60(2), Apr, pp. 170-173.

Świątek-Najwer, E., Otto, K., Krowicki, P., Krysztoforski, K., Keppler, P. and Kozak, J. (2014) '3D Bone Shape Modelling Basing on Dataset Recorded by Ultrasound Free-Hand Navigated Probe.' *In Information Technologies in Biomedicine, Volume 4*. Springer, pp. 45-56.

Tamari, K., Tinley, P., Briffa, K. and Aoyagi, K. (2006) 'Ethnic-, gender-, and age-related differences in femorotibial angle, femoral antetorsion, and tibiofibular torsion: Cross-sectional study among healthy Japanese and Australian Caucasians.' *Clinical anatomy*, 19(1) pp. 59-67.

Tanaka, H., Tarumi, T. and Rittweger, J. (2011) 'Aging and physiological lessons from master athletes.' *Comprehensive Physiology*, 10(1) pp. 261-296.

Tatsumi, S., Ishii, K., Amizuka, N., Li, M., Kobayashi, T., Kohno, K., Ito, M., Takeshita, S., et al. (2007) 'Targeted ablation of osteocytes induces osteoporosis with defective mechanotransduction.' *Cell metabolism*, 5(6) pp. 464-475.

Terjesen, T. and Anda, S. (1987) 'Femoral anteversion in children measured by ultrasound.' *Acta Orthopaedica Scandinavica*, 58(4) pp. 403-407.

Terjesen, T., Anda, S. and Rønningen, H. (1993) 'Ultrasound examination for measurement of femoral anteversion in children.' *Skeletal radiology*, 22(1) pp. 33-36.

Terjesen, T., Benum, P., Rossvoll, I., Svenningsen, S., Isern, A. E. F. and Nordbø, T. (1991) 'Leg-length discrepancy measured by ultrasonography.' *Acta Orthopaedica Scandinavica*, 62(2) pp. 121-124.

Thompson, W. R., Rubin, C. T. and Rubin, J. (2012) 'Mechanical regulation of signaling pathways in bone.' *Gene*, 503(2) pp. 179-193.

Tomczak, R., Guenther, K., Rieber, A., Mergo, P., Ros, P. and Brambs, H. (1997) 'MR imaging measurement of the femoral antetorsional angle as a new technique: comparison with CT in children and adults.' *American journal of roentgenology*, 168(3) pp. 791-794.

Tomczak, R., Günther, K., Pfeifer, T., Häberle, H., Rieber, A., Danz, B., Rilinger, N., Friedrich, J., et al. (1995) *Messung des femoralen Torsionswinkels von Kindern durch Magnetresonanztomographie im Vergleich mit CT und Ultraschall.* Vol. 162: Georg Thieme Verlag Stuttgart· New York.

Tönnis, D. and Heinecke, A. (1991a) 'Diminished femoral antetorsion syndrome: a cause of pain and osteoarthritis.' *Journal of pediatric orthopedics*, 11(4), 1991 Jul-Aug, pp. 419-431.

Tönnis, D. and Heinecke, A. (1991b) 'Diminished femoral antetorsion syndrome: a cause of pain and osteoarthritis.' *Journal of Pediatric Orthopedics*, 11(4), 1991 Jul-Aug, pp. 419-431.

Tönnis, D. and Heinecke, A. (1999) 'Current concepts review-acetabular and femoral anteversion: relationship with osteoarthritis of the hip.' *Jbjs*, 81(12) pp. 1747-1770.

Toogood, P. A., Skalak, A. and Cooperman, D. R. (2009) 'Proximal femoral anatomy in the normal human population.' *Clinical orthopaedics and related research*, 467(4), Apr, 2008/09/02, pp. 876-885.

Uda, Y., Azab, E., Sun, N., Shi, C. and Pajevic, P. D. (2017) 'Osteocyte mechanobiology.' *Current osteoporosis reports*, 15(4) pp. 318-325.

Uding, A., Bloom, N. J., Commean, P. K., Hillen, T. J., Patterson, J. D., Clohisy, J. C. and Harris-Hayes, M. (2019) 'Clinical tests to determine femoral version category in people with chronic hip joint pain and asymptomatic controls.' *Musculoskeletal Science and Practice*, 39, Feb, 2018/12/17, pp. 115-122.

Uemura, K., Atkins, P. R., Fiorentino, N. M. and Anderson, A. E. (2018) 'Hip rotation during standing and dynamic activities and the compensatory effect of femoral anteversion: An in-vivo analysis of asymptomatic young adults using three-dimensional computed tomography models and dual fluoroscopy.' *Gait & posture*, 61 pp. 276-281.

Upadhyay, S., O'neil, T., Burwell, R. and Moulton, A. (1987) 'A new method using ultrasound for measuring femoral anteversion (torsion): technique and reliability.' *The British journal of radiology*, 60(714) pp. 519-523.

van Arkel, R. J., Amis, A. A. and Jeffers, J. R. (2015) 'The envelope of passive motion allowed by the capsular ligaments of the hip.' *Journal of Biomechanics*, 48(14) pp. 3803-3809.

Varzi, D., Coupaud, S. A., Purcell, M., Allan, D. B., Gregory, J. S. and Barr, R. J. (2015) 'Bone morphology of the femur and tibia captured by statistical shape modelling predicts rapid bone loss in acute spinal cord injury patients.' *Bone*, 81 pp. 495-501.

Veilleux, L.-N., Cheung, M. S., Glorieux, F. H. and Rauch, F. (2013) 'The muscle-bone relationship in X-linked hypophosphatemic rickets.' *The Journal of Clinical Endocrinology & Metabolism*, 98(5) pp. E990-E995.

Veilleux, N. J., Kalore, N. V., Wegelin, J. A., Vossen, J. A., Jiranek, W. A. and Wayne, J. S. (2018) 'Automated femoral version estimation without the distal femur.' *J Orthop Res*, 36(12), Dec, 2018/08/04, pp. 3161-3168.

Verbruggen, S. W., Kainz, B., Shelmerdine, S. C., Hajnal, J. V., Rutherford, M. A., Arthurs, O. J., Phillips, A. T. and Nowlan, N. C. (2018a) 'Stresses and strains on the human fetal skeleton during development.' *Journal of The Royal Society Interface*, 15(138) p. 20170593.

Verbruggen, S. W., Kainz, B., Shelmerdine, S. C., Arthurs, O. J., Hajnal, J. V., Rutherford, M. A., Phillips, A. T. and Nowlan, N. C. (2018b) 'Altered biomechanical stimulation of the

developing hip joint in presence of hip dysplasia risk factors.' *Journal of biomechanics*, 78 pp. 1-9.

Vrezas, I., Elsner, G., Bolm-Audorff, U., Abolmaali, N., & Seidler, A. (2010). Case–control study of knee osteoarthritis and lifestyle factors considering their interaction with physical workload. *International archives of occupational and environmental health*, 83, 291-300.

Wade, S., Strader, C., Fitzpatrick, L., Anthony, M. and O'Malley, C. (2014) 'Estimating prevalence of osteoporosis: examples from industrialized countries.' *Archives of osteoporosis*, 9(1) pp. 1-10.

Waidelich, H.-A., Strecker, W. and Schneider, E. (1992) *Computertomographische Torsionswinkel-und Längenmessung an der unteren Extremität.* Vol. 157: Georg Thieme Verlag Stuttgart· New York.

Waidelich, H.-A. a. S., W and Schneider, E. (1992) *Computertomographische Torsionswinkel-und Längenmessung an der unteren Extremität Waidelich 1992.pdf>.* Vol. 157. Fortschritte auf dem Gebiet der Röntegenstrahlen und der bildgebenden Verfahren.

Waisbrod, G., Schiebel, F. and Beck, M. (2017) 'Abnormal femoral antetorsion-a subtrochanteric deformity.' *Journal of hip preservation surgery*, 4(2), Jul, 2017/06/21, pp. 153-158.

Walker, J. and Goldsmith, C. (1981) 'Morphometric study of the fetal development of the human hip joint: significance for congenital hip disease.' *The Yale journal of biology and medicine*, 54(6) p. 411.

Walmsley, T. (1933) 'The vertical axes of the femur and their relations. A contribution to the study of the erect position.' *Journal of anatomy*, 67(Pt 2) p. 284.

Ward, K., Caulton, J., Adams, J. and Mughal, M. (2006) 'Perspective: cerebral palsy as a model of bone development in the absence of postnatal mechanical factors.' *Journal of musculoskeletal and neuronal interactions*, 6(2) p. 154.

Watanabe, R. S. (1974) 'Embryology of the human hip.' *Clinical Orthopaedics and Related Research*, 98 pp. 8-26.

Weber, A. E., Nathani, A., Dines, J. S., Allen, A. A., Shubin-Stein, B. E., Arendt, E. A. and Bedi, A. (2016) 'An algorithmic approach to the management of recurrent lateral patellar dislocation.' *The Journal of bone and joint surgery. American volume*, 98(5) pp. 417-427.

Wedge, J. H., Munkacsi, I. and Loback, D. (1989) 'Anteversion of the femur and idiopathic osteoarthrosis of the hip.' *The Journal of bone and joint surgery. American volume*, 71(7), Aug, pp. 1040-1043.

Weiner, D. S., Cook, A. J., Hoyt, W. A. and Oravec, C. E. (1978) 'Computed tomography in the measurement of femoral anteversion.' *Orthopedics*, 1(4) pp. 299-306.

Wilkinson, J. A. (1962) 'Femoral anteversion in the rabbit.' *The Journal of bone and joint surgery. British volume*, 44(2) pp. 386-397.

Wilks, D. C., Gilliver, S. F. and Rittweger, J. (2009a) 'Forearm and tibial bone measures of distance-and sprint-trained master cyclists.' *Medicine & Science in Sports & Exercise*, 41(3) pp. 566-573.

Wilks, D. C., Winwood, K., Gilliver, S., Kwiet, A., Chatfield, M., Michaelis, I., Sun, L., Ferretti, J. L., et al. (2009b) 'Bone mass and geometry of the tibia and the radius of master sprinters, middle and long distance runners, race-walkers and sedentary control participants: a pQCT study.' *Bone*, 45(1) pp. 91-97.

Wills, A.K., Black, S., Cooper, R., Coppack, R.J., Hardy, R., Martin, K.R., Cooper, C. and Kuh, D., (2012). Life course body mass index and risk of knee osteoarthritis at the age of 53 years: evidence from the 1946 British birth cohort study. *Annals of the rheumatic diseases*, 71(5), pp.655-660.

Wissing, H. and Spira, G. (1986) 'Die Bestimmung von Rotationsfehlern am Femur durch computertomographische Bestimmung des Antetorsionswinkels des Schenkelhalses.' *Unfallchirurgie*, 12(1) p. 1.

Witzke, K. A. and Snow, C. M. (2000) 'Effects of polymetric jump training on bone mass in adolescent girls.' *Medicine and science in sports and exercise*, 32(6) pp. 1051-1057.

Wolff, J. (1892) 'Das Gesetz der Transformation der knochen. A. Hirschwald, Berlin.' *Translated as: the law of bone remodeling (1986). Springer-Verlag, Berlin*,

Wright, M. and Irving, M. (2012) 'Clinical management of achondroplasia.' *Archives of disease in childhood*, 97(2) pp. 129-134.

Xie, M., Gol'Din, P., Herdina, A. N., Estefa, J., Medvedeva, E. V., Li, L., Newton, P. T., Kotova, S., et al. (2020) 'Secondary ossification center induces and protects growth plate structure.' *Elife*, 9 p. e55212.

Xing, L., & Boyce, B. F. (2005). Regulation of apoptosis in osteoclasts and osteoblastic cells. *Biochemical and biophysical research communications*, 328(3), 709-720.

Yadav, P., Shefelbine, S. J., Ponten, E. and Gutierrez-Farewik, E. M. (2017) 'Influence of muscle groups' activation on proximal femoral growth tendency.' *Biomechanics and modeling in mechanobiology*, 16(6), Dec, 2017/06/24, pp. 1869-1883.

Yang, G., Dai, Y., Dong, C., Kang, H., Niu, J., Lin, W. and Wang, F. (2020) 'Distal femoral morphological dysplasia is correlated with increased femoral torsion in patients with trochlear dysplasia and patellar instability.' *The bone & joint journal*, 102(7) pp. 868-873.

Yaniv, M., Becker, T., Goldwirt, M., Khamis, S., Steinberg, D. M. and Weintroub, S. (2006) 'Prevalence of bowlegs among child and adolescent soccer players.' *Clinical journal of sport medicine*, 16(5) pp. 392-396.

Yavuzer, M. G. (2020) 'Evolution of bipedalism.' *In Comparative Kinesiology of the Human Body*. Elsevier, pp. 489-497.

Yoshioka, Y. and Cooke, T. D. V. (1987) 'Femoral anteversion: assessment based on function axes.' *Journal of orthopaedic research*, 5(1) pp. 86-91.

Yoshioka, Y., Siu, D. and Cooke, T. (1987a) 'The anatomy and functional axes of the femur.' *The Journal of bone and joint surgery. American volume*, 69(6) pp. 873-880.

Yoshioka, Y., Siu, D. and Cooke, T. (1987b) 'The anatomy and functional axes of the femur.' *J Bone Joint Surg Am*, 69(6) pp. 873-880.

Zeng, W.-N., Wang, F.-Y., Chen, C., Zhang, Y., Gong, X.-Y., Zhou, K., Chen, Z., Wang, D., et al. (2016) 'Investigation of association between hip morphology and prevalence of osteoarthritis.' *Scientific Reports*, 6(1), 2016/03/22, p. 23477.

Zhang, C., Zhao, Z., Sun, Y., Xu, L., JiaJue, R., Cui, L., Pang, Q., Jiang, Y., (2019) 'Clinical and genetic analysis in a large Chinese cohort of patients with X-linked hypophosphatemia.' *Bone*, 121 pp. 212-220.

Zhou H, Chernecky R and Davies JE.(1994) Deposition of cement at reversal lines in rat femoral bone. *Journal of Bone and Mineral Research*; 9: 367–374

Zhukouskaya, V. V., Rothenbuhler, A., Colao, A., Di Somma, C., Kamenický, P., Trabado, S., Prié, D., Audrain, C., et al. (2020) 'Increased prevalence of overweight and obesity in children with X-linked hypophosphatemia.' *Endocrine connections*, 9(2) pp. 144-153.

Zirkle, D. and Lovejoy, C. O. (2019) 'The hominid ilium is shaped by a synapomorphic growth mechanism that is unique within primates.' *Proceedings of the National Academy of Sciences*, 116(28) pp. 13915-13920.